



**UNIVERSIDADE ESTADUAL DE CAMPINAS**  
**FACULDADE DE ENGENHARIA DE ALIMENTOS**

**ANA LETÍCIA RODRIGUES COSTA LELIS**

**PRODUCTION OF PICKERING EMULSIONS BY HIGH AND LOW ENERGY  
PROCESSES**

**PRODUÇÃO DE EMULSÕES TIPO PICKERING POR PROCESSOS DE ALTA E  
BAIXA ENERGIA**

**CAMPINAS**

**2018**

**ANA LETÍCIA RODRIGUES COSTA LELIS**

**PRODUCTION OF PICKERING EMULSIONS BY HIGH AND LOW ENERGY PROCESSES**

**PRODUÇÃO DE EMULSÕES TIPO PICKERING POR PROCESSOS DE ALTA E BAIXA ENERGIA**

Thesis presented to the Faculty of Food Engineering of University of Campinas in partial fulfillment of the requirements for the degree of Doctor in Food Engineering.

Tese apresentada à Faculdade de Engenharia de Alimentos da Universidade Estadual de Campinas como parte dos requisitos exigidos para obtenção do título de Doutora em Engenharia de Alimentos.

**Orientadora:** Profa. Dra. Rosiane Lopes da Cunha

ESTE EXEMPLAR CORRESPONDE À VERSÃO FINAL DA TESE QUE DEFENDIDA PELA ALUNA ANA LETÍCIA RODRIGUES COSTA LELIS E ORIENTADA PELA PROFA. DRA. ROSIANE LOPES DA CUNHA

**CAMPINAS**

**2018**



**Agência(s) de fomento e nº(s) de processo(s):** CNPq, 140710/2015-9; CNPq, 204109/2017-5

Ficha catalográfica  
Universidade Estadual de Campinas  
Biblioteca da Faculdade de Engenharia de Alimentos  
Claudia Aparecida Romano - CRB 8/5816

L539p Lelis, Ana Letícia Rodrigues Costa, 1990-  
Produção de emulsões tipo Pickering por processos de alta e baixa energia / Ana Letícia Rodrigues Costa Lelis. – Campinas, SP : [s.n.], 2018.

Orientadores: Rosiane Lopes da Cunha e David A. Weitz.  
Tese (doutorado) – Universidade Estadual de Campinas, Faculdade de Engenharia de Alimentos.  
Em regime interinstitucional com: Harvard University .

1. Quitosana. 2. Celulose. 3. Estabilidade. 4. Digestibilidade. 5. Ultrassom. I. Cunha, Rosiane Lopes da. II. Weitz, David A.. III. Universidade Estadual de Campinas. Faculdade de Engenharia de Alimentos. V. Título.

Informações para Biblioteca Digital

**Título em outro idioma:** Production of Pickering emulsions by high and low energy processes

**Palavras-chave em inglês:**

Chitosan  
Cellulose  
Stability  
Digestibility  
Ultrasound

**Área de concentração:** Engenharia de Alimentos

**Titulação:** Doutora em Engenharia de Alimentos

**Banca examinadora:**

Rosiane Lopes da Cunha [Orientador]  
Chiu Chih Ming

Lucimara Gaziola de la Torre  
Márcio da Silveira Carvalho  
Pedro Esteves Duarte Augusto

**Data de defesa:** 12-12-2018

**Programa de Pós-Graduação:** Engenharia de Alimentos

## **BANCA EXAMINADORA**

**Profa. Dra. Rosiane Lopes da Cunha - Orientadora**  
Faculdade de Engenharia de Alimentos (FEA)  
Universidade Estadual de Campinas (UNICAMP), Campinas, SP

**Dr. Chiu Chih Ming**  
Faculdade de Engenharia de Alimentos (FEA)  
Universidade Estadual de Campinas (UNICAMP), Campinas, SP

**Profa. Dra. Lucimara Gaziola de la Torre**  
Faculdade de Engenharia Química  
Universidade Estadual de Campinas (UNICAMP), Campinas, SP

**Prof. Dr. Márcio da Silveira Carvalho**  
Departamento de Engenharia Mecânica  
Pontifícia Universidade Católica do Rio de Janeiro (PUC-RJ), Rio de Janeiro, RJ

**Prof. Dr. Pedro Esteves Duarte Augusto**  
Escola Superior de Agricultura Luiz de Queiroz (ESALQ)  
Universidade de São Paulo (USP), Piracicaba, SP

A Ata da defesa com as respectivas assinaturas dos membros encontram-se no SIGA/Sistema de Fluxo de Dissertação/Tese e na Secretaria do Programa da Unidade.

*“I will lead her into desert and speak to her heart”  
Hosea 2:16*

*Dedicado aos meus pais e marido,*

## AGRADECIMENTOS

À Deus, que permitiu que tudo isso pudesse ser realizado, sendo meu amparo e refúgio em todos os momentos, pois comprovado é o Teu amor por mim.

Ao meu marido Fábio, que depositou toda confiança e apoio durante este período da minha vida e que está disposto a sonhar e viver comigo o plano de Deus para nós.

À Cláudia Isabel e Joaquim Rodrigues, que souberam abrir mão dos seus sonhos para que os meus pudessem ser realizados e que são presença constante e grandes incentivadores.

A minha irmã Ana Clarice, fruto do cuidado de Deus para comigo, água e vinho. E como ela mesma diz: “Deixa chegar o sonho, prepara uma avenida que agente vai passar”.

Ao Eric, meu amigo fiel e poderosa proteção durante nossa longa caminhada juntos (mesmo separados e para sempre)! Sinal do cuidado de Deus na minha vida.

À Andresa, amizade que vale mais que qualquer tesouro! Sinal do cuidado de Deus na minha vida.

À Suelen, amiga de todas as horas (até em diferentes fusos horário)! Obrigada por me escutar, me acolher e ser voz de Deus na minha vida!

Ao Éder, Natália, Larissa e Núria, companheiros de caminhada e de fé!

Agradeço a Prof<sup>a</sup>. Dr<sup>a</sup>. Rosiane Lopes da Cunha pela oportunidade e confiança depositada em mim, seus ensinamentos foram essenciais para a minha formação profissional.

A todos os integrantes do Laboratório de Engenharia de Processos da Universidade Estadual de Campinas, pelo apoio técnico e científico durante o trabalho.

À Universidade Estadual de Campinas pela oportunidade concedida para a realização deste doutorado. Aos professores do Departamento de Engenharia de Alimentos pelos ensinamentos e conhecimento transmitido.

Ao Conselho Nacional de Pesquisa Científica e Tecnológica (CNPq), Fundação de Amparo à Pesquisa do Estado de São Paulo (FAPESP) e Financiadora de Estudos e Projetos (FINEP) pelo apoio financeiro. O presente trabalho foi realizado com apoio da Coordenação de Aperfeiçoamento de Pessoal de Nível Superior – Brasil (CAPES) – Código de Financiamento 001.

Ao Prof. Dr. Márcio da Silveira Carvalho pela oportunidade concedida para a realização de parte dos experimentos no Laboratório de Micro Hidrodinâmica e Meios Porosos do Departamento de Engenharia Mecânica da Pontifícia Universidade Católica do Rio de Janeiro (PUC-RJ).

Ao Professor David A. Weitz e todos os membros do grupo *Experimental Soft Condensed Matter* pela grande oportunidade do estágio sanduíche na *John Paulson School of Engineering and Applied Sciences* da *Harvard University*.

My very special thanks go to Shalom Catholic Community of Boston. Thank you for all the support and all the love that you've given me. I'm truly blessed for all the time of friendship that God has given us.

“Where you go... I will go...Your people shall be My people...” Ruth 1:16

## RESUMO

Partículas de quitosana (Ch) e celulose (nanofibras de celulose; CNFs e cristais de celulose; CCrys) foram utilizadas como estabilizantes de emulsões Pickering óleo em água (O/A) produzidas por técnicas de alta (ultrassom e homogeneizador a alta pressão) e baixa energia (dispositivos de microfluídica). As características das partículas e emulsões foram avaliadas frente às variáveis de processo de emulsificação e condições gastrointestinais. Em uma primeira etapa, Ch foram produzidas e caracterizadas quanto aos efeitos da variação da potência aplicada e tempo de processamento em ultrassom sobre a estabilidade destas partículas e das emulsões. Os intensos efeitos de cavitação gerados com altas potências de ultrassom foram capazes de quebrar as partículas de quitosana e as gotas de óleo em menores tamanhos promovendo a formação de uma rede tridimensional entre gotas. Além disso, a alta estabilidade das emulsões foi associada à redução da tensão interfacial entre o óleo e a água e aumento da hidrofobicidade das partículas. Os efeitos das condições de emulsificação usando ultrassom e homogeneizador a alta pressão sobre as propriedades das CNFs obtidas da casca da banana e das emulsões Pickering foram avaliados na segunda etapa deste projeto. O fenômeno de coalescência foi observado nas emulsões produzidas no homogeneizador a alta pressão, enquanto que, a floculação das gotas ocorreu naquelas obtidas em ultrassom de alta intensidade. Nesta última, a estabilidade à coalescência foi associada com o ligeiro aumento da viscosidade da emulsão e rompimento das CNFs durante o processo de ultrassonicação. Em uma terceira etapa, um protocolo de digestibilidade *in vitro* foi utilizado para elucidar o papel das partículas (Ch, CNFs and CCrys) na taxa de digestão lipídica das emulsões tipo Pickering. A alta carga positiva das emulsões estabilizadas por quitosana levou à desagregação das gotas após a etapa gástrica, o que favoreceu a maior digestão lipídica na etapa intestinal. Por outro lado, a emulsão estabilizada com CNFs apresentou menor digestão lipídica e a forte aderência das partículas de CCrys na interface das gotas tornou-as resistentes ao deslocamento por componentes tensoativos. Na última etapa, a formação e propriedades de emulsões estabilizadas por CCrys foi estudada usando um dispositivo microcapilar. Gotas de óleo altamente monodispersas e emulsões estáveis ao longo do tempo foram produzidas a partir do balanço entre o tempo de geração das gotas e adsorção das partículas. Por outro lado, grandes gotas de óleo e emulsões menos estáveis foram obtidas após a ocorrência de eventos de coalescência dentro do microcanal ou devido ao aumento da viscosidade da fase dispersa. A abordagem microfluídica contribuiu para uma melhor compreensão das condições dinâmicas de estabilização das emulsões Pickering dentro e fora dos microcanais revelando eventos discretos que geralmente estão escondidos em emulsões produzidas por métodos convencionais de emulsificação.

**Palavras-chave:** quitosana, celulose, estabilidade, digestibilidade, ultrassom, homogeneizador de alta-pressão, microcanal

## ABSTRACT

High-energy (ultrasound and high-pressure homogenizer) and low-energy (microfluidic devices) processes were used to obtain oil-in-water (O/W) Pickering emulsions stabilized by food-grade particles (chitosan nanoparticles; Ch, cellulose nanofibers; CNFs and cellulose crystals; CCrys). In the first step, the effect of time and ultrasound power on physicochemical properties of Ch and O/W Pickering emulsions were evaluated using an ultrasonic device. The surface activity of chitosan particles was evidenced with the reduction of interfacial tension between oil-water phases. The emulsion stability mechanism by deprotonated chitosan particles was also associated to an increase of the particle hydrophobicity and the formation of a droplet network structure due to the intense effects of cavitation generated at higher ultrasonication power. The effects of the emulsification conditions using ultrasound and high-pressure homogenization on the properties of the CNFs obtained from the banana peel and Pickering emulsions were evaluated in the second step. Coalescence phenomenon was observed in the emulsions produced using high-pressure homogenizer, whereas droplets flocculation occurred in emulsions processed by ultrasound. In the latter, coalescence stability was associated with effects of cavitation forces acting on the CNFs breakup. In the third step, an *in vitro* digestibility protocol was used to elucidate the role of different emulsifying polysaccharides particles (Ch, CNFs and CCrys) on the lipid digestion rate of oil-in-water Pickering emulsions. The highly positive charge of the emulsions stabilized by chitosan led to the disaggregation of droplets after the gastric step, which favored a more intense lipid digestion in the intestinal step. On the other hand, Tween 80, CCrys and CNFs were able to inhibit lipid digestion and no changes on droplet mean size were observed following intestinal step. CNFs-stabilized emulsion showed the lowest lipid digestion, whereas the strong adherence of the CCrys particles onto the droplet interface became them resistant to displacement by surface-active components. In the last step, the formation and stability of oil droplets in the presence of cellulose nanocrystals was studied using a microcapillary device. Monodisperse oil droplets and stable emulsions over time were produced from a balance between droplets generation time and particles adsorption. On the other hand, large oil droplets and less stable emulsions were obtained after coalescence events inside the microchannel or due to the increase on the dispersed phase viscosity. Microfluidic approach contributed to a better understanding of the dynamic conditions of stabilization inside and outside the microchannels revealing discrete events that usually are hidden in emulsions produced by conventional emulsification methods.

**Keywords:** chitosan, cellulose, stability, digestibility, ultrasound, high-pressure homogenizer, microchannel



## LISTA DE FIGURAS

<b>Figura 2.1.</b> (a) Representação de emulsões óleo em água (O/A) estabilizadas por emulsificantes convencionais e partículas sólidas. (b) Posição de uma partícula sólida na interface da gota com um ângulo de contato menor que $90^\circ$ correspondendo à formação de uma emulsão O/A .....	25
<b>Figure 3.1.</b> Particle size distribution of chitosan particles untreated or treated with different ultrasonication power. Process time, dashed line: 3 min and solid line: 5 min. ....	46
<b>Figure 3.2.</b> Dynamic interfacial tension of the systems between sunflower oil and different aqueous solutions (water, acid-chitosan (Ch) solution (pH 3.3), chitosan (Ch) particles untreated and chitosan (Ch) particles treated at 600 W/5 min (pH 6.9)).....	48
<b>Figure 3.3.</b> (a) Thixotropy and viscosity at $5\text{ s}^{-1}$ (process time: (■) 3 min and (■) 5 min) and (b) mechanical spectra (process time: ( $\Delta$ ) 3 min and (o) 5 min) of emulsions stabilized by chitosan particles. Open symbols: $G''$ and filled symbols: $G'$ . Different letters indicate significant differences ( $p < 0.05$ ) between emulsions viscosity at $5\text{ s}^{-1}$ . ....	49
<b>Figure 3.4.</b> (a) Optical micrograph of emulsions stabilized by chitosan particles (0.6% w/v) obtained from RS and US processes. (b) Confocal micrographs of emulsion stabilized by chitosan particles stained with FITC (green color). Process condition: 600 W/5 min. ....	52
<b>Figure 3.5.</b> (a) Size distribution of freshly emulsions stabilized by chitosan particles (0.6% w/v) obtained from RS and US process. Dispersant solvent, blue lines: Tween 20 and black lines: water. (b) Size distribution and optical microscopy of emulsions stabilized by chitosan particles (0.6% w/v) obtained from US process after 6 days of storage.....	53
<b>Figure 3.6.</b> (a) Backscattering profiles (in fresh and after 6 days of storage) of emulsions stabilized by chitosan particles (0.6% w/v) obtained from US process (dashed line: 3 min and solid line: 5 min). (b) Pictures of measuring cells containing emulsions stabilized by chitosan particles (0.6% w/v) obtained from US process after 6 days of storage.....	55
<b>Figure 4. 1.</b> AFM images of the untreated and treated cellulose nanofibers obtained after the strongest homogenization conditions using high-pressure homogenizer (HP) or ultrasound (US) (scanning area $2.0\text{ }\mu\text{m} \times 2.0\text{ }\mu\text{m}$ , scale bar = 200 nm).....	73
<b>Figure 4.2.</b> FTIR spectra of the cellulose nanofibers (0.01% w/w) obtained after different homogenization conditions using ultrasound (W) or high-pressure homogenizer (MPa).....	74
<b>Figure 4.3.</b> Dynamic interfacial tension between sunflower oil and water or cellulose nanofibers (CNFs) .....	76
<b>Figure 4.4.</b> (a) Backscattering profiles (in fresh (—) and after 1 (---) and 6 (...) days of storage) of emulsions stabilized by cellulose nanofibers (0.01% w/w) obtained from ultrasound (W) and high-pressure processes (MPa). (b) Pictures of measuring cells containing emulsions stabilized by cellulose nanofibers (0.01% w/w) obtained from ultrasound (W) and high-pressure homogenizer (MPa) after 6 days of storage.....	79
<b>Figure 4.5.</b> (a) Mean diameter ( $D_{32}$ ) and (b) size distribution of emulsions stabilized by cellulose nanofibers (0.01% w/w) obtained from ultrasound (W) or high-pressure homogenizer (MPa). Fresh emulsions (—) and after 6 days of storage (6d): (---) cream phase (...) serum phase.....	82
<b>Figure 4.6.</b> Optical micrograph emulsions stabilized by cellulose nanofibers (0.01% w/w) obtained from (a) ultrasound (P: power; W) or (b) high-pressure homogenizer (HP: pressure; MPa). Confocal micrograph of emulsion stabilized by cellulose nanofibers and stained with Congo red (red color). Process conditions in (c) ultrasound: 675 W and (d) high-pressure: 50 MPa. Scale bar: $10\text{ }\mu\text{m}$ .....	86

<b>Figure 5.1.</b> a) Mean droplet size ( $D_{4,3}$ ) and b) volume size distribution of the Pickering emulsions before digestion (initial or full line) and after gastric (dashed line) and intestinal (dotted line) steps.....	104
<b>Figure 5.2.</b> Microscopy of the Pickering emulsions before digestion (initial) and after gastric and intestinal steps. Scale bar: 10 $\mu\text{m}$ .....	104
<b>Figure 5.3.</b> Zeta potential values of Pickering emulsions before digestion (initial) and after gastric and intestinal steps .....	105
<b>Figure 5.4.</b> Visual aspect of the Pickering emulsions before digestion (initial) and after gastric and intestinal steps .....	105
<b>Figure 5.5.</b> Kinetics of free fat acids (FFA) release under simulated intestinal conditions ..	107
<b>Figure 5.6.</b> Schematic representation of the physicochemical mechanism involved in the in vitro digestion steps of each emulsifier/particles- stabilized emulsions.....	109
 <b>Figure 6.1.</b> AFM image of cellulose nanocrystals. a) Scanning area 3.0 $\mu\text{m}$ x 3.0 $\mu\text{m}$ , scale bar = 500 nm and b) scanning area 1.0 $\mu\text{m}$ x 1.0 $\mu\text{m}$ , scale bar = 200 nm .....	118
<b>Figure 6.2.</b> Schematic of the co-flow and flow-focusing microfluidic device used for production of Pickering emulsions .....	119
<b>Figure 6.3.</b> Coalescence events (%) of oil droplets as a function of the disperse phase flow rate ( $\mu\text{L}/\text{min}$ ) and cellulose nanocrystals (CNC) dispersion concentration (% w/w). Continuous phase flow rate= 200 $\mu\text{L}/\text{min}$ . .....	121
<b>Figure 6.4.</b> Particles (droplets) size distribution of O/W Pickering emulsions stabilized by cellulose nanocrystals. Fresh emulsions (solid line) and after 7 days of storage (dashed line) .....	124
<b>Figure 6.5.</b> Optical micrograph of O/W Pickering emulsions stabilized by cellulose nanocrystals after 7 days of storage. Scale bar: 200 $\mu\text{m}$ .....	125
<b>Figure 6.6.</b> Size distribution (fresh emulsions: solid line and after 7 days of storage: dashed line) and optical micrograph (after 7 days of storage) of Pickering emulsions produced at 3.0% w/w of cellulose nanocrystals and disperse phase flow rate of 10 $\mu\text{L}/\text{min}$ and collected in tubes with water. Scale bar: 200 $\mu\text{m}$ .....	126

## LISTA DE TABELAS

<b>Table 3.1.</b> Energy density applied in each process condition and physicochemical properties of non-treated and ultrasound treated chitosan (Ch) dispersions (0.01 % w/v). ....	46
<b>Table 3.2.</b> Mean diameter ( $D_{32}$ ) and span of emulsions stabilized by chitosan particles (0.6 % w/v) obtained from RS and US process. Fresh emulsion and after 6 days of storage.....	53
<b>Table 4.1.</b> Length and diameter size (nm), aspect ratio, zeta potential (mV), crystallinity index (ICr%) and contact angle ( $^{\circ}$ )* of the cellulose nanofibers (0.01% w/w) obtained after different homogenization conditions using ultrasound (US) or high-pressure homogenizer (HP). ....	72
<b>Table 4.2.</b> Viscosity of emulsions stabilized by cellulose nanofibers (0.01% w/w) obtained from ultrasound (US) or high-pressure homogenizer (HP). Fresh emulsion and after 6 days of storage (6d). ....	80
<b>Table 5.1.</b> Particle/emulsifier concentration and emulsification process conditions in high-intensity ultrasound.....	99
<b>Table 6.1.</b> Viscosity or apparent viscosity at $1000\text{ s}^{-1}$ ( $\eta$ ) and rheological parameters (k and n) of the cellulose nanocrystals (CNC) aqueous dispersion (% w/w). Viscosity ratio ( $\alpha$ ) and interfacial tension ( $\gamma$ ) between CNC aqueous dispersion (% w/w) and corn oil.....	122
<b>Table 6.2.</b> Mean diameter ( $D$ ; $\mu\text{m}$ ) and coefficient of variation (CV; %) of O/W Pickering emulsions stabilized by cellulose nanocrystals (CNC).....	123

## SUMÁRIO

<b>CAPÍTULO I.....</b>	<b>17</b>
1.1. <i>Introdução Geral.....</i>	18
1.2. <i>Objetivos .....</i>	19
1.2.1. <i>Geral.....</i>	19
1.2.2. <i>Específicos .....</i>	20
1.3. <i>Estruturação da tese.....</i>	20
<b>CAPÍTULO II .....</b>	<b>22</b>
2.1. <i>Revisão Bibliográfica.....</i>	23
2.1.1. <i>Emulsões .....</i>	23
2.1.2. <i>Emulsões tipo Pickering.....</i>	24
2.1.3. <i>Processos de produção de emulsões Pickering e seus desafios .....</i>	26
2.1.4. <i>Partículas de grau alimentício para estabilização de emulsões.....</i>	28
2.1.5. <i>Emulsões Pickering e a digestão lipídica .....</i>	29
<b>CAPÍTULO III.....</b>	<b>37</b>
<i>Highlights.....</i>	38
<i>Abstract .....</i>	38
<i>Graphical Abstract.....</i>	39
3.1. <i>Introduction.....</i>	39
3.2. <i>Material and Methods .....</i>	41
3.2.1. <i>Material.....</i>	41
3.2.2. <i>Methods .....</i>	41
3.2.2.1. <i>Preparation and characterization of chitosan particles .....</i>	41
3.2.2.2. <i>Preparation of Pickering emulsions .....</i>	42
3.2.2.3. <i>Characterization of Pickering emulsions.....</i>	43
3.3. <i>Results and discussion.....</i>	45
3.3.1. <i>Properties of chitosan particles .....</i>	45
3.3.2. <i>Properties of the Pickering emulsions.....</i>	47
3.4. <i>Conclusion .....</i>	55
<i>Acknowledgments.....</i>	56
<i>References .....</i>	56
<b>CAPÍTULO IV .....</b>	<b>62</b>
<i>Highlights.....</i>	63
<i>Abstract .....</i>	63
<i>Graphical Abstract.....</i>	64

4.1. Introduction.....	64
4.2. Material and Methods .....	66
4.2.1. Material.....	66
4.2.2.2. Characterization of CNFs.....	67
4.2.2.4. Characterization of Pickering emulsions.....	70
4.3. Results and discussion.....	71
4.3.1. Emulsification process influencing properties of CNFs particles .....	71
4.3.2. Contact angle and interfacial tension between oil-water phases .....	75
4.4. Conclusion .....	87
Acknowledgments.....	88
References .....	88
<b>CAPÍTULO V.....</b>	<b>94</b>
Abstract.....	95
5.1. Introduction.....	95
5.2. Material and Methods .....	97
5.2.1. Material.....	97
5.2.2. Methods .....	98
5.2.2.1. Particles preparation.....	98
5.2.2.2. Preparation of Pickering emulsions .....	99
5.2.2.3. <i>In vitro</i> digestion of the emulsions and free fatty acids release.....	99
5.2.2.4. Characterization of Pickering emulsions.....	100
5.3. Results and discussion.....	101
5.3.1. Characterizing Pickering emulsions in gastric step .....	101
5.3.2. Characterizing Pickering emulsions in intestinal step.....	106
5.4. Conclusion .....	110
Acknowledgments.....	110
References .....	110
<b>CAPÍTULO VI.....</b>	<b>115</b>
Abstract.....	116
6.1. Introduction.....	116
6.2. Material and Methods .....	118
6.2.1. Material.....	118
6.2.2. Glass microfluidic device .....	119
6.2.3. Physical properties of the phases and emulsion characterization.....	120
6.3. Results and discussion.....	120
6.3.1. Events inside the microchannel .....	120
6.3.2. Pickering emulsions outside the microchannel.....	122

<i>6.4. Conclusion .....</i>	<i>127</i>
<i>Acknowledgments.....</i>	<i>127</i>
<i>References .....</i>	<i>128</i>
<b><i>CAPÍTULO VII.....</i></b>	<b><i>135</i></b>
<i>7.1. Discussão Geral.....</i>	<i>136</i>
<b><i>CAPÍTULO VIII.....</i></b>	<b><i>139</i></b>
<i>8.1. Conclusão Geral .....</i>	<i>140</i>
<b><i>REFERÊNCIAS.....</i></b>	<b><i>142</i></b>
<b><i>ANEXOS.....</i></b>	<b><i>160</i></b>

# CAPÍTULO I

---

- INTRODUÇÃO GERAL

- OBJETIVOS

- ESTRUTURAÇÃO DA TESE

## 1.1. Introdução Geral

Alguns sistemas alimentícios possuem material particulado que se acumula na interface entre líquidos imiscíveis, como óleo e água, contribuindo para a estabilização coloidal de emulsões. As partículas envolvidas na estruturação desses sistemas possuem uma gama de tamanhos que varia desde alguns nanômetros até dezenas de micrômetros. Um exemplo importante deste tipo de sistema alimentício são as margarinas (emulsões A/O estabilizadas por cristais de triglicerídeos). Gotas de emulsão revestidas e estabilizadas por uma camada de partículas sólidas adsorvidas na interface óleo/água são denominadas tipo Pickering. Emulsões óleo em água (O/A) ou água em óleo (A/O) podem ser produzidas dependendo apenas da afinidade relativa das partículas por ambas as fases (mais hidrofílica ou mais hidrofóbica) (Dickinson, 2006).

A demanda de um mercado consumidor mais consciente da necessidade de cuidar da saúde e as expectativas da indústria alimentícia de aumentar investimentos na utilização de compostos naturais em substituição aos aditivos sintéticos impulsionam o desenvolvimento e a utilização de produtos seguros e saudáveis para o consumo humano. As emulsões Pickering podem ser uma alternativa potencial para substituição de emulsificantes sintéticos dependendo da natureza das partículas usadas como estabilizantes eliminando alguns efeitos alergênicos e citotoxicidade. Além disso, a deposição de determinadas partículas na interface das gotas contribui para o controle da digestibilidade lipídica, sendo estas emulsões adequadas no desenvolvimento de produtos que promovem a saciedade e combatem a obesidade (Chevalier & Bolzinger, 2013; Tzoumaki, Moschakis, Scholten, & Biliaderis, 2013).

As emulsões alimentares estão propensas a problemas de desestabilização física, química e microbiológica desde sua produção, armazenamento até o consumo final. A coalescência é um tipo de desestabilização física muito comum que compromete a aceitabilidade do mercado consumidor pelo produto emulsionado. Uma das maiores vantagens na utilização de emulsões Pickering é a forte barreira física e energética criada pelas partículas sólidas adsorvidas na interface das gotas que impede a coalescência das gotas de maneira mais efetiva que os emulsificantes convencionais, eliminando problemas com a aparência das emulsões alimentícias (Lopetinsky, Masliyah, & Xu, 2006; Dickinson, 2010; Kaz et al., 2012).

O diâmetro da partícula é um parâmetro relevante ao determinar a capacidade das partículas sólidas de atuarem como estabilizantes em emulsões. Alguns autores consideram que as partículas devem ser menores pelo menos uma ordem de magnitude do tamanho das gotas de emulsão (Binks & Lumsdon, 2001; Dickinson, 2012). Em emulsões alimentícias as gotas dispersas possuem tipicamente tamanho micrométrico, portanto, partículas sólidas



nanométricas são ideais na estabilização destas gotas. Uma limitação da utilização de partículas nanométricas é a aceitabilidade do seu uso em alimentos devido aos potenciais riscos da sua permanência dentro do corpo humano. Uma conclusão quanto à aceitabilidade e riscos irá depender de uma combinação de fatores, incluindo a composição, morfologia e principalmente a digestibilidade da partícula (Berton-Carabin & Schroën, 2015; Borel & Sabliov, 2014).

Até o momento, um trabalho considerável foi feito para compreender os fenômenos de estabilização de emulsões tipo Pickering, mas pouco tem sido feito para aplicar esses conhecimentos na potencialização do desempenho funcional dessas emulsões. Os desafios são muitos e começam com a escolha dos ingredientes, como por exemplo, a obtenção de nanopartículas por métodos livres de traços de contaminação química e a utilização de partículas proteicas, que provocam dúvidas em relação à obtenção de “verdadeiras” emulsões tipo Pickering (Berton-Carabin & Schroën, 2015). Além disso, deve-se considerar os efeitos dos métodos mecânicos de homogeneização utilizados, uma vez que a cinética de adsorção das partículas é mais lenta comparado aos surfactantes convencionais devido ao maior tamanho das partículas sólidas. Assim, o transporte de massa e a adsorção de partículas na interface podem não ser suficientemente rápidos para estabilizar as menores gotas formadas durante a homogeneização levando a geração de gotas de emulsão relativamente grandes e/ou com alta polidispersidade (Dickinson, 2010).

Com o exposto, tanto a escolha das partículas quanto a escolha dos métodos de emulsificação caracterizam-se como um grande desafio científico para aplicação de emulsões Pickering em sistemas alimentícios. Neste trabalho, partículas de quitosana e celulose (fibras e cristais) foram utilizadas como estabilizantes de emulsões óleo em água produzidas por técnicas de alta (ultrassom e homogeneizador a alta pressão) e baixa energia (técnicas microfluídicas). As características das partículas e emulsões foram avaliadas frente às variáveis de processo de emulsificação e condições gastrointestinais.

## **1.2. Objetivos**

### **1.2.1. Geral**

Utilizar nanopartículas de grau alimentício na produção de emulsões tipo Pickering obtidas por meio de processos de homogeneização de alta e baixa energia, bem como avaliar a estabilidade destes sistemas frente às variáveis de processo de emulsificação e condições gastrointestinais.

### 1.2.2. Específicos

(i) Produzir e caracterizar nanopartículas sólidas de quitosana e verificar os efeitos da variação da potência aplicada e tempo de processamento na estabilidade destas partículas e das emulsões produzidas em ultrassom de alta intensidade.

(ii) Avaliar o efeito das técnicas de alta energia na estabilidade das nanofibras de celulose obtidas da casca da banana e das emulsões produzidas em ultrassom e homogeneizador a alta pressão.

(iii) Avaliar a microestrutura e estabilidade das emulsões tipo Pickering frente a condições gastrointestinais.

(iv) Produzir emulsões estabilizadas por nanocristais de celulose usando dispositivos microcapilares de vidro e estudar eventos discretos de estabilização e coalescência de gotas em função da concentração de partículas e condições do processo.

### 1.3. Estruturação da tese

O projeto de pesquisa foi desenvolvido em etapas que estão apresentadas na forma de capítulos. Os Capítulos I e II abordam os temas gerais e os objetivos do estudo e uma breve revisão bibliográfica que contextualiza pesquisas atuais sobre a produção de emulsões Pickering relacionando-as com os objetivos pretendidos neste trabalho. O Capítulo III contempla um artigo que avaliou os efeitos da variação das condições de processo do ultrassom de alta intensidade na estabilidade das partículas de quitosana e das emulsões estabilizadas por essas partículas. O Capítulo IV apresenta os resultados de estabilidade e propriedades físico-químicas de emulsões produzidas em ultrassom e homogeneizador a alta pressão e estabilizadas por nanofibras de celulose obtidas da casca da banana. O Capítulo V contempla um artigo que avaliou a estabilidade dessas emulsões Pickering frente as condições gastrointestinais. No Capítulo VI são apresentados os dados experimentais sobre a produção de emulsões Pickering estabilizadas por nanocristais de celulose e obtidas por técnica de microfluídica utilizando dispositivos capilares de vidro. O Capítulo VII traz uma discussão geral de todos os resultados experimentais apresentados, destacando os dados mais relevantes. Por fim, no Capítulo VIII as conclusões gerais do projeto de pesquisa são apresentadas de forma sucinta.

**REFERÊNCIAS BIBLIOGRÁFICAS**

- Berton-Carabin, C. C., & Schroën, K. (2015). Pickering emulsions for food applications: Background, trends, and challenges. *Annual Review of Food Science and Technology*, 6, 263-297.
- Binks, B. P. (2002). Particles as surfactants—similarities and differences. *Current Opinion in Colloid & Interface Science*, 7(1–2), 21-41.
- Borel, T., & Sabliov, C. M. (2014). Nanodelivery of Bioactive components for food applications: Types of delivery systems, properties, and their effect on ADME profiles and toxicity of nanoparticles. *Annual Review of Food Science and Technology*, 5(1), 197-213.
- Dickinson, E. (2006). Interfacial Particles in Food Emulsions and Foams, Colloidal Particles at Liquid Interfaces. Ed. Bernard P. Binks and Tommy S. Horozov. 1st ed. Cambridge: Cambridge University Press, 298-327.
- Dickinson, E. (2010). Food emulsions and foams: Stabilization by particles. *Current Opinion in Colloid & Interface Science*, 15 (1–2), 40-49.
- Dickinson, E. (2012). Use of nanoparticles and microparticles in the formation and stabilization of food emulsions. *Trends in Food Science & Technology*, 24 (1), 4-12.
- Chevalier, Y., & Bolzinger, M.-A. (2013). Emulsions stabilized with solid nanoparticles: Pickering emulsions. *Colloids and Surfaces A: Physicochemical and Engineering Aspects*, 439, 23-34.
- Kaz, D. M. et al. (2012). Physical ageing of the contact line on colloidal particles at liquid interfaces. *Nat Mater*, 11 (2), 138-142.
- Lopetinsky, R. J. G., Masliyah, J. H., & Xu, Z. (2006). Solids-stabilized emulsions: A review. In: (Ed.). *Colloidal Particles at Liquid Interfaces*, 186-224.
- Tzoumaki, M. V., Moschakis, T., Scholten, E., & Biliaderis, C. G. (2013). In vitro lipid digestion of chitin nanocrystal stabilized o/w emulsions. *Food and Function*, 4(1), 121-129.

## **CAPÍTULO II**

---

- REVISÃO BIBLIOGRÁFICA

## 2.1. Revisão Bibliográfica

### 2.1.1. Emulsões

Emulsão é a mistura de dois líquidos imiscíveis, em que um líquido é disperso na forma de pequenas gotas em outro líquido que constitui a fase contínua. As emulsões podem ser classificadas de acordo com a distribuição relativa das diferentes fases, sendo os tipos mais comuns as emulsões óleo em água (O/A) e água em óleo (A/O). O processo de emulsificação inclui duas etapas, onde primeiramente uma alta tensão de cisalhamento leva à deformação da gota, aumentando sua área superficial específica até o seu rompimento e em seguida, a nova interface é estabilizada por um emulsificante (Perrier-Cornet, Marie & Gervais, 2005).

Devido à sua afinidade combinada para ambos os meios, polar e apolar, os emulsificantes são agentes com atividade superficial ou tensoativos que tem como principal função atuar na interface da gota, formando camadas protetoras que diminuem a tensão interfacial entre a fase dispersa (gotas) e a fase contínua da emulsão, impedindo a agregação da fase dispersa (McClements, Decker & Weiss, 2007). A área interfacial total de uma emulsão ( $\Delta A$ ) é muito grande devido à quebra da fase dispersa em pequenas gotas. Como a área interfacial está associada com a tensão interfacial ( $\gamma$ ), sistemas emulsionados são termodinamicamente instáveis, pois apresentam uma quantidade de energia livre ( $\Delta G_f$ ) de formação da emulsão sempre positiva, como demonstrado na análise da equação 2.1, derivada da Equação Fundamental da Termodinâmica (Claesson, Blomberg & Poptoshev, 2003; Anton, Benoit & Saulnier, 2008).

$$\Delta G_f = \gamma \Delta A - T \Delta S_f \quad (2.1)$$

sendo,  $\gamma$ = tensão interfacial ( $\text{N.m}^{-1}$ );  $\Delta A$ = ganho de área superficial após a emulsificação ( $\text{m}^2$ );  $T$ = temperatura absoluta (K);  $\Delta S_f$ = aumento da entropia devido ao processo de emulsificação ( $\text{J.K}^{-1}$ ) e  $\Delta G_f$ = variação na Energia Livre de Gibbs do sistema (J).

Menores valores de  $\gamma$  podem ser obtidos com adição de emulsificantes levando a uma diminuição da energia livre da emulsão e tornando-a assim mais cineticamente estável (McClements, 2005). Existem duas grandes classes de emulsificantes: os de baixa massa molecular que podem ter origem natural ou sintética (monoglicerídeos, polissorbato, lecitina, dentre outros) e os macromoleculares (usualmente proteínas, principalmente do leite, da soja e ovo) (Dickinson, 1992). Além disso, a estabilidade das emulsões pode ser aumentada pela adição de espessantes, que são agentes que modificam a viscosidade ou gelificam a fase

contínua. Os principais espessantes utilizados são os polissacarídeos, como as gomas carragena, xantana, gelana e jataí (McClements, Decker & Weiss, 2007).

Apesar do abaixamento da tensão interfacial com a adição de emulsificante em emulsões, o termo entálpico associado à tensão interfacial entre os líquidos permanece positivo, favorecendo a separação das fases. É por isso que as emulsões são definidas como metaestáveis, com um período de vida útil “razoável” até que ocorra a desestabilização física. A espessura da camada interfacial é aproximadamente  $\leq 1$  nm (Atkinson et al., 1995; Dickinson, 2009; Singh, 2011) e a carga superficial (quantidade adsorvida do emulsificante na interface) é geralmente  $\sim 1\text{-}2$  mg.m<sup>-2</sup> para os emulsificantes de baixa massa molecular e  $2\text{-}3$  mg.m<sup>-2</sup> para as proteínas (Bos & Van Vliet, 2001). A camada interfacial formada pelos emulsificantes determina as interações entre as gotas, sendo que interações repulsivas irão contribuir para a estabilidade da emulsão. A repulsão pode ser proveniente de interações eletrostáticas (emulsificantes carregados) e/ou a partir de forças estéricas (impedimento físico causado pelas moléculas interfaciais que impedem a aproximação entre as gotas) (McClements, 2005).

### 2.1.2. Emulsões tipo Pickering

Além dos espessantes e emulsificantes convencionais (emulsificantes de baixa massa molecular e macromoléculas), partículas sólidas podem ser utilizadas para estabilizar emulsões (Figura 2.1a). Este tipo de emulsão é comumente chamado de "emulsão tipo Pickering". Diferente do mecanismo de estabilização por emulsificantes convencionais, as partículas sólidas não precisam ser anfífilas e é a sua solubilidade parcial com o óleo e a água que promove a forte adsorção (quase irreversível) destas partículas na interface da gota (Berton-Carabin & Schroën, 2015; Pickering, 1907). A posição da partícula sólida na interface óleo-água depende da sua afinidade relativa por ambas as fases, podendo ser caracterizada por um ângulo de contato ( $\theta$ ). As partículas que são preferencialmente hidrofílicas e adequadas para a formação de emulsões óleo em água (O/A) possuem  $\theta$  menor que  $90^\circ$  (Figura 2.1b), enquanto que as partículas que são preferencialmente hidrofóbicas são adequadas para formação de emulsões água em óleo (A/O) e tem  $\theta$  maior que  $90^\circ$  (Aveyard, Binks, & Clint, 2003; Binks, 2002; Zhu, Jiang, Liu, Cui, & Binks, 2015).

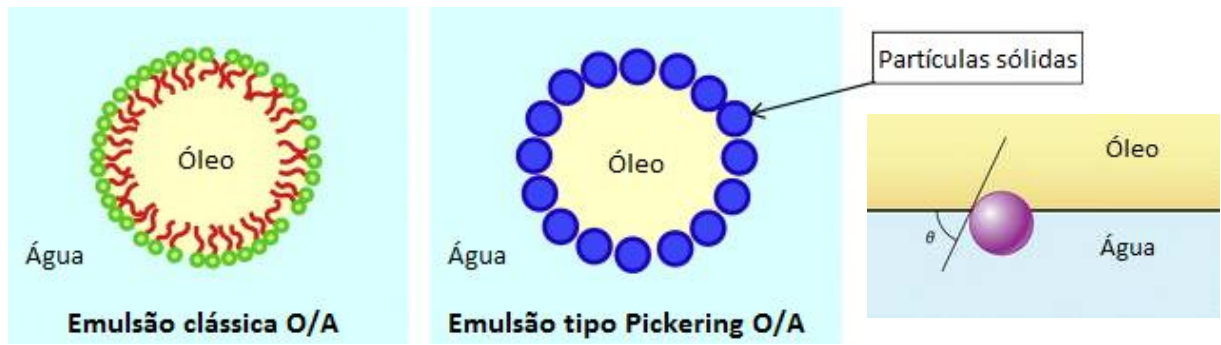


**Figura 2.1.** (a) Representação de emulsões óleo em água (O/A) estabilizadas por emulsificantes convencionais e partículas sólidas. (b) Posição de uma partícula sólida na interface da gota com um ângulo de contato menor que 90° correspondendo à formação de uma emulsão O/A.

As propriedades de estabilização das partículas sólidas foram descobertas por Ramsden e Pickering no início do século passado, mas o interesse da comunidade científica cresceu substancialmente somente nesta última década (Berton-Carabin & Schroën, 2015). A adsorção das partículas sólidas nas gotas forma uma camada interfacial que impede estericamente a sua aproximação. Além da barreira mecânica, existe uma barreira energética (energia de dessorção) associada às forças atrativas laterais entre partículas e as interações entre as partículas e as fases líquidas. Esta interação resulta na deformação da interface do líquido em volta das partículas e contribui ainda mais para a estabilidade quase intransponível da camada interfacial contra a coalescência das gotas e amadurecimento de Ostwald. A resistência da emulsão O/A à cremação aumenta consideravelmente quando a massa de partículas adsorvida por gota é suficiente para aumentar a densidade da gota diminuindo a diferença de densidade entre as fases (Rayner, Sjöö, Timgren, & Dejmek, 2012; Tcholakova, Denkov, & Lips, 2008).

A alta energia de dessorção também indica que ao contrário dos emulsionantes convencionais, que podem se locomover e espontaneamente adsorver na interface das gotas, a adsorção das partículas sólidas não é espontânea. Para estabilizar a interface da gota, a energia de adsorção das partículas deve ser muito maior que a energia cinética de uma partícula que se aproxima da interface da gota. A energia ( $\Delta E$ ) necessária para remover uma partícula adsorvida na interface depende do diâmetro da partícula e do ângulo de contato (relacionado com a solubilidade parcial das partículas com as fases) e pode ser determinada através da Equação 2.2 (Kaz et al., 2012; Salari et al., 2014).

$$\Delta E = \pi r^2 \gamma (1 - |\cos \theta|)^2 \quad (2.2)$$

sendo que,  $r$  = raio da partícula (m) e  $\gamma$  = tensão interfacial entre as fases (N.m<sup>-1</sup>).

Embora as considerações teóricas indiquem que partículas maiores possuam maior energia de dessorção, estudos mostram que a estabilidade é inversamente proporcional ao tamanho das partículas, pois menores partículas empacotam-se mais facilmente na interface da gota, formando uma camada mais homogênea que favorece as ligações interpartículas. Por exemplo, uma partícula de 10 nm e com um ângulo de contato de 90° com uma interface plana possui uma energia de dessorção de 103 kT. Esta magnitude energética é muito maior do que a energia de dessorção de emulsificantes convencionais, já que estes estão em estado de equilíbrio dinâmico constantemente sujeitos à adsorção e dessorção na interface da gota (Dickinson, 2012; Chevalier & Bolzinger, 2013; Berton-Carabin & Schroën, 2015). Além disso, o estudo feito por Berton-Carabin & Schroën (2015) mostrou que o efeito da variação do diâmetro da partícula na variação da energia de dessorção é maior comparado com o ângulo de contato, fazendo do diâmetro da partícula um parâmetro relevante ao determinar a capacidade das partículas sólidas de atuarem como estabilizantes de emulsões.

Em estudos iniciais, alguns autores consideravam que as partículas sólidas utilizadas na produção de emulsões tipo Pickering deveriam ser menores pelo menos uma ordem de magnitude do tamanho das gotas da emulsão (Binks & Lumsdon, 2001; Dickinson, 2012). Atualmente estudos relacionados com emulsões alimentícias relatam que partículas sólidas com tamanho (medido antes do processo de emulsificação) da mesma ordem de grandeza das gotas de óleo foram efetivas na estabilização dessas emulsões. A estabilidade das emulsões foi alcançada devido a uma quebra das partículas sólidas durante o processo de emulsificação (homogeneizador à alta pressão) aumentando a sua polidispersidade. Desta forma, as menores partículas se adsorveram na interface atuando como estabilizantes, enquanto que as maiores partículas que não foram adsorvidas na interface, formam uma rede na fase contínua promovida por interações hidrofóbicas (Yusoff & Murray, 2011; Gould, Vieira & Wolf, 2013; Kurukji et al., 2013).

### **2.1.3. Processos de produção de emulsões Pickering e seus desafios**

O processo de emulsificação pode ser uma operação simples de mistura realizada por dispositivos de alta pressão, ultrassônicos, tipo rotor-estator ou sistemas de membrana (Urban et al., 2006). Nos dispositivos tipo rotor-estator as principais forças para a formação e redução do tamanho de gotas são o impacto mecânico do fluido acelerado contra a parede e a tensão de cisalhamento no espaço entre o rotor e o estator, que é gerada pela rápida rotação do motor. Nestes dispositivos as gotas da emulsão são altamente polidispersas e não é possível alcançar tamanhos de gotas abaixo de 1 µm (Urban et al., 2006). Na homogeneização por ultrassom a redução do tamanho de gotas é realizada pela aplicação de micro-cisalhamento intenso,



resultante do colapso de microbolhas formadas durante a cavitação acústica fornecida através da sonda de ultrassom (Jafari, Assadpoor, He, & Bhandari, 2008). Neste processo, a potência do equipamento de ultrassom e o tempo de processamento podem ser manipulados de forma a obter emulsões com diferentes diâmetros médios de gotas (Silva, Gomes, Hubinger, Cunha, & Meireles, 2015).

A maioria das emulsões tipo Pickering contendo compostos GRAS foram produzidas por técnicas de homogeneização de baixa eficiência (dispositivo rotor-estator) resultando em alta polidispersidade e gotas de emulsão relativamente grandes (centenas de micrômetros) podendo desestabilizar por cremação ou sedimentação. Os fatores que limitam a diminuição do diâmetro das gotas são o tamanho das partículas sólidas e as técnicas de emulsificação (Berton-Carabin & Schroën, 2015). Em emulsões produzidas com emulsificantes convencionais, o tamanho das gotas pode ser reduzido consideravelmente usando técnicas de alto cisalhamento. Na literatura, homogeneizadores de alta pressão (Gupta & Rousseau, 2012; Kurukji, Pichot, Spyropoulos, & Norton, 2013; Luo et al., 2011), ultrassom (Liu & Tang, 2013; Tzoumaki, Moschakis, Kiosseoglou, & Biliaderis, 2011) e microfluidizadores (Gao et al., 2014; Liu & Tang, 2013) também têm sido relatados como processos que alcançam menores tamanhos de gotas em emulsões tipo Pickering.

Estudos alternativos sobre a adequação de técnicas de emulsificação de baixo consumo de energia e alta eficiência para emulsões Pickering ainda são escassos. A emulsificação em dispositivos de microfluídica demanda baixa energia para a produção de gotas de diâmetro reduzido e com distribuição monodispersa de tamanho de gotas. A principal vantagem dessa técnica é a geração individual das gotas devido ao valor extremamente reduzido de número de Reynolds. O tamanho das gotas pode ser controlado com precisão através do ajuste da geometria dos dispositivos de microfluídica, das propriedades das duas fases líquidas (viscosidade e tensão interfacial) e dos parâmetros operacionais (vazão/velocidade de entrada das duas fases) (Shah et al., 2008; C.-X. Zhao & Middelberg, 2011; Zhao, 2013; Zhou et al., 2013). Partículas de sílica em tamanho nanométrico são bastante usadas no estudo da hidrodinâmica de estabilização de emulsões por partículas (Priest, Reid, & Whitby, 2011; Xu, Nakajima, & Binks, 2005; Yuan, Cayre, Manga, Williams, & Biggs, 2010), porém nenhum estudo foi realizado até o momento sobre a fluidodinâmica de formação de gotas e estabilidade de emulsões produzidas em dispositivos de microfluídica estabilizadas com partículas sólidas de grau alimentício.

#### 2.1.4. Partículas de grau alimentício para estabilização de emulsões

Emulsões tipo Pickering podem ser estabilizadas por partículas inorgânicas ou orgânicas, como por exemplo, sílica, carbonato de cálcio, microgéis, entre outras. No entanto, materiais inorgânicos ou sintéticos possuem aplicabilidade limitada na indústria de alimentos e farmacêutica por questões legais. Portanto, o desenvolvimento de sistemas a base de produtos naturais tem sido alvo de investigação em estabilizantes tipo Pickering. Nanocristais de celulose (Wen, Yuan, Liang, & Vriesekoop, 2014), partículas de amido modificado (Song et al., 2015), zeína (de Folter, Van Ruijven, & Velikov, 2012), proteína de soja (Liu & Tang, 2013), proteína de ervilha (Liang & Tang, 2014) e nanocristais de quitina (Tzoumaki et al., 2013) são alguns dos emulsificantes estudados para aplicações em alimentos, pois são seguros e aceitos como ingredientes alimentares.

A quitina é o segundo biopolímero mais abundante encontrado na natureza, extraído do exoesqueleto de camarão e outros crustáceos. A partir da reação de hidrólise básica da quitina é sintetizada a quitosana. A quitosana é um polímero constituído por unidades de  $\beta$ - (1,4)-2-amino-2-desóxi-D-glicopirano, que tem como característica marcante ser um dos poucos biopolímeros naturais carregados positivamente existentes no mundo. Além disso, é barato, comercialmente disponível e amplamente utilizado em aplicações alimentares para revestimento e encapsulação. A protonação dos grupos amino livres da quitosana em soluções ácidas torna-a solúvel em água e fortemente catiônica. As aminas catiônicas ( $NH_3^+$ ) e os grupos hidroxila ( $OH^-$ ) ao longo da cadeia conferem à quitosana baixa atividade superficial e, portanto, baixa capacidade emulsificante. Recentemente foi demonstrado o potencial uso de auto-agregados de quitosana na formação de emulsões Pickering O/A, sem a necessidade de modificação química (Liu, Wang, Zou, Wei, & Tong, 2012). Partículas de quitosana obtidas a partir da quitosana desprotonada mostraram ser eficazes como emulsificantes na formação de emulsões que respondem a alterações de pH (pH-responsive) (Ho et al., 2016), porém são poucos os estudos sobre as propriedades e estabilidade destas emulsões frente a condições de “stress” ambiental, tais como, presença de solutos e condições gastrointestinais.

A celulose é o biopolímero mais abundante e um excelente candidato para a estabilização interfacial entre líquidos imiscíveis, por causa de sua capacidade de renovação, sustentabilidade, biodegradabilidade e não toxicidade (Kalashnikova, Bizot, Cathala, & Capron, 2011; Salas, Nypelö, Rodriguez-Abreu, Carrillo, & Rojas, 2014; Xhanari, Syverud, Chinga-Carrasco, Paso, & Stenius, 2011). Os monômeros da glicose na celulose são esterificados por ligações do tipo  $\beta$ (1-4)-glicosídicas responsáveis pela formação da cadeia de

celulose ser essencialmente linear. Estas cadeias formam feixes paralelos (microfibrilas) que se agregam para formar fibras de celulose. Essas microfibrilas são o menor agregado de cadeias de celulose, uma vez que são formados por arranjos de cristais de celulose separados por domínios amorfos. O tamanho da microfibrila é dado em função do grau de polimerização das cadeias de celulose e apresentam forte dependência com sua origem (Zhao et al., 2007). Embora haja vários métodos de produzir nanopartículas de celulose, o seu isolamento geralmente envolve três passos: (1) pré-tratamento da matéria-prima, (2) hidrólise parcial e (3) desintegração mecânica (Sun, Sun, Fowler, & Baird, 2004). As nanofibrilas de celulose são obtidas com tratamentos mecânicos como cisalhamento e pressão (Stenstad, Andresen, Tanem, & Stenius, 2008), apresentando dimensões que podem variar de 20 a 40 nm de diâmetro a vários micrômetros de comprimento (Svagan, Azizi Samir, & Berglund, 2007). Tratamentos químicos ou enzimáticos são aplicados com a finalidade de separar as fibras, facilitando o processo mecânico de fibrilação (Henriksson, Henriksson, Berglund, & Lindström, 2007).

Geralmente, a hidrólise ácida é empregada para isolar os domínios cristalinos de celulose. Os íons de hidrogênio, na hidrólise ácida podem penetrar entre as cadeias de celulose nas regiões amorfas, promover a clivagem hidrolítica de ligações glicosídicas e isolar as estruturas cristalinas no formato de agulhas, designadas nanocristais de celulose (Beck-Candanedo, Roman, & Gray, 2005; Kvien, Tanem, & Oksman, 2005). O isolamento de cristais de celulose foi feito primeiramente com ácido sulfúrico (Ranby, 1951) e, posteriormente, foi descoberto que a obtenção de cristais também podia ser alcançada com ácido clorídrico combinado com desintegração mecânica. Nessas condições, geralmente são obtidos nanocristais cujas dimensões estão entre 100 a 400 nm de comprimento e diâmetros inferiores a 10 nm (Alemdar & Sain, 2008), sendo esta a celulose cristalina hidrolisada comercializada hoje nas indústrias alimentícia e farmacêutica.

### **2.1.5. Emulsões Pickering e a digestão lipídica**

A concepção de sistemas coloidais como controladores da taxa de digestão de lipídeos no interior do trato gastrointestinal tem recebido grande atenção em estudos recentes (Majeed et al., 2016; Tikekar, Pan, & Nitin, 2013; Tzoumaki et al., 2013). Inibir ou retardar a digestão do lipídeo através da modificação adequada da interface de emulsões O/A é considerado um meio eficaz de reduzir o apetite e promover a saciedade. Portanto, estes sistemas podem auxiliar no desenvolvimento de produtos alimentícios que contribuam no combate de doenças crônicas, como a obesidade, câncer, diabetes, hipertensão e problemas cardíacos (Maljaars, Peters, Mela, & Masclee, 2008; Renzaho & Mellor, 2010; Tzoumaki et al., 2013).

Na digestão, as emulsões estabilizadas com emulsificantes convencionais são expostas a um meio altamente ácido (pH 1-3) no estômago, no qual também estão presentes as proteases e a lipase gástrica responsáveis pela hidrólise enzimática, além dos fosfolípidos, mucinas e proteínas que são substâncias tensoativas. Estas substâncias competem e podem substituir os emulsificantes presentes na superfície das gotas de óleo, alterando a composição interfacial e suas propriedades. No intestino delgado, as emulsões também são expostas ao contato com substâncias com atividade de superfície que também podem competir e substituir os tensoativos presentes na superfície das gotas. A hidrólise lipídica envolve as etapas de adsorção do sal biliar, para a posterior adsorção da lipase pancreática na interface das gotas de óleo, permitindo assim que a enzima hidrolise os triacilgliceróis em ácidos graxos livres (Wilde & Chu, 2011). Os ácidos graxos são incorporados nas micelas e vesículas de sais biliares/fosfolípidos e transportados para posterior absorção pelas células epiteliais (Hur, Decker, & McClements, 2009).

Embora haja uma série de pesquisas sobre emulsões estabilizadas por partículas sólidas existem poucos estudos que investigam o rompimento da camada interfacial estabilizada por partículas nas condições gastrointestinais e o potencial das emulsões Pickering em inibir ou retardar a digestão do lípido. Tzoumaki et al. (2013) compararam a cinética da digestão lipídica de emulsões O/A estabilizadas por nanocristais de quitina e por um emulsificante convencional de proteína de leite, WPI. A hidrólise lipídica de emulsões estabilizadas com os nanocristais de quitina foi significativamente mais lenta e a concentração de lípidos liberados foi muito mais baixa comparado com as emulsões estabilizadas pelo emulsificante convencional. Além disso as emulsões estabilizadas com os nanocristais de quitina foram mais estáveis à coalescência do que as emulsões de WPI, que exibiram um aumento significativo no tamanho da gota durante a digestão lipídica.

Neste contexto, o estudo de emulsões Pickering estabilizadas com partículas sólidas de quitosana e celulose com digestibilidade lipídica controlada se faz necessário, já que a busca pelo desenvolvimento de produtos de baixa caloria que promovem a saciedade e combatem a obesidade ainda é um objetivo a ser atingido pela indústria de alimentos.

**REFERÊNCIAS BIBLIOGRÁFICAS**

- Alemдар, A., & Sain, M. (2008). Isolation and characterization of nanofibers from agricultural residues – Wheat straw and soy hulls. *Bioresource Technology*, 99(6), 1664-1671.
- Anton, N., Benoit, J.-P., & Saulnier, P. (2008). Design and production of nanoparticles formulated from nano-emulsion templates-A review. *Journal of Controlled Release*, 128(3), 185-199.
- Atkinson, P. J. et al. (1995). Neutron reflectivity of adsorbed  $\beta$ -casein and  $\beta$ -lactoglobulin at the air/water interface. *Journal of the Chemical Society*, 91(17), 2847-2854.
- Aveyard, R., Binks, B. P., & Clint, J. H. (2003). Emulsions stabilised solely by colloidal particles. *Advances in Colloid and Interface Science*, 100, 503-546.
- Beck-Candanedo, S., Roman, M., & Gray, D. G. (2005). Effect of Reaction Conditions on the Properties and Behavior of Wood Cellulose Nanocrystal Suspensions. *Biomacromolecules*, 6(2), 1048-1054.
- Berton-Carabin, C. C., & Schroën, K. (2015). Pickering emulsions for food applications: Background, trends, and challenges. *Annual Review of Food Science and Technology*, 6, 263-297.
- Binks, B. P. (2002). Particles as surfactants-similarities and differences. *Current Opinion in Colloid & Interface Science*, 7(1-2), 21-41.
- Binks, B. P., & Lumsdon, S. O. (2001). Pickering Emulsions Stabilized by Monodisperse Latex Particles: Effects of Particle Size. *Langmuir*, 17(15), 4540-4547.
- Bos, M. A., & Van Vliet, T. (2001). Interfacial rheological properties of adsorbed protein layers and surfactants: A review. *Advances in Colloid and Interface Science*, 91(3), 437-471.
- Chevalier, Y., & Bolzinger, M.-A. (2013). Emulsions stabilized with solid nanoparticles: Pickering emulsions. *Colloids and Surfaces A: Physicochemical and Engineering Aspects*, 439, 23-34.
- Claesson, P. M. et al. (2003). Surface Forces and Emulsion Stability. In: Friberg, S., Larsson, K., & Sjöblom, J. *Food Emulsions*. Ed. CRC Press, 900.
- de Folter, J. W. J., van Ruijven, M. W. M., & Velikov, K. P. (2012). Oil-in-water Pickering emulsions stabilized by colloidal particles from the water-insoluble protein zein. *Soft Matter*, 8(25), 6807-6815.
- Dickinson, E. (1992). An introduction to food colloids. *Oxford University Press*, 4(1), 26-27.

- Dickinson, E. (2009). Hydrocolloids as emulsifiers and emulsion stabilizers. *Food Hydrocolloids*, 23(6), 1473-1482.
- Dickinson, E. (2012). Use of nanoparticles and microparticles in the formation and stabilization of food emulsions. *Trends in Food Science & Technology*, 24(1), 4-12.
- Gao, Z. M., Yang, X. Q., Wu, N. N., Wang, L. J., Wang, J. M., Guo, J., & Yin, S. W. (2014). Protein- based pickering emulsion and oil gel prepared by complexes of zein colloidal particles and stearate. *Journal of Agricultural and Food Chemistry*, 62(12), 2672-2678.
- Gould, J., Vieira, J., & Wolf, B. Cocoa particles for food emulsion stabilisation. *Food & Function*, 4(9), 1369-1375.
- Gupta, R., & Rousseau, D. (2012). Surface-active solid lipid nanoparticles as Pickering stabilizers for oil-in-water emulsions. *Food & Function*, 3(3), 302-311.
- Henriksson, M., Henriksson, G., Berglund, L. A., & Lindström, T. (2007). An environmentally friendly method for enzyme-assisted preparation of microfibrillated cellulose (MFC) nanofibers. *European Polymer Journal*, 43(8), 3434-3441.
- Ho, K. W., Ooi, C. W., Mwangi, W. W., Leong, W. F., Tey, B. T., & Chan, E. S. (2016). Comparison of self-aggregated chitosan particles prepared with and without ultrasonication pretreatment as Pickering emulsifier. *Food Hydrocolloids*, 52, 827-837.
- Hur, S. J., Decker, E. A., & McClements, D. J. (2009). Influence of initial emulsifier type on microstructural changes occurring in emulsified lipids during in vitro digestion. *Food Chemistry*, 114(1), 253-262.
- Jafari, S. M., Assadpoor, E., He, Y., & Bhandari, B. (2008). Re-coalescence of emulsion droplets during high-energy emulsification. *Food Hydrocolloids*, 22(7), 1191-1202.
- Kalashnikova, I., Bizot, H., Cathala, B., & Capron, I. (2011). New pickering emulsions stabilized by bacterial cellulose nanocrystals. *Langmuir*, 27(12), 7471-7479.
- Kaz, D. M. et al. (2012). Physical ageing of the contact line on colloidal particles at liquid interfaces. *Nat Mater*, 11(2), 138-142.
- Kurukji, D., Pichot, R., Spyropoulos, F., & Norton, I. T. (2013). Interfacial behaviour of sodium stearoyllactylate (SSL) as an oil-in-water pickering emulsion stabiliser. *Journal of Colloid and Interface Science*, 409, 88-97.
- Kvien, I., Tanem, B. S., & Oksman, K. (2005). Characterization of cellulose whiskers and their nanocomposites by atomic force and electron microscopy. *Biomacromolecules*, 6(6), 3160- 3165.

- Liang, H. N., & Tang, C. H. (2014). Pea protein exhibits a novel Pickering stabilization for oil-in-water emulsions at pH 3.0. *LWT - Food Science and Technology*, 58(2), 463-469.
- Liu, F., & Tang, C.-H. (2013). Soy Protein Nanoparticle Aggregates as Pickering Stabilizers for Oil-in-Water Emulsions. *Journal of Agricultural and Food Chemistry*, 61(37), 8888-8898.
- Liu, H., Wang, C., Zou, S., Wei, Z., & Tong, Z. (2012). Simple, reversible emulsion system switched by pH on the basis of chitosan without any hydrophobic modification. *Langmuir*, 28(30), 11017-11024.
- Luo, Z., Murray, B. S., Yusoff, A., Morgan, M. R. A., Povey, M. J. W., & Day, A. J. (2011). Particle-Stabilizing Effects of Flavonoids at the Oil-Water Interface. *Journal of Agricultural and Food Chemistry*, 59(6), 2636-2645.
- Majeed, H., Antoniou, J., Hategekimana, J., Sharif, H. R., Haider, J., Liu, F., . . . Zhong, F. (2016). Influence of carrier oil type, particle size on in vitro lipid digestion and eugenol release in emulsion and nanoemulsions. *Food Hydrocolloids*, 52, 415-422.
- Maljaars, P. W. J., Peters, H. P. F., Mela, D. J., & Masclee, A. A. M. (2008). Ileal brake: A sensible food target for appetite control. A review. *Physiology & Behavior*, 95(3), 271-281.
- McClements, D. J. (2005). Food Emulsions: Principles, Practices, and Techniques. Ed Crc Press. Washington, 632.
- McClements, D. J., Decker, E. A., & Weiss, J. (2007). Emulsion-based delivery systems for lipophilic bioactive components. *Journal of Food Science*, 72(8), R109-R124.
- Perrier-Cornet, J. M., Marie, P., & Gervais, P. (2005). Comparison of emulsification efficiency of protein-stabilized oil-in-water emulsions using jet, high pressure and colloid mill homogenization. *Journal of Food Engineering*, 66(2), 211-217.
- Pickering, S. U. (1907). CXCVI.-Emulsions. *Journal of the Chemical Society, Transactions*, 91(0), 2001-2021.
- Priest, C., Reid, M. D., & Whitby, C. P. (2011). Formation and stability of nanoparticle-stabilised oil-in-water emulsions in a microfluidic chip. *Journal of Colloid and Interface Science*, 363(1), 301-306.
- Ranby, B. G. (1951). Fibrous macromolecular systems. Cellulose and muscle. The colloidal properties of cellulose micelles. *Discussions of the Faraday Society*, 11(0), 158-164.
- Rayner, M., Sjöö, M., Timgren, A., & Dejmek, P. (2012). Quinoa starch granules as stabilizing particles for production of Pickering emulsions. *Faraday Discussions*, 158, 139-155.

- Renzaho, A. M. N., & Mellor, D. (2010). Food security measurement in cultural pluralism: Missing the point or conceptual misunderstanding. *Nutrition*, 26(1), 1-9.
- Salari, J. W. O. et al. (2014) Deformation of the water/oil interface during the adsorption of sterically stabilized particles. *Langmuir*, 30(25), 7327-7333.
- Salas, C., Nypelö, T., Rodriguez-Abreu, C., Carrillo, C., & Rojas, O. J. (2014). Nanocellulose properties and applications in colloids and interfaces. *Current Opinion in Colloid & Interface Science*, 19(5), 383-396.
- Shah, R. K., Shum, H. C., Rowat, A. C., Lee, D., Agresti, J. J., Utada, A. S., . . . Weitz, D. A. (2008). Designer emulsions using microfluidics. *Materials Today*, 11(4), 18-27.
- Silva, E. K., Gomes, M. T. M. S., Hubinger, M. D., Cunha, R. L., & Meireles, M. A. A. (2015). Ultrasound-assisted formation of annatto seed oil emulsions stabilized by biopolymers. *Food Hydrocolloids*, 47, 1-13.
- Singh, H. (2011). Aspects of milk-protein-stabilised emulsions. *Food Hydrocolloids*, 25(8), 1938-1944.
- Song, X., Pei, Y., Qiao, M., Ma, F., Ren, H., & Zhao, Q. (2015). Preparation and characterizations of Pickering emulsions stabilized by hydrophobic starch particles. *Food Hydrocolloids*, 45, 256- 263.
- Stenstad, P., Andresen, M., Tanem, B. S., & Stenius, P. (2008). Chemical surface modifications of microfibrillated cellulose. *Cellulose*, 15(1), 35-45.
- Sun, X. F., Sun, R. C., Fowler, P., & Baird, M. S. (2004). Isolation and characterisation of cellulose obtained by a two-stage treatment with organosolv and cyanamide activated hydrogen peroxide from wheat straw. *Carbohydrate Polymers*, 55(4), 379-391.
- Svagan, A. J., Azizi Samir, M. A. S., & Berglund, L. A. (2007). Biomimetic Polysaccharide Nanocomposites of High Cellulose Content and High Toughness. *Biomacromolecules*, 8(8), 2556-2563.
- Tcholakova, S., Denkov, N. D., & Lips, A. (2008). Comparison of solid particles, globular proteins and surfactants as emulsifiers. *Physical Chemistry Chemical Physics*, 10(12), 1608-1627.
- Tikekar, R. V., Pan, Y., & Nitin, N. (2013). Fate of curcumin encapsulated in silica nanoparticle stabilized Pickering emulsion during storage and simulated digestion. *Food Research International*, 51(1), 370-377.



- Tzoumaki, M. V., Moschakis, T., Kiosseoglou, V., & Biliaderis, C. G. (2011). Oil-in-water emulsions stabilized by chitin nanocrystal particles. *Food Hydrocolloids*, 25(6), 1521-1529.
- Tzoumaki, M. V., Moschakis, T., Scholten, E., & Biliaderis, C. G. (2013). In vitro lipid digestion of chitin nanocrystal stabilized o/w emulsions. *Food and Function*, 4(1), 121-129.
- Urban, K. et al. (2006). Rotor-stator and disc systems for emulsification processes. *Chemical Engineering and Technology*, 29(1), 24-31.
- Wen, C., Yuan, Q., Liang, H., & Vriesekoop, F. (2014). Preparation and stabilization of d-limonene Pickering emulsions by cellulose nanocrystals. *Carbohydrate Polymers*, 112, 695-700.
- Wilde, P. J., & Chu, B. S. (2001). Interfacial & colloidal aspects of lipid digestion. *Advances in Colloid and Interface Science*, 165(1), 14-22.
- Xhanari, K., Syverud, K., Chinga-Carrasco, G., Paso, K., & Stenius, P. (2011). Structure of nanofibrillated cellulose layers at the o/w interface. *Journal of Colloid and Interface Science*, 356(1), 58-62.
- Xu, Q. Y., Nakajima, M., & Binks, B. P. (2005). Preparation of particle-stabilized oil-in-water emulsions with the microchannel emulsification method. *Colloids and Surfaces A: Physicochemical and Engineering Aspects*, 262(1-3), 94-100.
- Yuan, Q., Cayre, O. J., Manga, M., Williams, R. A., & Biggs, S. (2010). Preparation of particle-stabilized emulsions using membrane emulsification. *Soft Matter*, 6(7), 1580-1588.
- Yusoff, A., & Murray, B. S. (2011). Modified starch granules as particle-stabilizers of oil-in-water emulsions. *Food Hydrocolloids*, 25(1), 42-55.
- Zhao, C.-X., & Middelberg, A. P. J. (2011). Two-phase microfluidic flows. *Chemical Engineering Science*, 66(7), 1394-1411.
- Zhao, C. X. (2013). Multiphase flow microfluidics for the production of single or multiple emulsions for drug delivery. *Advanced Drug Delivery Reviews*, 65(11-12), 1420-1446.
- Zhao, H., Kwak, J. H., Conrad Zhang, Z., Brown, H. M., Arey, B. W., & Holladay, J. E. (2007). Studying cellulose fiber structure by SEM, XRD, NMR and acid hydrolysis. *Carbohydrate Polymers*, 68(2), 235-241.
- Zhou, G., Zhao, Y., Hu, J., Shen, L., Liu, W., & Yang, X. (2013). A new drug-loading technique with high efficiency and sustained-releasing ability via the Pickering emulsion

interfacial assembly of temperature/pH-sensitive nanogels. *Reactive and Functional Polymers*, 73(11), 1537-1543.

Zhu, Y., Jiang, J., Liu, K., Cui, Z., & Binks, B. P. (2015). Switchable pickering emulsions stabilized by silica nanoparticles hydrophobized in situ with a conventional cationic surfactant. *Langmuir*, 31(11), 3301-3307.

## CAPÍTULO III

---

One-step ultrasound producing O/W emulsions stabilized by chitosan particles

*Published in Food Research International, v. 107, 717-725, 2018*

## **One-step ultrasound producing O/W emulsions stabilized by chitosan particles**

<sup>1</sup>Ana Letícia Rodrigues Costa, <sup>1</sup>Andresa Gomes, <sup>1</sup>Rosiane Lopes Cunha

<sup>1</sup>Department of Food Engineering, Faculty of Food Engineering, University of Campinas (UNICAMP), 13083-862 Campinas, SP, Brazil

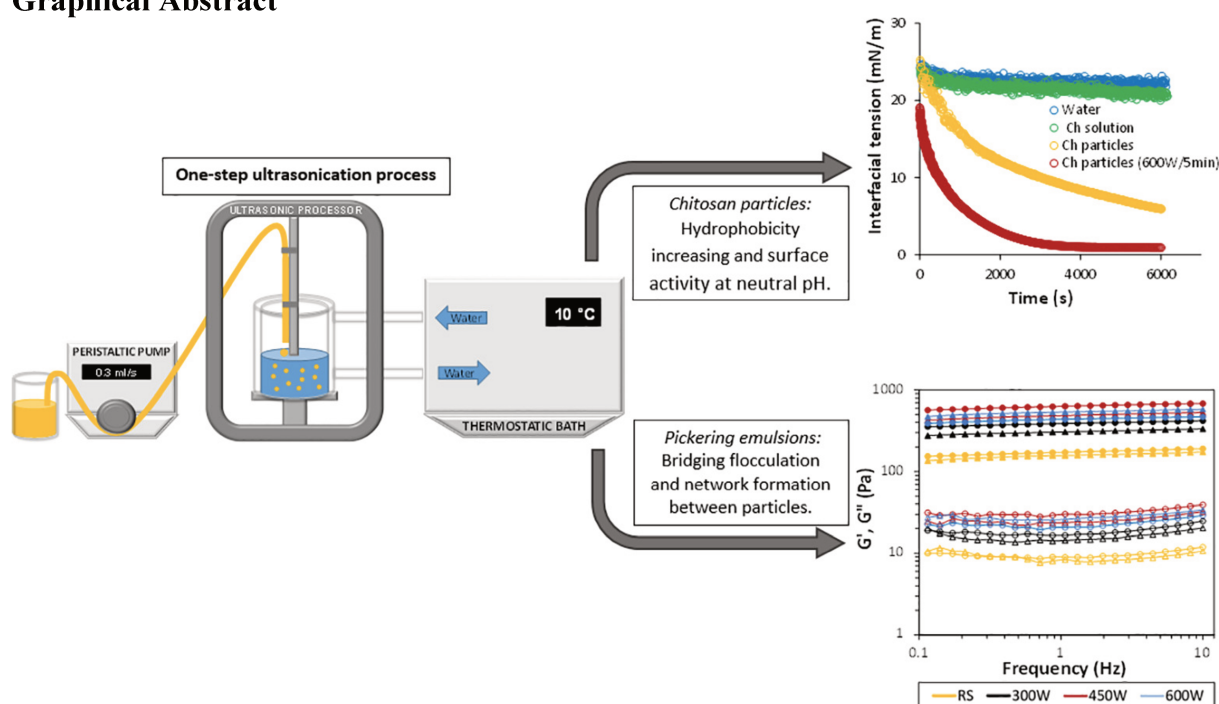
### **Highlights**

- One-step ultrasound was used to produce chitosan nanoparticles and O/W Pickering emulsions.
- Chitosan particles size reduced and hydrophobicity increased at more drastic process conditions.
- Chitosan particles present surface activity at neutral pH.
- Bridging flocculation occurred between adsorbed particles onto the droplet interface.
- Interactions between droplets resulted in network formation that avoided the emulsion destabilization.

### **Abstract**

Deprotonated chitosan nanoparticles have shown a potential to act as a food-grade particle stabilizer of oil-in-water (O/W) Pickering emulsions. The effect of one-step emulsification conditions using ultrasonic device was studied changing time and ultrasonication (US) power. The physicochemical properties of chitosan particles and O/W Pickering emulsions produced at the same time from different process conditions were evaluated. The surface activity of chitosan particles was evidenced with the reduction of interfacial tension between oil-water phases. This behavior was associated to the great capacity of hydrophobic groups acting onto the interface during the ultrasonic emulsification. The combined intensification of time and US power also led to an increase of hydrophobicity and polydispersity, changes in zeta potential and reduction on size of chitosan particles. At higher US power, the decrease of droplet size favored the interaction between oil droplets through weak attractive forces and particles sharing (bridging flocculation) leading to an increase in viscosity of emulsions. Thus, the major finding of this work was to elucidate the emulsion stability mechanism by deprotonated chitosan particles, which was associated to an increase of their hydrophobicity and the formation of a droplet network structure. In addition, a one-step homogenization could be performed allowing to produce these emulsions using less energy and process time.

## Graphical Abstract



**Keywords:** Solid particle; Chitin; Homogenization process; Emulsification; Hydrophobicity; Bridging flocculation

### 3.1. Introduction

Emulsions stability mechanism provided by solid particles is different from conventional emulsifiers since the strong adsorption of these particles onto the droplet interface is caused by the partial wettability of the particles in oil and water. Adsorbed particles promote the formation of an interfacial layer preventing sterically the emulsion destabilization (Berton-Carabin & Schroën, 2015; Pickering, 1907). Besides the mechanical barrier, there is an energy barrier (desorption energy) associated with the attractive forces between particles onto the interface and interactions between the particles and liquid phases. These interactions result in the deformation of the liquid interface around the particles favoring the formation of an interfacial layer almost insurmountable against droplets coalescence and Ostwald ripening (Leal-Calderon & Schmitt, 2008; Tcholakova, Denkov, & Lips, 2008).

Some of the Pickering emulsions reported in the literature show potential application in food products due to safety and acceptance of their ingredients. Rotor-stator homogenizers have been widely used in obtaining Pickering emulsions stabilized by a number of food-grade particles, such as modified starch (Dokić, Krstonošić, & Nikolić, 2012; Saravacos et al., 2011; Song et al., 2015), microcrystalline cellulose (Kargar, Fayazmanesh, Alavi, Spyropoulos, & Norton, 2012; Wen, Yuan, Liang, & Vriesekoop, 2014), zein protein (de Folter, van Ruijven,

& Velikov, 2012), soy protein (Liu & Tang, 2013; Liu & Tang, 2014) and micellar casein (Ye, Zhu, & Singh, 2013). Modified starch granules were also successfully employed as particle-stabilizers of O/W emulsions using high-pressure homogenization (Yusoff & Murray, 2011). Ultrasound technique has been used directly as a homogenization process and/or as a pretreatment of the emulsifier particles aiming their physicochemical changes followed by other emulsification processes (Ho et al., 2016; Tzoumaki, Moschakis, Kiosseoglou, & Biliaderis, 2011; Wang et al., 2016). Food particle dispersions of rutin hydrate, naringin and cellulose were previously treated using ultrasound, which resulted in some changes on size particles and consequently stability of emulsions produced with these particles (Duffus, Norton, Smith, Norton, & Spyropoulos, 2016). In addition, Pickering emulsions stabilized by chitin and cellulose nanocrystals particles were successfully produced using an ultrasonic device. A higher particles concentration led to smaller droplet size and higher stability to creaming process (Tzoumaki et al., 2011; Wang et al., 2016). Despite these studies, no extensive discussion has been carried out about possible changes on the particles structure caused by ultrasound process conditions and their consequence on emulsion properties.

Chitin is the second most abundant natural polymer after cellulose and it is the supporting material of crustaceans (Elsabee, Morsi, & Al-Sabagh, 2009). Chitosan is obtained from alkaline deacetylation of chitin consisting of repeated *D*-glucosamine (2-amino-2-deoxy-*D*-glucopyranose) and *N*-acetyl-*D*-glucosamine (2-acetamido-2-deoxy-*D*-glucopyranose) units linked *via*  $\beta(1 \rightarrow 4)$  glycosidic bonds (Mohammed, Williams, & Tverezovskaya, 2013; Philippova & Korchagina, 2012). Chitosan has been permitted in many countries for use as a food additive (JFCRF, 2014), food processing aid (EU, 2011; FDA, 2011; FSANZ, 2013) and dietary supplement (EU, 2012; FSANZ, 2013) due to its non-toxicity and potential health benefits (Mwangi, Ho, Tey, & Chan, 2016). Ultrasonication can depolymerize chitosan by the action of intense mechanical forces associated with the cavitation phenomenon that promotes the disruption of lower energy glycosidic linkages (Baxter, Zivanovic, & Weiss, 2005; Suslick & Price, 1999). Recently, the physicochemical properties of chitosan particles formed from ultrasonicated and non-ultrasonicated chitosan solution were studied. Ultrasonication pretreatment on chitosan aqueous solution resulted in the formation of smaller and monodisperse particles. However, this treatment caused a reduction on particle hydrophobicity and emulsions with higher creaming index compared to the Pickering emulsions stabilized by non-pretreated chitosan using rotor-stator homogenizers (Ho et al., 2016).

In general, hydrophobicity, size, aggregation degree and polymer concentration are factors that determine the capacity of the solid particles acting as emulsifiers (Ho et al., 2016; Kalashnikova, Bizot, Cathala, & Capron, 2011). However, in the same way as

conventional emulsifiers, the particles nature and emulsion properties, such as droplet size and viscosity, can be affected by the choice of homogenization method and the energy input level during the emulsification process (Liu & Tang, 2014). Ultrasound-assisted emulsification (Chemat & Khan, 2011; Soria & Villamiel, 2010) is a technique widely studied to produce food emulsions since sound waves are generally considered safe, non-toxic, and environmentally friendly (Kentish & Ashokkumar, 2011). Besides, ultrasound has the potential to development of new products with unique properties and functionality (Silva, Rosa, & Meireles, 2015). Therefore, this study aimed to investigate the effects of one-step emulsification process conditions using ultrasonic device, power and processing time, on the physicochemical properties of chitosan particles and O/W Pickering emulsions produced at the same time.

## **3.2. Material and Methods**

### **3.2.1. Material**

Low molecular chitosan with a deacetylation degree of 75–85%, fluorescein isothiocyanate (FITC), pyrene, glacial acetic acid and sodium hydroxide (NaOH) were purchased from Sigma-Aldrich (USA). Anhydrous ethanol and sodium hydroxide were purchased from PanReac AppliChem (Spain). Sunflower oil (Bunge Alimentos, Brazil) was acquired in the local market and deionized water was obtained from a Milli-Q system. All the chemicals used were of analytical grade.

### **3.2.2. Methods**

#### **3.2.2.1. Preparation and characterization of chitosan particles**

Chitosan particles were synthesized according to the method previously described by Liu, Wang, Zou, Wei, and Tong (2012). Briefly, an acetic acid solution (4 M) was prepared, and then the chitosan powder was added to this solution. The mass ratio chitosan to acetic acid was fixed at 2:3. The acid-chitosan solution (0.8% w/v) was gently stirred for 12 h before to be filtered using a Whatman paper (Grade 1). The chitosan particles were formed by in situ deprotonation of the amine groups after adjusting the pH value of the acid-chitosan solution (0.8% w/v) from 3.3 to 6.9 using 4 M NaOH. Aqueous dispersion of chitosan particles was subjected to the same conditions of homogenization used for emulsions preparation (Section 3.2.2.2). Chitosan particles suspension were diluted to 0.01% w/v using MilliQ water for the measurements. The zeta potential and particle size were measured on a Zetasizer (Nano ZS, Malvern Instruments, UK) using the refractive indices of water and chitosan particles as 1.330

and 1.332, respectively. Quantitative information about the hydrophobic microdomains of chitosan particles was obtained from fluorescence spectroscopy using a ISS K2 fluorometer (ISS, USA) with probe pyrene at a final concentration of  $2 \times 10^{-6}$  mol/L. Pyrene is expected to localize preferentially in the hydrophobic domains (molecule hydrophobic portion) of amphipathic molecules, once it is a hydrophobic molecule with low water solubility. Fluorescence spectrum was obtained at the excitation wavelength of 338 nm with the fluorescence emission spectra ranging from 350 to 550 nm (slit width 0.5 nm). Emission spectra are associated with vibronic lines structures whose intensities show a strong dependence on the polarity of the microenvironment (Amiji, 1995). The relative micropolarity surrounding the pyrene environmental was determined from the fine structure of pyrene monomers fluorescence, namely the ratio  $I_1/I_3$  corresponding to the monomers peaks at 373 nm ( $I_1$ ) and 383 nm ( $I_3$ ) (Tan, Xie, Zhang, Cai, & Xia, 2016).

Interfacial tension between the organic (sunflower oil) and aqueous phase was performed using a tensiometer Tracker-S (Teclis, France) by the rising droplet method. The initial droplet volume was 6  $\mu$ l. The aqueous phase was water, acid-chitosan solution at pH 3.3 or aqueous dispersions of chitosan particles untreated and treated at the more drastic process conditions (600 W/5 min) at pH 6.9.

### 3.2.2.2. Preparation of Pickering emulsions

Oil-in-water emulsions (75 ml) stabilized by chitosan particles were prepared by blending 25% (v/v) sunflower oil and 75% (v/v) chitosan aqueous suspensions using two emulsification processes, resulting in a final concentration of chitosan nanoparticles in the emulsion of 0.6% w/v. The emulsification process was performed in only one-step in contrast to conventional emulsification processes involving two-steps for the formation of fine emulsions, i.e. rotor-stator followed by ultrasonication or high-pressure (Domian, Brynda-Kopytowska, & Oleksza, 2015; Kurukji, Pichot, Spyropoulos, & Norton, 2013; Silva, Gomes, Hubinger, Cunha, & Meireles, 2015). In one-step emulsification process, oil phase was added dropwise to the chitosan aqueous suspensions using a peristaltic pump Masterflex L/S (Cole-Parmer Instrument Company, EUA) with a mean flow rate of 0.3 ml/s during homogenization in an ultrasonic processor (QR 750 W, Ultronique, Campinas, Brazil) with a 13 mm diameter titanium probe. The effect of nominal power (W) and processing time (min) on the emulsions properties (Section 3.2.2.3) was investigated with power variation between 300 and 600 W during 3 min or 5 min. The same procedure was used to prepare control emulsions in a rotor-stator (RS) system (Ultra Turrax T18, IKA, Germany) at 10,000 rpm during 3 or 5 min, once this emulsification process has been widely used in obtaining Pickering emulsions stabilized



by food-grade particles. The one-step emulsification processes were carried out into a jacketed vessel attached to a thermostatic bath (Quimis, Brasil) at  $10 \pm 2$  °C, in order to avoid over heating of emulsions. The temperature of preparation did not exceed 37 °C during both emulsification processes. Energy density provided by both emulsification methods was calculated according to Equation 3.1.

$$ED = \frac{P \times t}{V} \quad (3.1)$$

where  $ED$  is the energy density ( $\frac{J}{cm^3}$ ),  $P$  is the nominal applied power (W),  $t$  is the process time (s) and  $V$  is the volume ( $cm^3$ ).

### 3.2.2.3. Characterization of Pickering emulsions

#### 3.2.2.3.1. Kinetic stability-laser scanning turbidimetry

Emulsion stability was monitored using the optical scanning instrument Turbiscan ASG (Formulaction, France). Fresh emulsions were placed in flat-bottomed cylindrical glass tubes (140 mm, height; 16 mm, diameter) and stored at  $25 \pm 2$  °C before to be subjected to backscattered light at 880 nm. Measurements were performed on fresh emulsions and after 6 days of storage. A plot of backscattered light, BS (%) on the y-axis and the sample height (mm) on the x-axis was performed. A sample height of 0 mm corresponds to the bottom of the measuring cell.

#### 3.2.2.3.2. Optical microscopy and confocal scanning laser microscopy (CSLM)

The emulsion microstructure was observed by an optical microscope (Axio Scope.A1, Carl Zeiss, Germany) with 100× oil immersion objective lens. The images were captured with the software AxioVision Rel. 4.8 (Carl Zeiss, Germany). The optical microscopy was performed on the freshly prepared emulsions and after 6 days of storage.

Chitosan-stabilized emulsions (process condition: 600 W/5 min) were examined using a Zeiss LSM 780-NLO confocal on an Axio Observer Z.1 microscope (Carl Zeiss, Germany) with an objective 100×. The images were collected using wavelengths of 488 nm and 525 nm for excitation and emission of the FITC, respectively. Synthesis of FITC-labeled chitosan was based on the reaction between the isothiocyanate group of FITC and the primary amino group

of chitosan. Freeze-dried chitosan (1 g) was firstly dissolved in 100 ml of 0.1 M acetic acid under magnetic stirring during 24 h. After that, 100 ml of anhydrous ethanol was slowly added to this solution under continuous stirring. In addition, 50 ml of FITC dissolved in anhydrous ethanol (0.5 w/v) was slowly added to the chitosan solution. The mixture was stirred at 350 rpm, room temperature and dark conditions for 3 h. FITC-labeled chitosan was precipitated in 0.2 M sodium hydroxide solution. The precipitate was washed and centrifuged extensively with deionized distilled water until the total absence of free FITC fluorescence signal in the washing water. The labeled polymer was then freeze-dried (Qaqish & Amiji, 1999).

### 3.2.2.3.3. Droplet size distribution and rheological assays

The droplet size distribution was determined by the laser diffraction method using a Mastersizer 2000 (Malvern Instruments Ltd., Malvern, UK). Water or an aqueous solution of Tween 20 (2% v/v) were used as dispersant. Size measurements of individual droplets could be only performed with dispersant Tween 20, once a flocculated state of droplets could be evidenced in the size measurements using water as dispersant. Ultrasound was applied for 2 min in order to avoid the presence of bubbles and the rotational velocity of the equipment was kept at 2100 rpm. The droplet size was expressed as the volume-surface mean diameter ( $D_{32}$ ) calculated according to Equation 3.2. Polydispersity index (*span*) was calculated according to Equation 3.3. Measurements were performed on the freshly prepared emulsions and after 6 days of storage.

$$D_{32} = \frac{\sum n_i d_i^3}{\sum n_i d_i^2} \quad (3.2)$$

$$Span = \frac{d_{(90)} - d_{(10)}}{d_{(50)}} \quad (3.3)$$

where  $n_i$  is the droplets number with diameter  $d_i$  and  $d_{10}$ ,  $d_{50}$  and  $d_{90}$  are the diameters at 10%, 50% and 90% of cumulative volume, respectively.

For dynamic viscoelastic measurements, firstly the viscoelastic linear domain was determined from a strain sweep (0.01–10%) at a fixed frequency of 1 Hz. After that, a frequency sweep was performed with a fixed strain 0.1%, which was within the linear region, over a frequency range between 0.1 and 10 Hz. The dynamic mechanical spectra were obtained recording the storage modulus  $G'$ , and the loss modulus  $G''$  as a function of frequency.

#### **3.2.2.3.4. Statistical analysis**

All experiments were performed in triplicate. Analysis of variance (ANOVA) was performed using the Minitab 16® software and significant differences ( $p < 0.05$ ) between the treatments were evaluated using Tukey analysis.

### **3.3. Results and discussion**

#### **3.3.1. Properties of chitosan particles**

The effect of the different homogenization processes on the physicochemical properties of chitosan particles is shown in Figure 3.1 and Table 3.1. Untreated particles showed a monomodal size distribution with a mode of approximately 1000 nm and a polydispersity index of 0.47. Peak size shifted toward lower values with the increase of ultrasonic treatment and progressively a bimodal size distribution was observed. Higher ultrasonication time and/or amplitude also caused a reduction on the intensity of the larger peak and increased intensity of the smaller peak (Figure 3.1). Based on our results and from other the authors, we can assume that during emulsification will occur a disruption of the chitosan particles concomitantly to the process of oil droplets breakup (Kurukji et al., 2013; Liu & Tang, 2014; Yusoff & Murray, 2011). Solid particles used to stabilize Pickering emulsions should be at least one order of magnitude smaller than emulsion droplets size (Binks, 2002; Dickinson, 2012). At stronger emulsification process conditions, a vast majority of nanometer-sized particle (between 100 and 500 nm) was produced due to the breaking of chitosan particles and aggregates (Figure 3.1). Smaller particles could be more easily adsorbed onto the droplet interface producing a more homogenous layer around the droplet and enhancing the emulsion stability (Binks, 2002; Gould, Vieira, & Wolf, 2013).

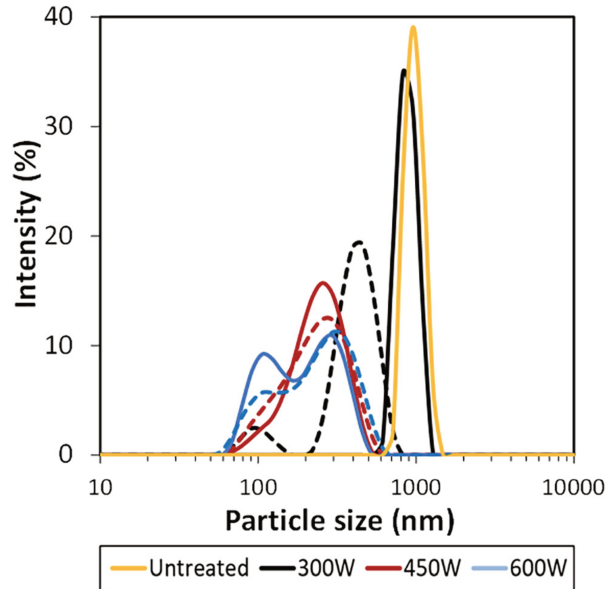


**Figure 3.1.** Particle size distribution of chitosan particles untreated or treated with different ultrasonication power. Process time, dashed line: 3 min and solid line: 5 min.

**Table 3.1.** Energy density applied in each process condition and physicochemical properties of non-treated and ultrasound treated chitosan (Ch) dispersions (0.01 % w/v).

Sample	Time (min)	Energy density (J/cm <sup>3</sup> )	pH	I <sub>1</sub> /I <sub>3</sub>	Zeta potential (mV)
Ch solution	—	—	3.3	—	+60.0 ± 3.1 <sup>a</sup>
Ch particles	—	—	6.9	1.70 ± 0.01 <sup>a</sup>	+13.1 ± 0.5 <sup>bc</sup>
RS	3	708	6.9	1.74 ± 0.11 <sup>a</sup>	+13.5 ± 0.2 <sup>b</sup>
	5	1180	6.9	1.64 ± 0.02 <sup>ab</sup>	+11.6 ± 0.4 <sup>c</sup>
300W	3	720	7.0	1.64 ± 0.01 <sup>ab</sup>	+7.9 ± 0.4 <sup>de</sup>
	5	1200	6.9	1.52 ± 0.02 <sup>b</sup>	+7.2 ± 0.5 <sup>e</sup>
450W	3	1080	7.0	1.63 ± 0.02 <sup>ab</sup>	+7.8 ± 0.5 <sup>de</sup>
	5	1800	6.9	1.29 ± 0.05 <sup>c</sup>	+8.7 ± 0.6 <sup>de</sup>
600W	3	1440	6.8	1.08 ± 0.01 <sup>d</sup>	+9.1 ± 0.2 <sup>d</sup>
	5	2400	6.9	1.09 ± 0.01 <sup>d</sup>	+9.6 ± 0.8 <sup>d</sup>

Means with the same letters in the same column do not show statistical differences ( $p > 0.05$ )

The amino groups of chitosan are protonated below the pKa of the polysaccharide, conferring a positive surface charge to this polysaccharide. Zeta potential of chitosan solution at pH 3.3 was +60 mV and decreased to +13 mV as pH increased to 6.9. Such a reduction is associated with the proximity of the chitosan pKa (between 6.2 and 7), which leads to formation of chitosan aggregates stabilized by additional hydrogen bonds involving neutralized amino groups (Philippova & Korchagina, 2012). The pKa value depends mainly on the degree of chitosan deacetylation and chain length of chitosan (Arrascue, Garcia, Horna, & Guibal, 2003; Philippova & Korchagina, 2012). Shorter chain shows higher pKa, whereas the aggregation is

more pronounced with an increase in the chitosan deacetylation (Philippova & Korchagina, 2012). An additional reduction of zeta potential was observed with application of RS/5 min and ultrasonic treatments, but more drastic treatment conditions were accompanied by an increase in zeta potential. These results suggest a higher exposition of protonated amino groups residues ( $-\text{NH}_3^+$ ) on disrupted chitosan polymer chains during the ultrasonication process (Mwangi et al., 2016).

Breakup of aggregated chitosan particles favored exposure of hydrophobic domains as detected by  $I_1/I_3$  values. Table 3.1 shows that the  $I_1/I_3$  values of chitosan particles untreated or treated from RS and low US intensity were close to the pure water ( $I_1/I_3 = 1.8$ ), whereas,  $I_1/I_3$  values of chitosan treated at high US intensity were similar to the anionic surfactant micelles, around 1.0 (Wilhelm et al., 1991). Ho et al. (2016) suggested a reduction in the hydrophobicity of chitosan particles after treatment in ultrasound, which reflected in the formation of less stable emulsions. However in our work, the decrease of  $I_1/I_3$  values confirmed the higher exposition of hydrophobic domains on the chitosan nanoparticles (size reduction and surface area increasing) due to mechanical treatments. Thus, the lower polarity around the pyrene molecules indicated that these particles could be able to bind more strongly to the oily phase (Estrada-Fernández et al., 2018) providing an important mechanism against to the emulsion destabilization.

### 3.3.2. Properties of the Pickering emulsions

The adsorption of chitosan (Ch) particles onto the oil-water interface was studied by tensiometry (Figure 3.2). The interfacial tension between sunflower oil and pure water or acid-chitosan solution (pH 3.3) was also measured as control experiments. The initial interfacial tension of the water, acid-chitosan solution and untreated chitosan particles was almost identical (about 25 mN/m), whereas of the treated chitosan particles (600 W/5 min) was 19 mN/m. All interfacial tension values decreased over time. After 6000 s, the control systems showed interfacial tension around 20 mN/m, whereas values lower than 6 mN/m and 2 mN/m were obtained in the presence of untreated and treated chitosan particles, respectively at neutral pH. The faster reduction of interfacial tension of treated particles could be associated to their lower polarity since more hydrophobic domains were exposed after ultrasonication treatment. Values of initial (12 mN/m) and equilibrium (5 mN/m) interfacial tension between palm olein oil and chitosan particles solution showed a similar behavior (Ho et al., 2016). The authors suggested that the interfacial tension reduction over time could be attributed to the presence of residual material from chitin, showing some surface activity. However in our work, this hypothesis was

discarded, since the chitosan solution could not reduce the interfacial tension at pH 3.3 and such a reduction of interfacial tension should be related to the chitosan properties at neutral pH.

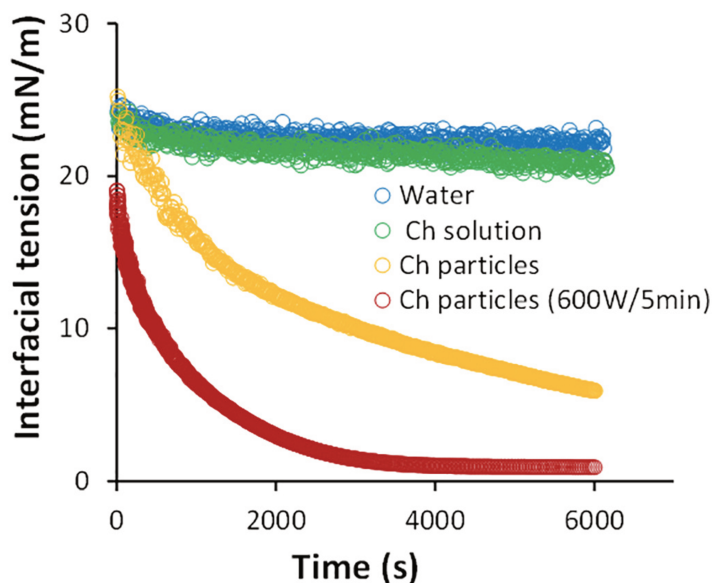


**Figure 3.2.** Dynamic interfacial tension of the systems between sunflower oil and different aqueous solutions (water, acid-chitosan (Ch) solution (pH 3.3), chitosan (Ch) particles untreated and chitosan (Ch) particles treated at 600 W/5 min (pH 6.9)).

The faster reduction of the interfacial tension between oil and treated and untreated chitosan particles was caused by particles adsorption onto the oil-water interface. This effect was described in a recent study using soy glycinin nanoparticles-stabilized emulsion and it was related to diffusion of nanoparticles from the bulk onto the interface, followed by their penetration, structural rearrangement and formation of viscoelastic films (Liu & Tang, 2016). Such viscoelastic film can be thick since chitosan will aggregate at a pH above pKa because the amount of charged units or repulsive forces between particles decreases, and neutralized amine groups can form additional hydrogen bonds stabilizing the aggregates. On the other hand, the non-polar acetyl units (*N*-acetyl-D-glucosamine) on the chitosan polymer will confer the hydrophobicity character of chitosan aggregates (Ho et al., 2016; Philippova & Korchagina, 2012). Therefore, we could attribute the surface activity of chitosan to the greater capacity of hydrophobic groups to act onto the oil-water interface after the formation of self-aggregated chitosan with hydrophilic and hydrophobic features.

Some studies showed that the strong adsorption of chitosan particles onto the oil-water interface hindered the droplets coalescence by a mechanical barrier formation (steric hindrance) (Ho et al., 2016; Mwangi et al., 2016; Payet & Terentjev, 2008). However, the stabilization mechanism of the self-aggregated chitosan-stabilized emulsions was not totally elucidated once other effects, such as the formation of a network between the oil droplets resulting from the

chitosan adsorption onto the oil-water interface, can promote changes on the emulsions properties providing more stability for the systems.

Apparent viscosity at  $5 \text{ s}^{-1}$  and rheological properties of the Pickering emulsions obtained from the fitting of power law model are presented in Figure 3.3a. Shear-thinning behavior and the viscosity increase were more remarkable in emulsions produced with higher US power ( $n = 0.33\text{--}0.53$ ;  $\eta$  at  $5 \text{ s}^{-1} = 0.94\text{--}1.09 \text{ Pa.s}$ ) than ones produced with rotor-stator or the lowest US power ( $n = 0.62\text{--}0.75$ ;  $\eta$  at  $5 \text{ s}^{-1} = 0.40\text{--}0.46 \text{ Pa.s}$ ). Particles concentration and oil loading were kept fixed for all the systems indicating that the increase of consistency index (0.2 to  $1.9 \text{ Pa.s}$ ) and viscosity depended only on the effects of emulsification process. Thus, viscosity changes can be associated with the application of ultrasonic waves that result in pressure fluctuations. These fluctuations propagate into the liquid macroscopic dispersion leading to the formation of microscopic bubbles which tend to collapse within a few milliseconds, resulting in the formation of very fine emulsions (smaller droplets or higher droplets surface area) by cavitation phenomenon (Kaltsa, Michon, Yanniotis, & Mandala, 2013; Silva, Gomes, et al., 2015; Silva, Zabet, & Meireles, 2015). The increase of droplets surface area using higher US power can favor the interaction between oil droplets through weak attractive forces leading to an increase of viscosity and pseudoplasticity. In general in emulsion systems, the resistance provided by the weak interaction forces are readily overcome by the application of shear forces (Torres, Iturbe, Snowden, Chowdhry, & Leharne, 2007), which is associated to the pseudoplasticity.

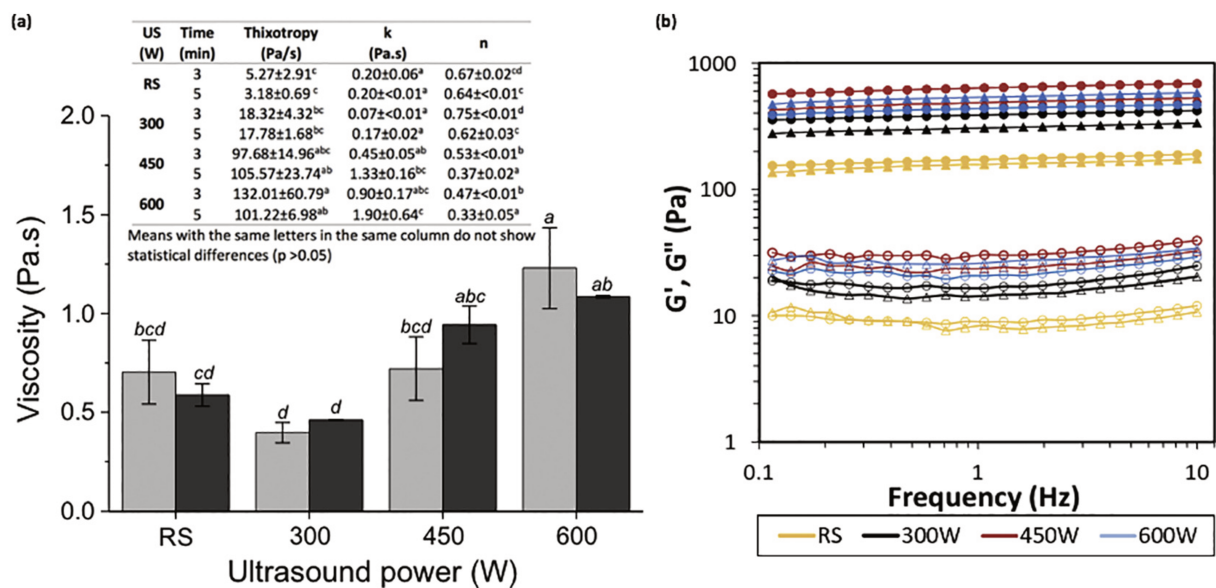


**Figure 3.3.** (a) Thixotropy and viscosity at  $5 \text{ s}^{-1}$  (process time: (□) 3 min and (■) 5 min) and (b) mechanical spectra (process time: (Δ) 3 min and (○) 5 min) of emulsions stabilized

by chitosan particles. Open symbols:  $G''$  and filled symbols:  $G'$ . Different letters indicate significant differences ( $p < 0.05$ ) between emulsions viscosity at  $5 \text{ s}^{-1}$ .

Formation of a network structure between droplets was supported by the presence of thixotropy in the samples. In general, thixotropy values increased with the increase of ultrasonic power treatment (3.18 to 132.01 Pa/s), but did not vary with the processing time (Figure 3.3a). The extent of network formation can be inferred from dynamic mechanical spectra of the emulsions, once the storage ( $G'$ ) and loss ( $G''$ ) moduli indicate whether the droplets are weakly or strongly associated (Torres et al., 2007). The dynamic mechanical spectra of the emulsions are depicted in Figure 3.3b. All emulsions exhibited  $G'$  higher than  $G''$  within the angular frequency range and both were independent of frequency. In Pickering emulsions, this behavior can be associated to the flocculation of droplets through the sharing of the colloidal particles onto the interface providing an important stabilizing mechanism against droplets coalescence (Stancik & Fuller, 2004; Torres et al., 2007). Besides, concentrated emulsions with lower droplet size can show more interactions between them, which could result in network formation with more pronounced viscoelastic properties (McClements, 2005).

The interaction between oil droplets in Pickering emulsions can also be further supported by microscopy showed in Figure 3.4a. Droplets flocculation mechanism was more clearly observed increasing the sonication intensity due to the increase in the superficial area of the oil droplets and chitosan particles. Pickering emulsions produced with an ultrasonic homogenizer and stabilized by chitin nanocrystals were also studied (Tzoumaki et al., 2011). The authors observed shear thinning behavior and more pronounced elastic response at high chitin concentration. They also associated this result to the chitin adsorption onto the oil-water interface and formation of a weak droplet network structure. Confocal micrographs confirmed the deposition of chitosan (green fluorescent layer) onto the oil-water interface (Figure 3.4b). Some differences in oil droplets size can be observed in different micrographs for a same process condition due to the emulsion polydispersity and flocculation phenomenon. Therefore micrographs showing larger droplets were chosen in the confocal microscopy to improve visualization.



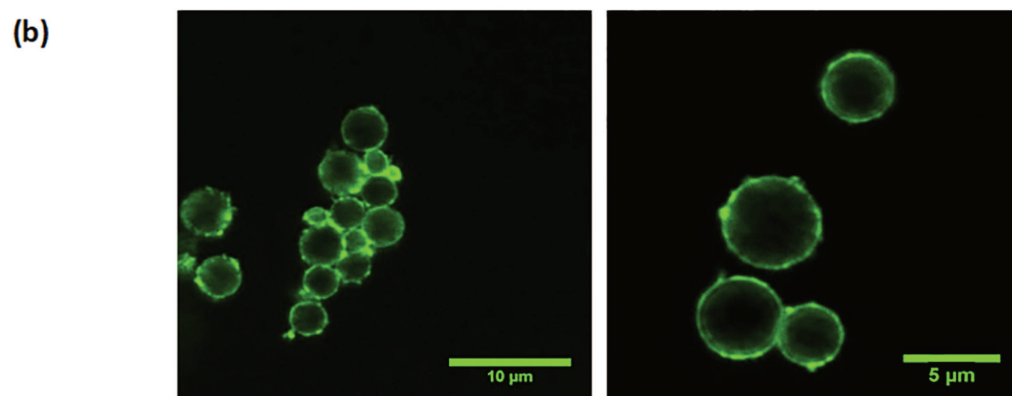
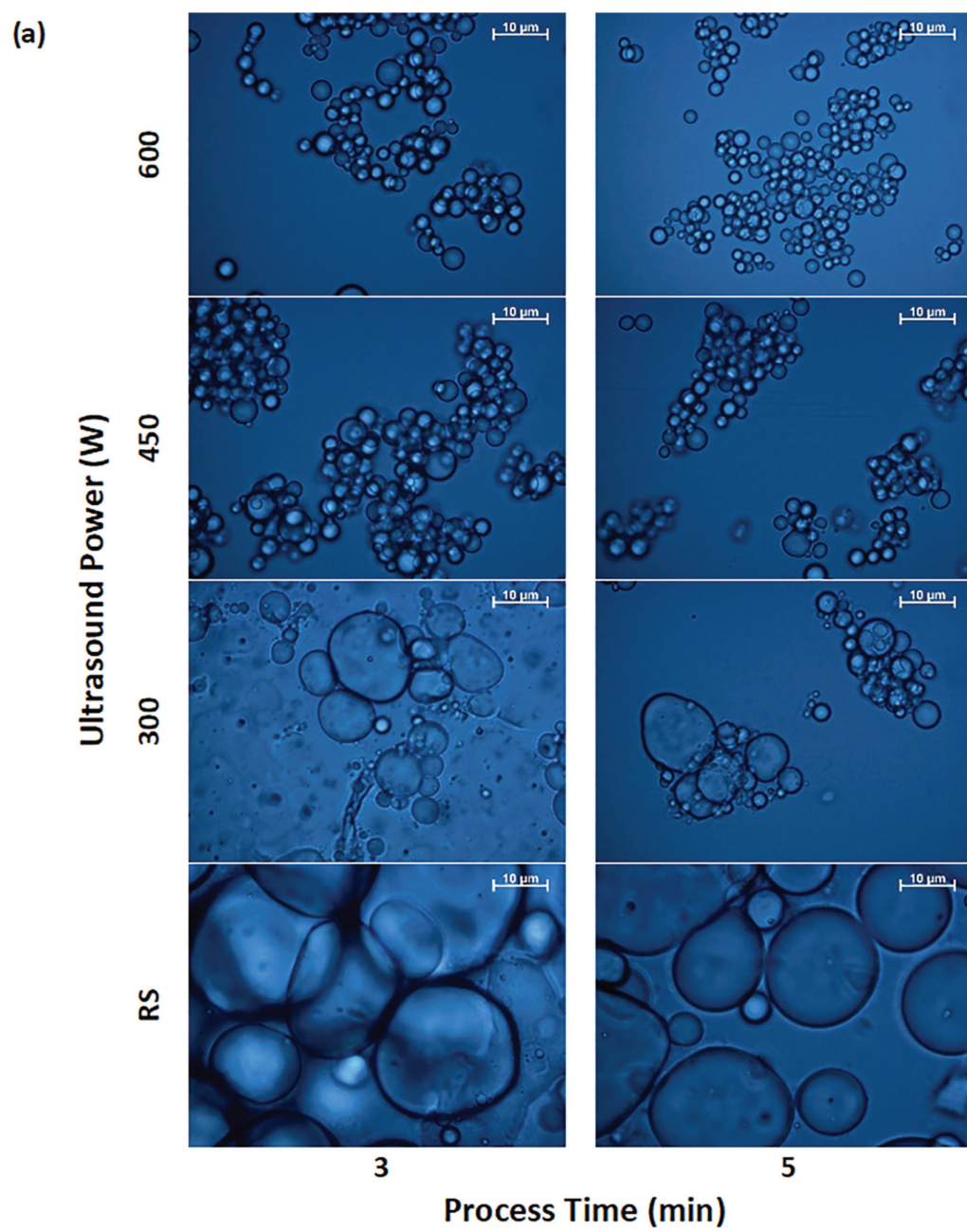


**Figure 3.4.** (a) Optical micrograph of emulsions stabilized by chitosan particles (0.6% w/v) obtained from RS and US processes. (b) Confocal micrographs of emulsion stabilized by chitosan particles stained with FITC (green color). Process condition: 600 W/5 min.

Figure 3.5a shows the effects of the ultrasonication operation conditions (power and time) on the droplet size distribution of the fresh Pickering emulsions, diluted in water or 2% (v/v) Tween 20. The corresponding average diameter ( $D_{32}$ ) is presented in Table 3.2. In general, the size distribution shifted toward lower sizes when Tween 20 (Figure 3.5a, blue lines) was used as dispersing solvent, indicating that the non-covalent interactions between adsorbed particles onto droplets were broken and replaced by the emulsifier. Thus, size measurements of individual droplets could be performed with dispersant Tween 20, once the effect of flocculated droplets on the emulsions properties was already evaluated by the rheological analysis. Emulsions prepared using rotor-stator exhibited a prominent size distribution peak closed to 40  $\mu\text{m}$ , while after ultrasonication process the droplet size distribution (all dispersed in Tween 20) was bimodal reflecting in the increase of droplets polydispersity. Bimodal distribution could also indicate destabilization of the Pickering emulsions or chitosan particles disruption, but the microscopic images (Figure 3.4a) showed indeed the formation of smaller droplets size (Table 3.2). After 6 days, some emulsions showed a slight increase in the mean droplet size compared to fresh emulsions (Table 3.2). The most remarkable droplet size increase was observed for emulsions produced at the highest power intensity (450 and 600 W), probably due to the higher surface area and intense flocculation (Figure 3.5b).

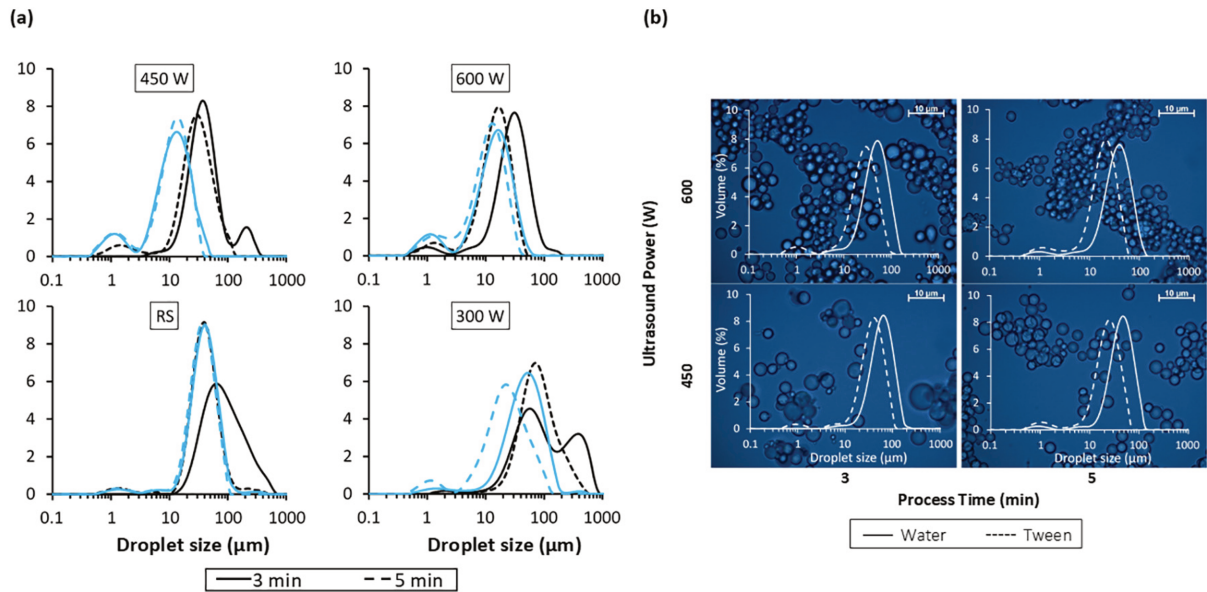


**Figure 3.5.** (a) Size distribution of freshly emulsions stabilized by chitosan particles (0.6% w/v) obtained from RS and US process. Dispersant solvent, blue lines: Tween 20 and black lines: water. (b) Size distribution and optical microscopy of emulsions stabilized by chitosan particles (0.6% w/v) obtained from US process after 6 days of storage.

**Table 3.2.** Mean diameter ( $D_{32}$ ) and span of emulsions stabilized by chitosan particles (0.6 % w/v) obtained from RS and US process. Fresh emulsion and after 6 days of storage.

US (W)	Time (min)	$D_{32}$ (μm)	Span	$D_{32}$ (μm)	Span
		Fresh-Tween 20	Fresh-Tween 20	6 days-Tween 20	6 days-Tween 20
RS	3	$21.6 \pm 3.1^a$	$1.40 \pm 0.08^{cd}$	$22.3 \pm 2.7^a$	$1.21 \pm 0.04^b$
	5	$19.0 \pm 0.3^a$	$1.33 \pm 0.06^d$	$21.7 \pm 0.4^a$	$1.67 \pm 0.55^{ab}$
300	3	$19.4 \pm 0.8^a$	$1.93 \pm 0.14^b$	$20.9 \pm 1.3^{ab}$	$2.30 \pm 0.02^a$
	5	$9.1 \pm 0.5^b$	$2.50 \pm 0.09^a$	$19.1 \pm 0.7^{ab}$	$2.28 \pm 0.26^a$
450	3	$5.7 \pm 0.8^b$	$1.79 \pm 0.07^{bc}$	$16.1 \pm 0.3^b$	$1.47 \pm 0.06^{ab}$
	5	$5.1 \pm 0.6^b$	$1.84 \pm 0.07^{bc}$	$10.0 \pm 0.4^c$	$1.52 \pm 0.05^{ab}$
600	3	$6.1 \pm 0.9^b$	$1.89 \pm 0.19^b$	$11.2 \pm 0.5^c$	$1.68 \pm 0.06^{ab}$
	5	$5.5 \pm 0.9^b$	$1.87 \pm 0.11^{bc}$	$8.8 \pm 0.7^c$	$1.61 \pm 0.16^{ab}$

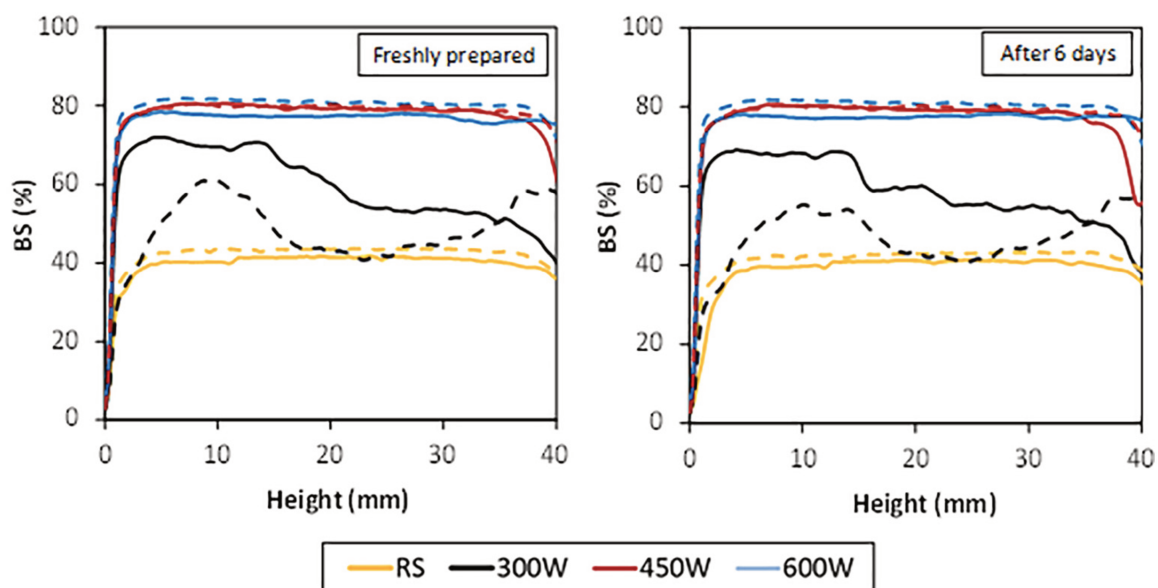
Means with the same letters in the same column do not show statistical differences ( $p > 0.05$ )

Overall, increasing ultrasound power was more efficient on the changes of chitosan particles and Pickering emulsions properties than shear stress promoted by RS systems and/or energy density input during the mechanical processes (Table 3.1). Cavitation phenomenon can lead to a more pronounced increase of local temperature as the power intensity and emulsification time are increased, which also favors the local decrease of apparent viscosity and interfacial tension between the phases, as well as, the droplets breakup (smaller droplets) (Gaikwad & Pandit, 2008). However, droplets can present a flocculation state attributed to the insufficient amount of nanoparticles completely recovering the created interface (bridging

flocculation) (Liu & Tang, 2016). Bridging flocculation is observed from two neighboring droplets sharing the same nanoparticles (droplets covering) and forming a bridge (Liu & Tang, 2014; Liu & Tang, 2016). In this work, droplets flocculation was associated to the emulsions prepared at higher shear rate (Destribats et al., 2013), since stronger mechanical forces lead to the formation of a higher amount of smaller droplets promoting bridging flocculation between adsorbed chitosan nanoparticles onto droplets.

The physical stability of the emulsion was determined immediately after preparation and on the sixth day of storage at  $25 \pm 2$  °C. The backscattering (BS) profiles versus height of the measuring cell are shown in Figure 3.6a. Fresh emulsions with larger mean size droplets (19–21.6  $\mu\text{m}$ ) presented BS value about 40%, while the smaller droplets (5–6  $\mu\text{m}$ ) showed BS values higher than 75%. The BS intensity is sensitive to the droplet size and their concentration since BS decreases with the decrease of droplets concentration and increases when the droplet size is smaller than the incident wavelength of the light (Leclercq & Nardello-Rataj, 2016; Mengual, Meunier, Cayré, Puech, & Snabre, 1999). Changes of the BS values in the height of the measuring cell were observed at the lowest ultrasonication condition (300 W), which indicates different droplet size throughout the height of the measuring cell. This instability may be explained by the fact that mechanical forces applied during one-step homogenization were not enough to ensure the formation of a fine emulsion. On the other hand, a higher stability of emulsions was reached with stronger ultrasonication conditions, namely emulsions with the highest level of power (450 and 600 W) applied during homogenization process. Under these conditions, the gel-like properties and increased viscosity can avoid the coalescence and destabilization. Thus, the slight displacement of the size distribution profiles toward larger sizes did not cause phase separation (Figure 3.6b). A high resistance against coalescence is the major benefit of the stabilization by solid particles compared to conventional emulsions (Leclercq & Nardello-Rataj, 2016). However, it should be worth notice that the ultrasonication treatment has an important role through disruption or disaggregation of initially formed chitosan particles into smaller ones and satisfactory homogenization of oil droplets into the aqueous phase. Intense effects of cavitation phenomenon (at 450 and 600 W) lead to the production of smaller droplets and an increase in non-covalent interactions between oil droplets (bridging flocculation), as well as, changes in viscosity and gel-like properties of systems that provided an enhancement in the kinetic stability of Pickering emulsions.

(a)



(b)

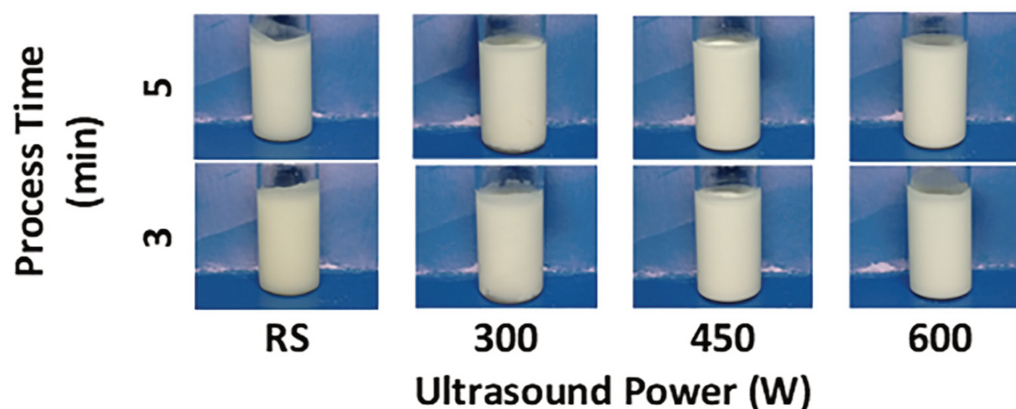


**Figure 3.6.** (a) Backscattering profiles (in fresh and after 6 days of storage) of emulsions stabilized by chitosan particles (0.6% w/v) obtained from US process (dashed line: 3 min and solid line: 5 min). (b) Pictures of measuring cells containing emulsions stabilized by chitosan particles (0.6% w/v) obtained from US process after 6 days of storage.

### 3.4. Conclusion

The effects of one-step emulsification process conditions by ultrasonic device on the physicochemical properties of chitosan particles and O/W Pickering emulsions simultaneously produced were studied. The combined intensification of time and ultrasonication power led to size reduction and polydispersity increase of chitosan particles and emulsion droplets. In addition, a droplet network structure was formed resulting from the chitosan adsorption onto the oil-water interface (reduction of O/W interfacial tension). This adsorption was associated

to the greater capacity of hydrophobic groups to act onto the interface during the droplet breakup (increase of chitosan particles hydrophobicity) and to the non-covalent interactions between oil droplets (bridging flocculation). Additionally, an increase in droplets flocculation changed viscosity and a gel-like structure was observed that also provided an enhancement in the Pickering emulsion stability. Therefore, the major finding of this work was to elucidate the emulsion stability mechanism by deprotonated chitosan particles and propose a one-step emulsification method that spends less time and energy but that can produce at the same time chitosan nanoparticles and fine kinetically stable emulsions.

### Acknowledgments

The authors thank CAPES – Brazil (DEA/FEA/PROEX) and FAPESP – Brazil (FAPESP 2007/58017-5 and 2011/06083-0) for their financial support. Ana Letícia Rodrigues Costa Lelis thanks CNPq – Brazil (CNPq 140710/2015-9) and Andresa Gomes Brunassi thanks CNPq – Brazil (CNPq 140705/2015-5) for the fellowship; Rosiane Lopes Cunha thanks CNPq – Brazil (CNPq 305477/2012-9) for the productivity grant. The authors also acknowledge the Spectroscopy and Calorimetry Facility at Brazilian Biosciences National Laboratory (LNBio) for Research in Energy and Materials (CNPEM, Brazil) for their support with the use of fluorimeter.

### References

- Amiji, M. M. (1995). Pyrene fluorescence study of chitosan association in aqueous solution. *Carbohydrate Polymers*, 26, 211–213.
- Arrascue, M. L., Garcia, H. M., Horna, O., & Guibal, E. (2003). Gold sorption on chitosan derivatives. *Hydrometallurgy*, 71(1–2), 191–200.
- Baxter, S., Zivanovic, S., & Weiss, J. (2005). Molecular weight and degree of acetylation of high-intensity ultrasonicated chitosan. *Food Hydrocolloids*, 19(5), 821–830.
- Berton-Carabin, C. C., & Schroën, K. (2015). Pickering emulsions for food applications: Background, trends, and challenges. *Annual Review of Food Science and Technology*, 6, 263–297.
- Binks, B. P. (2002). Particles as surfactants—Similarities and differences. *Current Opinion in Colloid & Interface Science*, 7(1–2), 21–41.
- Chemat, F., & Khan, M. K. (2011). Applications of ultrasound in food technology: Processing, preservation and extraction. *Ultrasonics Sonochemistry*, 18, 813–835.



- de Folter, J. W. J., van Ruijven, M. W. M., & Velikov, K. P. (2012). Oil-in-water Pickering emulsions stabilized by colloidal particles from the water-insoluble protein zein. *Soft Matter*, 8(25), 6807–6815.
- Destribats, M., Wolfs, M., Pinaud, F., Lapeyre, V., Sellier, E., Schmitt, V., & Ravaine, V. (2013). Pickering emulsions stabilized by soft microgels: Influence of the emulsification process on particle interfacial organization and emulsion properties. *Langmuir*, 29(40), 12367–12374.
- Dickinson, E. (2012). Use of nanoparticles and microparticles in the formation and stabilization of food emulsions. *Trends in Food Science & Technology*, 24(1), 4–12.
- Dokić, L., Krstonošić, V., & Nikolić, I. (2012). Physicochemical characteristics and stability of oil-in-water emulsions stabilized by OSA starch. *Food Hydrocolloids*, 29(1), 185–192.
- Domian, E., Brynda-Kopytowska, A., & Oleksza, K. (2015). Rheological properties and physical stability of o/w emulsions stabilized by OSA starch with trehalose. *Food Hydrocolloids*, 44, 49–58.
- Duffus, L. J., Norton, J. E., Smith, P., Norton, I. T., & Spyropoulos, F. (2016). A comparative study on the capacity of a range of food-grade particles to form stable O/W and W/O Pickering emulsions. *Journal of Colloid and Interface Science*, 473, 9–21.
- Elsabee, M. Z., Morsi, R. E., & Al-Sabagh, A. M. (2009). Surface active properties of chitosan and its derivatives. *Colloids and Surfaces B: Biointerfaces*, 74(1), 1–16.
- Estrada-Fernández, A. G., Román-Guerrero, A., Jiménez-Alvarado, R., Lobato-Calleros, C., Alvarez-Ramirez, J., & Vernon-Carter, E. J. (2018). Stabilization of oil-in-water-in-oil (O1/W/O2). Pickering double emulsions by soluble and insoluble whey protein concentrate-gum Arabic complexes used as inner and outer interfaces. *Journal of Food Engineering*, 221, 35–44.
- EU (2011). Commission Regulation (EU) No 53/2011 of 21 January 2011 amending Regulation (EC) No 606/2009 laying down certain detailed rules for implementing Council Regulations (EC) No 479/2008 as regards the categories of grapevine products, oenological practices and the applicable restrictions. <http://eur-lex.europa.eu/LexUriServ/LexUriServ.do?uri=OJ:L:2011:019:0001:0006:EN:PDF>, Accessed date: 2 October 2018.
- EU (2012). Commission Regulations (EU) No 432/2012 of 16 May 2012, establishing a list of permitted health claims made on foods, other than those referring to the reduction of

- disease risk and to children's development and health. <http://eur-lex.europa.eu/LexUriServ/LexUriServ.do?uri=OJ:L:2012:136:0001:0040:EN:PDF>, Accessed date: 2 October 2018.
- FDA (2011). Agency response letter GRAS notice no. GRN 000397. <https://www.fda.gov/Food/IngredientsPackagingLabeling/GRAS/NoticeInventory/ucm287638.htm>, Accessed date: 2 October 2018.
- FSANZ (2013). Food standards Australia New Zealand (FSANZ). Approval report - Application A1077. Fungal chitosan as a processing aid. <https://www.foodstandards.gov.au/code/applications/Documents/A1077-ChitosanAppR.pdf>, Accessed date: 2 October 2018.
- Gaikwad, S. G., & Pandit, A. B. (2008). Ultrasound emulsification: Effect of ultrasonic and physicochemical properties on dispersed phase volume and droplet size. *Ultrasonics Sonochemistry*, 15(4), 554–563.
- Gould, J., Vieira, J., & Wolf, B. (2013). Cocoa particles for food emulsion stabilisation. *Food & Function*, 4(9), 1369–1375.
- Ho, K. W., Ooi, C. W., Mwangi, W. W., Leong, W. F., Tey, B. T., & Chan, E. S. (2016). Comparison of self-aggregated chitosan particles prepared with and without ultrasonication pretreatment as Pickering emulsifier. *Food Hydrocolloids*, 52, 827–837.
- JFCRF (2014). Japan food chemical research foundation. List of existing food additives. [http://www.ffcr.or.jp/zaidan/FFCRHOME.nsf/7bd44c20b0dc562649256502001b65e9/346b67d78f8905324925685c0027a6e0/\\$FILE/En2014.1.30.pdf](http://www.ffcr.or.jp/zaidan/FFCRHOME.nsf/7bd44c20b0dc562649256502001b65e9/346b67d78f8905324925685c0027a6e0/$FILE/En2014.1.30.pdf), Accessed date: 2 October 2018.
- Kalashnikova, I., Bizot, H., Cathala, B., & Capron, I. (2011). New pickering emulsions stabilized by bacterial cellulose nanocrystals. *Langmuir*, 27(12), 7471–7479.
- Kaltsa, O., Michon, C., Yanniotis, S., & Mandala, I. (2013). Ultrasonic energy input influence on the production of sub-micron o/w emulsions containing whey protein and common stabilizers. *Ultrasonics Sonochemistry*, 20(3), 881–891.
- Kargar, M., Fayazmanesh, K., Alavi, M., Spyropoulos, F., & Norton, I. T. (2012). Investigation into the potential ability of Pickering emulsions (food-grade particles) to enhance the oxidative stability of oil-in-water emulsions. *Journal of Colloid and Interface Science*, 366(1), 209–215.



- Kentish, S., & Ashokkumar, M. (2011). The physical and chemical effects of ultrasound. In H. Feng, G. Barbosa-Canovas, & J. Weiss (Eds.). *Ultrasound technologies for food and bioprocessing* (pp. 1–12). New York, NY: Springer Food Engineering Series.
- Kurukji, D., Pichot, R., Spyropoulos, F., & Norton, I. T. (2013). Interfacial behaviour of sodium stearylactylate (SSL) as an oil-in-water pickering emulsion stabiliser. *Journal of Colloid and Interface Science*, 409, 88–97.
- Leal-Calderon, F., & Schmitt, V. (2008). Solid-stabilized emulsions. *Current Opinion in Colloid & Interface Science*, 13(4), 217–227.
- Leclercq, L., & Nardello-Rataj, V. (2016). Pickering emulsions based on cyclodextrins: A smart solution for antifungal azole derivatives topical delivery. *European Journal of Pharmaceutical Sciences*, 82, 126–137.
- Liu, F., & Tang, C. H. (2014). Emulsifying properties of soy protein nanoparticles: Influence of the protein concentration and/or emulsification process. *Journal of Agricultural and Food Chemistry*, 62(12), 2644–2654.
- Liu, F., & Tang, C.-H. (2013). Soy protein nanoparticle aggregates as Pickering stabilizers for oil-in-water emulsions. *Journal of Agricultural and Food Chemistry*, 61(37), 8888–8898.
- Liu, F., & Tang, C.-H. (2016). Soy glycinin as food-grade Pickering stabilizers: Part. I. Structural characteristics, emulsifying properties and adsorption/arrangement at interface. *Food Hydrocolloids*, 60, 606–619.
- Liu, H., Wang, C., Zou, S., Wei, Z., & Tong, Z. (2012). Simple, reversible emulsion system switched by pH on the basis of chitosan without any hydrophobic modification. *Langmuir*, 28(30), 11017–11024.
- McClements, D. J. (2005). *Food emulsions: Principles, practices, and techniques*. Washington: CRC Press 632.
- Mengual, O., Meunier, G., Cayré, I., Puech, K., & Snabre, P. (1999). TURBISCAN MA 2000: Multiple light scattering measurement for concentrated emulsion and suspension instability analysis. *Talanta*, 50(2), 445–456.
- Mohammed, M. H., Williams, P. A., & Tverezovskaya, O. (2013). Extraction of chitin from prawn shells and conversion to low molecular mass chitosan. *Food Hydrocolloids*, 31(2), 166–171.
- Mwangi, W. W., Ho, K.-W., Tey, B.-T., & Chan, E.-S. (2016). Effects of environmental factors on the physical stability of pickering-emulsions stabilized by chitosan particles. *Food Hydrocolloids*, 60, 543–550.

- Payet, L., & Terentjev, E. M. (2008). Emulsification and stabilization mechanisms of O/W emulsions in the presence of chitosan. *Langmuir*, 24(21), 12247–12252.
- Philippova, O. E., & Korchagina, E. V. (2012). Chitosan and its hydrophobic derivatives: Preparation and aggregation in dilute aqueous solutions. *Polymer Science, Series A*, 54(7), 552–572.
- Pickering, S. U. (1907). CXCVI.-emulsions. *Journal of the Chemical Society, Transactions*, 91(0), 2001–2021.
- Qaqish, R., & Amiji, M. (1999). Synthesis of a fluorescent chitosan derivative and its application for the study of chitosan–mucin interactions. *Carbohydrate Polymers*, 38(2), 99–107.
- Saravacos, G., Taoukis, P., Krokida, M., Karathanos, V., Lazarides, H., Stoforos, N., ... Dejmeck, P. (2011). 11th international congress on engineering and food (ICEF11) starch particles for food based Pickering emulsions. *Procedia Food Science*, 1, 95–103.
- Silva, E. K., Gomes, M. T. M. S., Hubinger, M. D., Cunha, R. L., & Meireles, M. A. A. (2015). Ultrasound-assisted formation of annatto seed oil emulsions stabilized by biopolymers. *Food Hydrocolloids*, 47, 1–13.
- Silva, E. K., Rosa, M. T. M. G., & Meireles, M. A. A. (2015). Ultrasound-assisted formation of emulsions stabilized by biopolymers. *Current Opinion in Food Science*, 5, 50–59.
- Silva, E. K., Zabot, G. L., & A Meireles, M. A. (2015). Ultrasound-assisted encapsulation of annatto seed oil: Retention and release of a bioactive compound with functional activities. *Food Research International*, 78, 159–168.
- Song, X., Pei, Y., Qiao, M., Ma, F., Ren, H., & Zhao, Q. (2015). Preparation and characterizations of Pickering emulsions stabilized by hydrophobic starch particles. *Food Hydrocolloids*, 45, 256–263.
- Soria, A. C., & Villamiel, M. (2010). Effect of ultrasound on the technological properties and bioactivity of food: A review. *Trends in Food Science & Technology*, 21, 323–331.
- Stancik, E. J., & Fuller, G. G. (2004). Connect the drops: Using solids as adhesives for liquids. *Langmuir*, 20(12), 4805–4808.
- Suslick, K. S., & Price, G. J. (1999). Applications of ultrasound to materials chemistry. *Annual Review of Materials Science*, 29(1), 295–326.

- Tan, C., Xie, J., Zhang, X., Cai, J., & Xia, S. (2016). Polysaccharide-based nanoparticles by chitosan and gum arabic polyelectrolyte complexation as carriers for curcumin. *Food Hydrocolloids*, 57, 236–245.
- Tcholakova, S., Denkov, N. D., & Lips, A. (2008). Comparison of solid particles, globular proteins and surfactants as emulsifiers. *Physical Chemistry Chemical Physics*, 10(12), 1608–1627.
- Torres, L. G., Iturbe, R., Snowden, M. J., Chowdhry, B. Z., & Leharne, S. A. (2007). Preparation of o/w emulsions stabilized by solid particles and their characterization by oscillatory rheology. *Colloids and Surfaces A: Physicochemical and Engineering Aspects*, 302(1–3), 439–448.
- Tzoumaki, M. V., Moschakis, T., Kiosseoglou, V., & Biliaderis, C. G. (2011). Oil-in-water emulsions stabilized by chitin nanocrystal particles. *Food Hydrocolloids*, 25(6), 1521–1529.
- Wang, W., Du, G., Li, C., Zhang, H., Long, Y., & Ni, Y. (2016). Preparation of cellulose nanocrystals from asparagus (*Asparagus officinalis* L.) and their applications to palm oil/water Pickering emulsion. *Carbohydrate Polymers*, 151, 1–8.
- Wen, C., Yuan, Q., Liang, H., & Vriesekoop, F. (2014). Preparation and stabilization of D-limonene Pickering emulsions by cellulose nanocrystals. *Carbohydrate Polymers*, 112, 695–700.
- Wilhelm, M., Zhao, C.-L., Wang, Y., Xu, R., Winnik, M. A., Mura, J.-L., ... Croucher, M. D. (1991). Poly(styrene-ethylene oxide) block copolymer micelle formation in water. A fluorescence probe study. *Macromolecules*, 24(5), 1033–1040.
- Ye, A., Zhu, X., & Singh, H. (2013). Oil-in-water emulsion system stabilized by protein coated nanoemulsion droplets. *Langmuir*, 29(47), 14403–14410.
- Yusoff, A., & Murray, B. S. (2011). Modified starch granules as particle-stabilizers of oil-in-water emulsions. *Food Hydrocolloids*, 25(1), 42–55.

## CAPÍTULO IV

---

Cellulose nanofibers from banana peels as a Pickering emulsifier: high-energy emulsification processes

*Published in Carbohydrate Polymers, v. 194, 122-131, 2018*

## **Cellulose nanofibers from banana peels as a Pickering emulsifier: high-energy emulsification process**

<sup>1</sup>Ana Letícia Rodrigues Costa, <sup>1</sup>Andresa Gomes,<sup>1</sup>Heloisa Tibolla,<sup>1</sup>Florencia Cecilia Menegalli,<sup>1</sup>Rosiane Lopes Cunha

<sup>1</sup> Department of Food Engineering, Faculty of Food Engineering, University of Campinas (UNICAMP), 13083-862, Campinas, SP, Brazil.

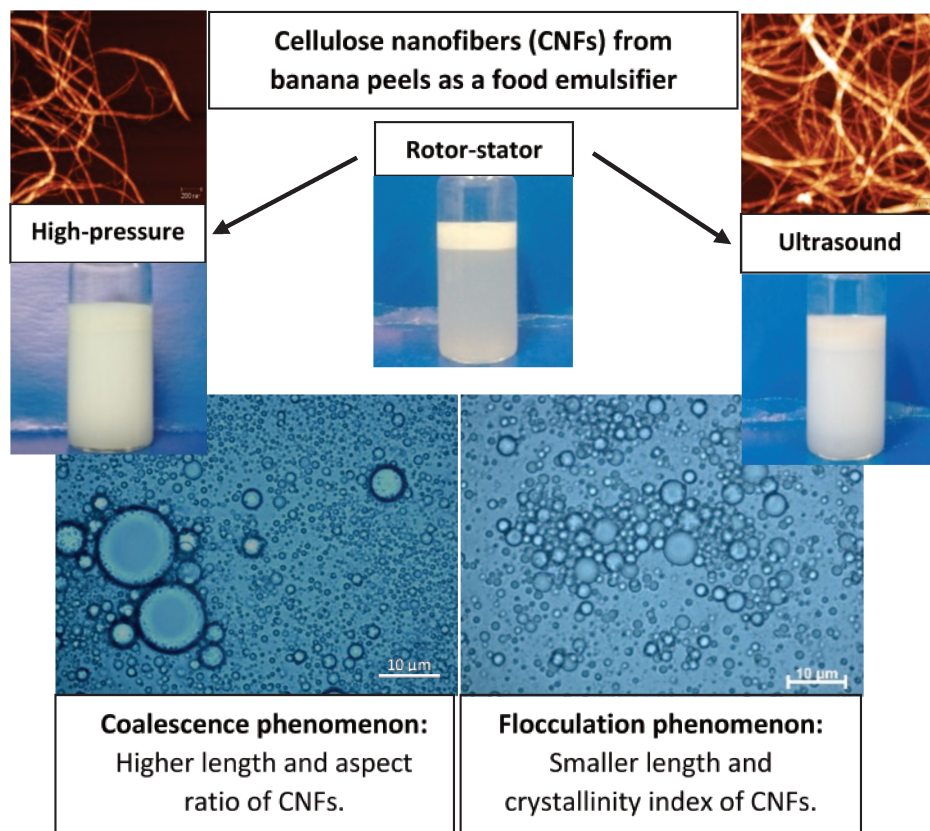
### **Highlights**

- CNFs-stabilized emulsions were produced using high-pressure and ultrasound.
- Cavitation phenomenon and shear forces led to a reduction on the CNFs length.
- Droplets flocculation were observed in the emulsions produced using ultrasound.
- Smaller nanofibers acted as an effective barrier against droplets coalescence.
- Changes on particle properties influence the application of CNFs as an emulsifier

### **Abstract**

Cellulose nanofibers (CNFs) from banana peels was evaluated as promising stabilizer for oil-in-water emulsions. CNFs were treated using ultrasound and high-pressure homogenizer. Changes on the size, crystallinity index and zeta potential of CNFs were associated with the intense effects of cavitation phenomenon and shear forces promoted by mechanical treatments. CNFs-stabilized emulsions were produced under the same process conditions as the particles. Coalescence phenomenon was observed in the emulsions produced using high-pressure homogenizer, whereas droplets flocculation occurred in emulsions processed by ultrasound. In the latter, coalescence stability was associated with effects of cavitation forces acting on the CNFs breakup. Thus, smaller droplets created during the ultrasonication process could be recovered by particles that acted as an effective barrier against droplets coalescence. Our results improved understanding about the relationship between the choice of emulsification process and their effects on the CNFs properties influencing the potential application of CNFs as a food emulsifier.

## Graphical Abstract



**Keywords:** Solid particle; High-pressure homogenizer; Ultrasound; Emulsification; Flocculation; Destabilization mechanism

### 4.1. Introduction

Currently consumers have become more health-conscious and as a consequence the food industry has increased the use of natural ingredients aiming the development of safer and healthier products. Oil-in-water food emulsions have been studied as delivery systems for active compounds or flavors and also to control lipid absorption within the gastrointestinal tract. Stabilization of food emulsions is not an easy task since the number of suitable emulsifiers is limited, increasing the research interest in the development of new food-grade ingredients as emulsions stabilizers (Ho et al., 2016; Mwangi, Ho, Tey, & Chan, 2016; Paximada, Tsouko, Kopsahelis, Koutinas, & Mandala, 2016). Emulsions with droplets coated and stabilized by a layer of adsorbed solid particles onto the oil-water interface are named Pickering emulsions. One of the most important features of the particle-stabilized emulsions is the high physical and energy barrier that prevent droplets coalescence more efficiently than conventional emulsifiers (Berton-Carabin & Schroën, 2015; Pickering, 1907). In addition, depending on the nature of these particles, some allergenic and cytotoxicity effects caused by synthetic emulsifiers could

be eliminated. Irreversible adsorption of some particles onto the interface also contributes to the control of the lipid digestibility, making these systems suitable for the development of products presenting low lipid adsorption that promote satiety and reduce obesity (Chevalier & Bolzinger, 2013; Tzoumaki, Moschakis, Scholten, & Biliaderis, 2013).

Cellulose is the main component of plant cell walls and a potential ingredient for the food industry considering the biocompatibility, biodegradability, renewability and sustainability of this polysaccharide (Kim, Yun, & Ounaies, 2006). Turbak, Snyder, and Sandberg (1983a, 1983b) and Herrick, Casebier, Hamilton, and Sandberg (1983) presented the first method for producing a new type of cellulose morphology, called microfibrillated cellulose (MFC). This new method consisted in the fabrication of cellulose with a large surface area using a homogenization procedure. A series of scientific publications and patents were published by them proposing some applications of MFC as a food additive and as stabilizers of oil-in-water emulsions (Turbak, Snyder, & Sandberg, 1982; Turbak et al., 1983a ; Turbak et al., 1983b; Turbak, Snyder, & Sandberg, 1984). Currently, there are numerous terms to describe microfibrillated cellulose, which include: cellulose nanofibrils, nanofibrillated cellulose, and cellulose nanofibers. Besides, the term “nanocellulose” have been proposed to describe different cellulose-based nanomaterials that have one dimension in the nanometer range including cellulose whiskers, cellulose nanocrystals and nanocrystalline cellulose (NCC) (Gómez et al., 2016; Lee, Aitomäki, Berglund, Oksman, & Bismarck, 2014; TAPPI, 2011). NCCs are derived from cellulose fibers through an acid treatment that results in the removal of amorphous cellulosic domains and retention of crystalline regions (Bondeson, Mathew, & Oksman, 2006; Dong, Revol, & Gray, 1998). Cellulose particles obtained from the byproducts of pharmaceutical and food industries and their application as emulsion stabilizers has been cited in the literature (Mikulcová, Bordes, & Kašpárková, 2016; Paximada et al., 2016; Winuprasith & Supphantharika, 2013). MFC obtained from mangosteen rind was used as emulsion stabilizer and an effective mechanism against coalescence and creaming of oil droplets was observed (Winuprasith & Supphantharika, 2015).

Banana is a popular fruit that grows in tropical and subtropical regions. The high amount of cellulose-rich waste generated by banana during food processing increases the interest to use this biomass aiming to reduce the environmental impact and add value to the cellulose byproduct (Rosa et al., 2010; Tibolla, Pelissari, & Menegalli, 2014). Cellulose nanofibers from banana peels can be produced by chemical and enzymatic treatments (Pelissari, Sobral, & Menegalli, 2014; Tibolla et al., 2014). Acid hydrolysis is the most common technique and sulfuric acid is usually the chosen reactive (Pirani & Hashaikeh, 2013; Teixeira et al., 2011). However, enzymatic treatment is an environmentally friendly process that arises as an

alternative to overcome the drawbacks of the acid hydrolysis process, which involves solvents and/or chemical reagents (Meyabadi & Dadashian, 2012; Siqueira, Bras, & Dufresne, 2010). Xylanases are usually employed in enzymatic hydrolysis. They can initiate the random hydrolysis of the  $\beta$ -1,4 non-reducing terminal regions located between the glycosidic linkages of the glucose units (Hubbe, Rojas, Lucia, & Sain, 2008; Pääkko et al., 2007) and then produce CNFs in colloidal suspensions (Hubbe et al., 2008; Pääkko et al., 2007). Optimum conditions to produce CNFs from banana peel bran by enzymatic hydrolysis was previously established by Tibolla, Pelissari, Rodrigues, and Menegalli (2017). Fixed values of pH (6.0), concentration of the xylanase enzyme (70 U/g of substrate) and substrate (banana peels bran at concentration of 15% w/v), and temperatures ranging between 35 and 55 °C afforded the best conditions.

Cellulose fibers contain crystalline and amorphous domains and their hydrophilic nature allows the formation of oil-in-water emulsions (Binks, 2002). However, in the same way as conventional emulsifiers, the physicochemical properties of cellulose particles such as crystallinity degree and length can be affected by the choice of homogenization method and the energy input amount during the emulsification process. As a consequence, the physical properties of the emulsions can be affected exerting influence on the kinetic stability of Pickering emulsions stabilized by cellulose fibers (Winuprasith & Suphantharika, 2013). Therefore, this study aimed to investigate the simultaneous effect of mechanical treatments on the emulsions production and structure of cellulose nanofibers (CNFs) from banana peels obtained by enzymatic hydrolysis. The physicochemical properties of CNFs were determined aiming to evaluate the influence of emulsification process from ultrasound and high-pressure homogenizer on these particles. In addition, changes on CNFs characteristics during the oil droplets breakup can modify some properties of Pickering emulsions, such as, droplets size and rheological properties, which can enhance their stability over time.

## **4.2. Material and Methods**

### **4.2.1. Material**

The banana peels bran was prepared from unripe banana peels (mature green) of the variety “Terra” (*Musa paradisiaca*) obtained from the southeastern region of Brazil, according to the methodology described by Pelissari, Andrade-Mahecha, Sobral, and Menegalli (2012). Sunflower oil, a long chain triacylglycerol (Bunge Alimentos S.A., Brazil) was purchased in the local market. Its main fatty acid composition was 5.29% palmitic acid (16:0), 3.72% stearic acid (18:0), 41.48% oleic acid (18:1) and 47.64% linoleic acid (18:2). Xylanase enzyme, kindly provided by Novozymes (Araucária – PR, Brazil), was used to produce CNFs by enzymatic



hydrolysis. Deionized water was obtained from a Milli-Q system and all the other chemicals were of analytical grade.

#### **4.2.2. Methods**

##### **4.2.2.1. Production of CNFs**

The bran was delignified to reduce the large amount of amorphous compounds contained in banana peels. An alkaline treatment was performed according to the method described by Tibolla et al. (2014). This process was done using 5% w/v KOH alkaline solution and a bran/solution ratio of 1:20 under vigorous stirring at room temperature during 14 h. Then the substrate was subjected to successive washings with deionized water followed by centrifugation after each washing (15,317xg, 5 °C, 15 min). This treatment partially removed some compounds present in the fiber, such as starch, pectin, and other polysaccharides, as well as the amorphous compounds, hemicellulose and lignin, improving the next step of enzymatic hydrolysis (Tibolla et al., 2017).

Enzymatic hydrolysis was conducted according to the method adapted from Tibolla et al. (2017). Erlenmeyer flasks containing the substrate previously delignified (banana peels bran at concentration of 15% w/v) and 0.1 M acetate buffer at pH 6.0 were placed in a thermostatic shaker at temperature of 35 °C for 10 min to adapt for the medium. Then enzyme xylanase at concentration of 70 U/g of bran (U is defined as 1 mL of xylose released per minute per mL of enzyme) was added to the mixture and left at the same temperature for 24 h under agitation (150 rpm). This step aimed to remove hemicelluloses fractions present in the plant fibers. In addition to attack the amorphous regions, xylanase helped to cleave the  $\beta$ -1,4 glycosidic bonds, isolating the CNFs (Tibolla et al., 2014). After that the suspensions were placed in a thermostatic bath at 80 °C for 30 min to denature the enzyme. Next, the residual pulp was successively washed with deionized water and the solid was separated by centrifugation (15,317xg, 5 °C, 15 min) until neutral pH was reached. The final residue was diluted in deionized water. At the end of these procedures, a colloidal suspension of CNFs was obtained and stored at 4 °C in a sealed container. Yield of CNFs from banana peels obtained under same process conditions of enzymatic hydrolysis was determined and is around 83% (Tibolla et al., 2017). The process to obtain CNFs from banana peels was conducted in duplicate.

##### **4.2.2.2. Characterization of CNFs**

Aqueous dispersion of CNFs were subjected to the same conditions of homogenization used to emulsions preparation (Section 4.2.2.3) without oil phase. Untreated aqueous dispersion

of CNFs were also used as control system. Changes on the physicochemical properties of CNFs caused by ultrasonication or high-pressure were monitored by Fourier-transform infrared spectroscopy, X-ray diffraction, atomic force microscopy and dynamic light scattering measurements.

#### 4.2.2.2.1. Fourier-transform infrared spectroscopy (FTIR) and X-Ray diffraction (XRD)

Aqueous dispersions of CNFs were freeze-dried before to be evaluated for XRD and FTIR analyses (Terroni, model LS 3000, São Paulo, Brazil). An infrared Fourier-transform spectrometer (Perkin Elmer, model Spectrum One, Ohio, USA) equipped with a UATR (universal attenuator total reflectance) accessory was used to analyze the functional groups by absorption spectroscopy in the infrared region ( $4000\text{--}700\text{ cm}^{-1}$ ) with a resolution of  $4\text{ cm}^{-1}$  and 16 scans (Vicentini, Dupuy, Leitzelman, Cereda, & Sobral, 2005).

The crystallinity of the freeze-dried samples was determined by XRD according to Van Soest, Hulleman, de Wit, and Vliegthart (1996). An X-ray diffractometer (Siemens, model D5005, Baden-Wurttemberg, Germany) operating at a voltage of 40 kV and a current of 30 mA was employed; the target was Cu. The crystallinity index (ICr%) of CNFs was calculated by using Equation 4.1 (Segal, Creely, Martin, & Conrad, 1959). In this method, ICr was calculated as the ratio of height between the maximum intensity of the crystalline peak close to  $2\theta = 22^\circ$  ( $I_{200}$ ) and the intensity of the non-crystalline material diffraction peak close to  $2\theta = 18^\circ$  ( $I_{\text{non-cr}}$ ).

$$I_{Cr} = \frac{I_{200} - I_{\text{non-cr}}}{I_{200}} \times 100 \quad (4.1)$$

#### 4.2.2.2.2. Atomic force microscopy (AFM)

Aqueous dispersions of CNFs ( $1.5\text{ }\mu\text{L}$ ) were placed on a grid with mica surface and dried at room temperature to perform AFM analysis. The images were obtained with a microscope (Park systems, model Nx-10, Suwon, Korea) equipped with a camera, under controlled conditions (relative moisture = 10% and temperature =  $25^\circ\text{C}$ ). AFM analyses were performed at the Laboratory for Surface Science (LCS) of the National Nanotechnology Laboratory (LNNano) (Campinas, Brazil). The AFM images were processed using processing analysis software (Gwyddion 2.48) to determine the diameter of the fibers.

#### 4.2.2.2.3. Dynamic light scattering (DLS) measurements

The DLS measurements were performed with a Zetasizer (Malvern Instruments Ltd., Zetasizer Nano Series-model Nano ZS, Worcestershire, England) to determine the surface charge (zeta potential) and to estimate the CNF length in aqueous suspension, at room temperature (25 °C). All the experiments were done in triplicate, and the results are presented as mean values.

#### 4.2.2.3. Preparation of Pickering emulsions

Oil-in-water emulsions (40 g) were firstly prepared by homogenizing the sunflower oil (10% w/w) and aqueous phases (90% w/w) containing 0.01% (w/w) CNFs untreated mechanically (determined from preliminary experiments) in a rotor-stator (Ultra Turrax T18, IKA, Germany) at 10,000 rpm for 2 min. After pre-emulsification, the emulsions were subjected to an emulsification process in a double-stage homogenizer (Panda 2 K NS1001L, Parma, Italy) or a QR 750 W ultrasonic probe (Ultrasonic, Campinas) with a 13 mm diameter titanium probe and a frequency of 20 kHz. The effect of pressure (10, 30, 50 or 70 MPa/5 MPa) or ultrasonication power (225, 375, 525 or 675 W during 2 min) on the properties of the emulsions was evaluated (Section 4.2.2.4.). The emulsification process using ultrasound was carried out into a jacketed vessel attached to a thermostatic bath (Quimis, Brasil) at  $10 \pm 2$  °C, in order to avoid emulsions overheating. A pre-emulsification process followed to a more intense treatment in a rotor-stator homogenizer (Ultra Turrax T18, IKA, Germany) at 13,000 rpm for 2 min was used to prepare control emulsions (RS), once this emulsification method has been widely used in obtaining Pickering emulsions stabilized by food-grade particles. The temperature of preparation did not exceed 37 °C during both emulsification processes. The process to obtain Pickering emulsions stabilized by CNFs from banana peels was conducted in duplicate.

Contact angle measurements between sunflower oil and freeze-dried samples of CNFs as well as interfacial tension between the oily phase (sunflower oil) and aqueous phase (CNFs suspension) were measured using a tensiometer Tracker-S (Teclis, France) at room temperature ( $25 \pm 2$  °C). A 2 µL of oil droplet was deposited with a micro-syringe on the CNFs film surface and the contact angle values were automatically measured after 30 s. CNFs film (diameter = 1 cm) was produced inserting 0.5 g of each sample of CNFs into a circular mold, followed by pressure using a hydraulic press (Shimadzu model SSP-10A) to 0.01 MPa during 2 min. The rising droplet method was used in interfacial tension measurements and the initial oil droplet volume was 6 µL. Measurements were performed in triplicate.

#### **4.2.2.4. Characterization of Pickering emulsions**

##### **4.2.2.4.1. Kinetic stability-laser scanning turbidimetry**

Emulsion stability was monitored using the optical scanning instrument Turbiscan ASG (Formulaction, France). Emulsions were placed in flat-bottomed cylindrical glass tubes (140 mm, height; 16 mm, diameter) and stored at  $25 \pm 2$  °C of storage. The backscattered light at 880 nm was measured just after emulsions preparation and after 6 days. A plot of backscattered light, BS (%) on the y-axis and the sample height (mm) on the x-axis was performed. A sample height of 0 mm corresponds to the bottom of the measuring cell. Measurements were performed in triplicate.

##### **4.2.2.4.2. Optical microscopy and confocal scanning laser microscopy (CSLM)**

The emulsion microstructure was observed by an optical microscope (Axio Scope.A1, Carl Zeiss, Germany) with 100× oil immersion objective lens. The images were captured with the software AxioVision Rel. 4.8 (Carl Zeiss, Germany). The optical microscopy was performed on the freshly prepared emulsions and after 6 days of storage. CNFs-stabilized emulsions was mixed to Congo red dye, stirred for 5 min and incubated overnight in the dark at room temperature (Winuprasith & Suphantharika, 2013). These CNFs-stabilized emulsions were examined using a Zeiss LSM 780-NLO confocal on an Axio Observer Z.1 microscope (Carl Zeiss, Germany) with an objective lens 100x. The images were collected using wavelengths of 488 nm and 605 nm for excitation and emission of the Congo red, respectively.

##### **4.2.2.4.3. Particle size distribution**

The droplet size distribution was determined by laser diffraction using a Mastersizer 2000 (Malvern Instruments Ltd, Malvern, UK) and the rotational velocity was 2100 rpm. Water was used as dispersant and ultrasound was applied for 2 min (before sample introduction) in order to avoid the presence of bubbles. The droplet size was expressed as the volume-surface mean diameter ( $D_{32}$ ), calculated according to Equation 4.2. Measurements were performed on the freshly prepared emulsions and after 6 days of storage in triplicate.

$$D_{32} = \frac{\sum n_i d_i^3}{\sum n_i d_i^2} \quad (4.2)$$

where  $n_i$  is the droplets number with diameter  $d_i$ .

#### 4.2.2.4.4. Rheological assays

Rheological properties of the fresh Pickering emulsions were measured in triplicate at  $25 \pm 2$  °C using a Physica MCR301 modular compact rheometer (Anton Paar, Austria) with stainless steel flat-plate geometry (4 cm) and a 1000 µm gap. The shear rate varied between 0 and  $300 \text{ s}^{-1}$  and the flow curves were obtained in sequential three flow steps: up-down-up cycles. The third flow curve data were fitted to the Newton model (Equation 4.3).

$$\sigma = \eta \dot{\gamma} \quad (4.3)$$

where  $\sigma$  is the shear stress (Pa),  $\eta$  is the viscosity (Pa s) and  $\dot{\gamma}$  is the shear rate ( $\text{s}^{-1}$ ).

#### 4.2.2.4. Statistical analysis

Analysis of variance (ANOVA) was performed using the Minitab 16<sup>®</sup> software and significant differences ( $p < 0.05$ ) between the treatments were evaluated using Tukey analysis.

### 4.3. Results and discussion

#### 4.3.1. Emulsification process influencing properties of CNFs particles

Table 4.1 shows some properties of CNFs measured after different homogenization conditions using ultrasound or high-pressure homogenization. All the CNFs exhibited a reduction on the length after the homogenization processes. The highest length reduction was observed increasing the ultrasound power from 525 W or pressure at 70 MPa. Probably the amorphous zones were degraded and the crystalline zones of the fibers were partly destroyed during both mechanical treatments, resulting in shorter nanofibers (Pelissari et al., 2014). However, the effect of mechanical treatment on the length reduction was more pronounced on CNFs treated with ultrasound than those treated using high-pressure homogenizer. On the other hand, nanofibers diameter was not affected by both mechanical treatments (Table 4.1). Higher diameters were obtained for cellulose nanofibers from banana peels by softer enzymatic hydrolysis (xylanase concentration: 50 U/g of bran) with values of 8.8 nm (Tibolla et al., 2014),

whereas, cellulose nanofibers from potato mechanically treated at high pressure (50 MPa/15 passes) presented diameters around 5 nm (Dufresne, Dupeyre, & Vignon, 2000). Other authors obtained cellulose nanofibrils from cassava bagasse whose diameter and length were found to be in the range of 2–11 and 360–1700 nm, respectively (Teixeira et al., 2011).

**Table 4.1.** Length and diameter size (nm), aspect ratio, zeta potential (mV), crystallinity index (ICr%) and contact angle (°)\* of the cellulose nanofibers (0.01% w/w) obtained after different homogenization conditions using ultrasound (US) or high-pressure homogenizer (HP).

Treatment	Treatment condition	Length (nm)	Diameter (nm)	Aspect ratio	Zeta potential (mV)	ICr (%)	Contact angle (°)
Untreated	-	3444±508 <sup>a</sup>	3.5±0.8 <sup>a</sup>	972±103 <sup>a</sup>	-24.3±2.2 <sup>a</sup>	66.7	23.6±2.0 <sup>a</sup>
	10	3440±119 <sup>a</sup>	3.5±1.3 <sup>a</sup>	985±72 <sup>a</sup>	-49.2±1.4 <sup>b</sup>	68.0	16.1±2.2 <sup>b</sup>
HP (MPa)	30	3493±518 <sup>a</sup>	3.4±2.0 <sup>a</sup>	1043±135 <sup>a</sup>	-52.9±1.5 <sup>bc</sup>	77.7	19.9±1.8 <sup>ab</sup>
	50	3251±914 <sup>ab</sup>	3.4±3.6 <sup>a</sup>	934±156 <sup>ab</sup>	-52.2±2.8 <sup>bc</sup>	64.3	19.9±0.6 <sup>ab</sup>
	70	1978±269 <sup>abc</sup>	3.4±1.4 <sup>a</sup>	577±36 <sup>bc</sup>	-55.5±1.9 <sup>bc</sup>	64.7	23.6±1.2 <sup>a</sup>
	225	2421±204 <sup>abc</sup>	3.4±1.1 <sup>a</sup>	716±121 <sup>abc</sup>	-54.6±4.3 <sup>bc</sup>	51.9	20.7±2.0 <sup>ab</sup>
US (W)	375	2319±252 <sup>abc</sup>	3.4±1.7 <sup>a</sup>	689±18 <sup>abc</sup>	-57.9±1.7 <sup>c</sup>	52.2	21.7±0.6 <sup>ab</sup>
	525	1594±191 <sup>bc</sup>	3.4±1.3 <sup>a</sup>	462±29 <sup>c</sup>	-56.8±2.2 <sup>bc</sup>	51.3	15.9±2.3 <sup>b</sup>
	675	1492±13 <sup>c</sup>	3.3±1.7 <sup>a</sup>	450±22 <sup>c</sup>	-55.5±3.5 <sup>bc</sup>	51.0	16.1±0.2 <sup>b</sup>

<sup>a-c</sup> Means with the same letters in the same column do not differ statistically ( $p < 0.05$ ).

\*Contact angle measurements between sunflower oil and freeze-dried samples of CNFs.

AFM images of untreated and treated nanofibers subjected to ultrasonication or high-pressure conditions confirmed the presence of CNFs with nanometric diameter. Our results also suggest that cellulose nanofibers were initially a network of entangled filaments (untreated), which were dispersed in a more separate network after mechanical treatments (Figure 4.1). Aspect ratio (defined as the ratio of fiber length to diameter) of untreated CNFs was 972, whereas treated CNFs presented aspect ratio ranging from 716 to 450 increasing the intensity of ultrasound power and from 1043 to 577 with the increase of homogenization pressure (Table 4.1). Fibers with a smaller diameter and shorter length, as the fibers obtained after homogenization processes are more suitable to be used as emulsion stabilizers since they can accommodate better onto the oil droplet interface enhancing the emulsion stability.

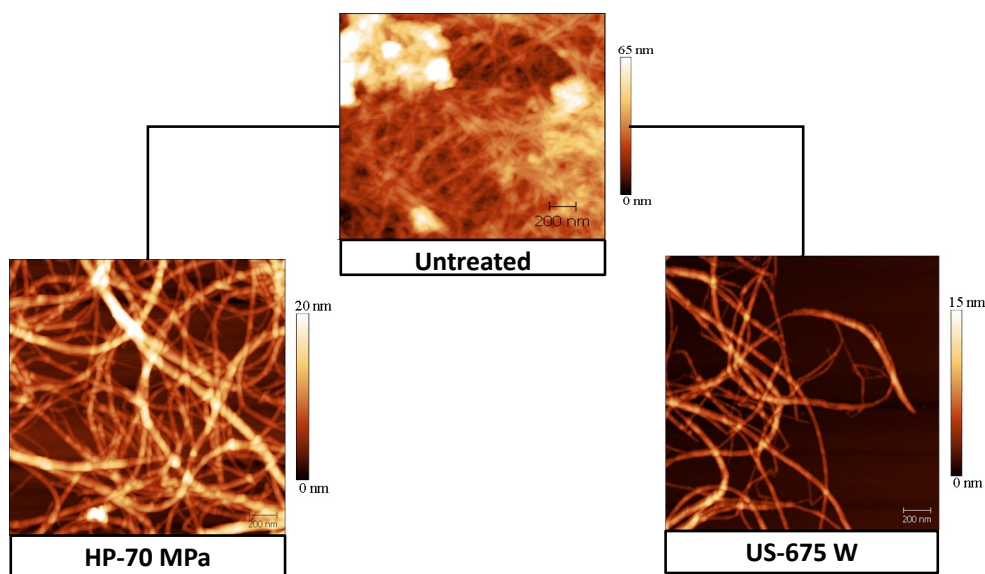


**Figure 4. 1.** AFM images of the untreated and treated cellulose nanofibers obtained after the strongest homogenization conditions using high-pressure homogenizer (HP) or ultrasound (US) (scanning area  $2.0\ \mu\text{m} \times 2.0\ \mu\text{m}$ , scale bar = 200 nm).

All the nanofiber aqueous suspensions exhibited negative zeta potential (Table 4.1), but the untreated CNFs presented the lowest zeta potential value ( $-24.3\ \text{mV}$ ). Application of ultrasound or high-pressure led to an increase in zeta potential values, but the values kept unchanged with the increase of treatments intensity. The high-pressure homogenizer and ultrasound probably promoted better agitation of the suspension and greater contact between CNFs and oxygen, favoring the generation of negative charge on the CNFs surface due to the partial oxidation of the particles (Kitamura, Okawa, Kato, & Sugawara, 2016). A similar increase of the zeta potential values ( $-16.1$  to  $-44.1\ \text{mV}$ ) has been reported for cellulose nanofibers isolated from banana peels using a high-pressure homogenizer (Pelissari et al., 2014). During the droplets breakup, a relative high charge density is required to CNFs aqueous dispersion providing less aggregation (Wang et al., 2016). Therefore, an increase on CNFs zeta potential can favor the emulsion stability by the formation of a stable layer onto the oil droplet due to electrostatic repulsion effect between CNFs, however can limit the confinement of particles onto the interface (Kalashnikova, Bizot, Cathala, & Capron, 2012). Therefore the charge density is also an important parameter to control the kinetic stability of Pickering emulsions and could be changed with the mechanical treatment.

FTIR spectroscopy is a suitable technique to ascertain the vibrations or stretch caused by mechanical treatments on the chemical structure of the CNFs (Bhattacharya et al., 2013). Figure 4.2 depicts the FTIR spectra of the fibers obtained after mechanical treatments and the identified peaks reveal the functional groups present on the samples. The spectra of all

samples present a broad absorption band in the  $3650\text{--}3000\text{ cm}^{-1}$  region corresponding to the -OH groups. The band observed at  $3337\text{ cm}^{-1}$  corresponds to changes in intramolecular hydrogen bonding of cellulose II. The transition from cellulose I to II was confirmed by the shoulder at  $1102\text{ cm}^{-1}$  (Zuluaga et al., 2009). The spectrum of the control exhibited a small peak in these regions, showing the highest intensification in the spectrum of the treated CNFs at 70 MPa. The peak at  $1731\text{ cm}^{-1}$  and  $1034\text{ cm}^{-1}$  became more intense in the spectra of all samples. These peaks correspond to deformation of C=O groups of xylan (main hemicellulose component) and fractions of xyloglucans associated with non-hydrolyzed hemicellulose strongly bound inside the cellulose fibrils (Cherian et al., 2008; Zuluaga et al., 2009). The region at  $2920\text{ cm}^{-1}$  referred to stretching vibrations of the C-H bonds of cellulose and hemicellulose (Pelissari et al., 2014), which intensified in the spectra at 525 W and 675 W, i.e., the highest ultrasound power. The peak at  $2853\text{ cm}^{-1}$  intensified after ultrasound treatments, which corresponds to O-H stretching of the waxes and lignin that remained after enzymatic treatment (Xu, Sun, Sun, Fowler, & Baird, 2006; Zuluaga et al., 2009). On the other hand, the absorption band around  $1609\text{ cm}^{-1}$  attested that all CNFs contained aromatic rings and conjugated carbonyl groups present in the polyphenolic groups of the lignin structure (Hassan, Mathew, Hassan, & Oksman, 2010; Tibolla et al., 2017), which were not affected by mechanical treatments.

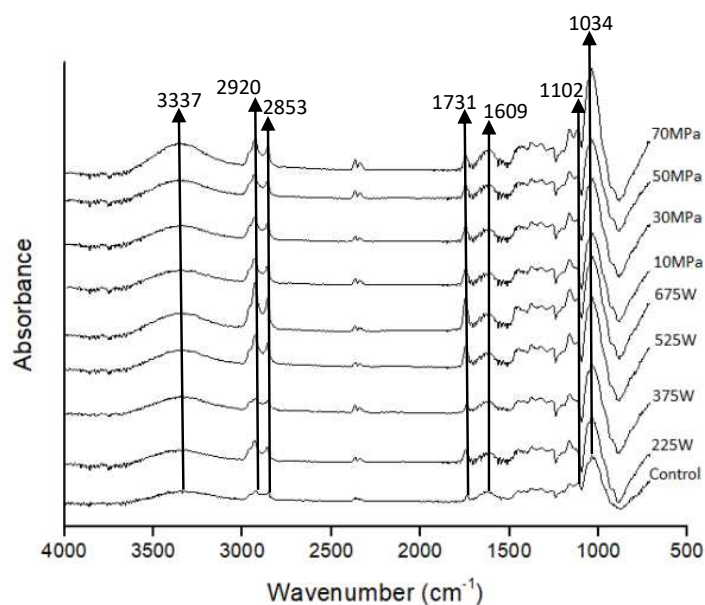


**Figure 4.2.** FTIR spectra of the cellulose nanofibers (0.01% w/w) obtained after different homogenization conditions using ultrasound (W) or high-pressure homogenizer (MPa).

The effect of the mechanical treatment on the crystallinity index of the CNFs was presented in Table 4.1. A slight increase in the ICr values was observed after treatment at 10



and 30 MPa, followed by a reduction with more intense pressure treatment (50 and 70 MPa). All CNFs subjected to mechanical treatment using ultrasound showed lower crystallinity. The increase of crystallinity index was reported for cellulose nanofibers isolated from banana peels with the increase of passages (3, 5 and 7 times) in a high-pressure homogenizer (50/5 MPa) (Pelissari et al., 2014) and increasing the ultrasound power (0–1000 W) (Khawas & Deka, 2016). However, a decrease in the crystallinity index after homogenization process was also observed for microfibrillated cellulose (MFC) from mangosteen rind (Winuprasith & Supphantharika, 2013), sugarcane bagasse (Li et al., 2012) and prickly pear fruit peels (Habibi, Mahrouz, & Vignon, 2009). Our results indicate that the intermolecular hydrogen bonds of cellulose were broken during the homogenization process, causing the collapse of the crystal structure (Winuprasith & Supphantharika, 2013). Structural changes caused by mechanical treatments were confirmed with a pronounced reduction of CNFs length using ultrasound than those obtained from high-pressure homogenizer (Table 4.1). Thus, structural changes can be associated with the forces type occurring during mechanical treatments. Overall, the effects of shear forces promoted by high-pressure homogenizer probably removed only the amorphous cellulosic domains leading to an increase in the crystallinity values. On the other hand, intense cavitation forces promoted by ultrasound could remove the amorphous zone and also degrade the crystalline one causing the reduction in the crystallinity index and length of CNFs.

#### **4.3.2. Contact angle and interfacial tension between oil-water phases**

Interfacial tension and contact angle measurements were performed with the aim to elucidate the stabilization mechanism of oil-in-water emulsions stabilized by CNFs suspensions. The interfacial tension of the sunflower oil droplet in pure water was measured as the control experiment. Values of the initial interfacial tension of both systems (water or CNF) were similar, around 25 mN/m, with a progressive decrease over time. At equilibrium, the interfacial tension between the oil droplet and water was 22 mN/m, while for CNFs suspensions the value was reduced to 20 mN/m (Figure 4.3).

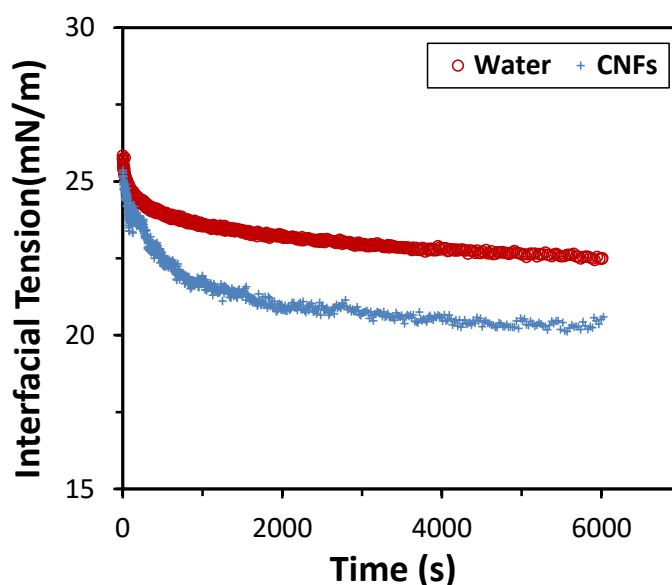


**Figure 4.3.** Dynamic interfacial tension between sunflower oil and water or cellulose nanofibers (CNFs).

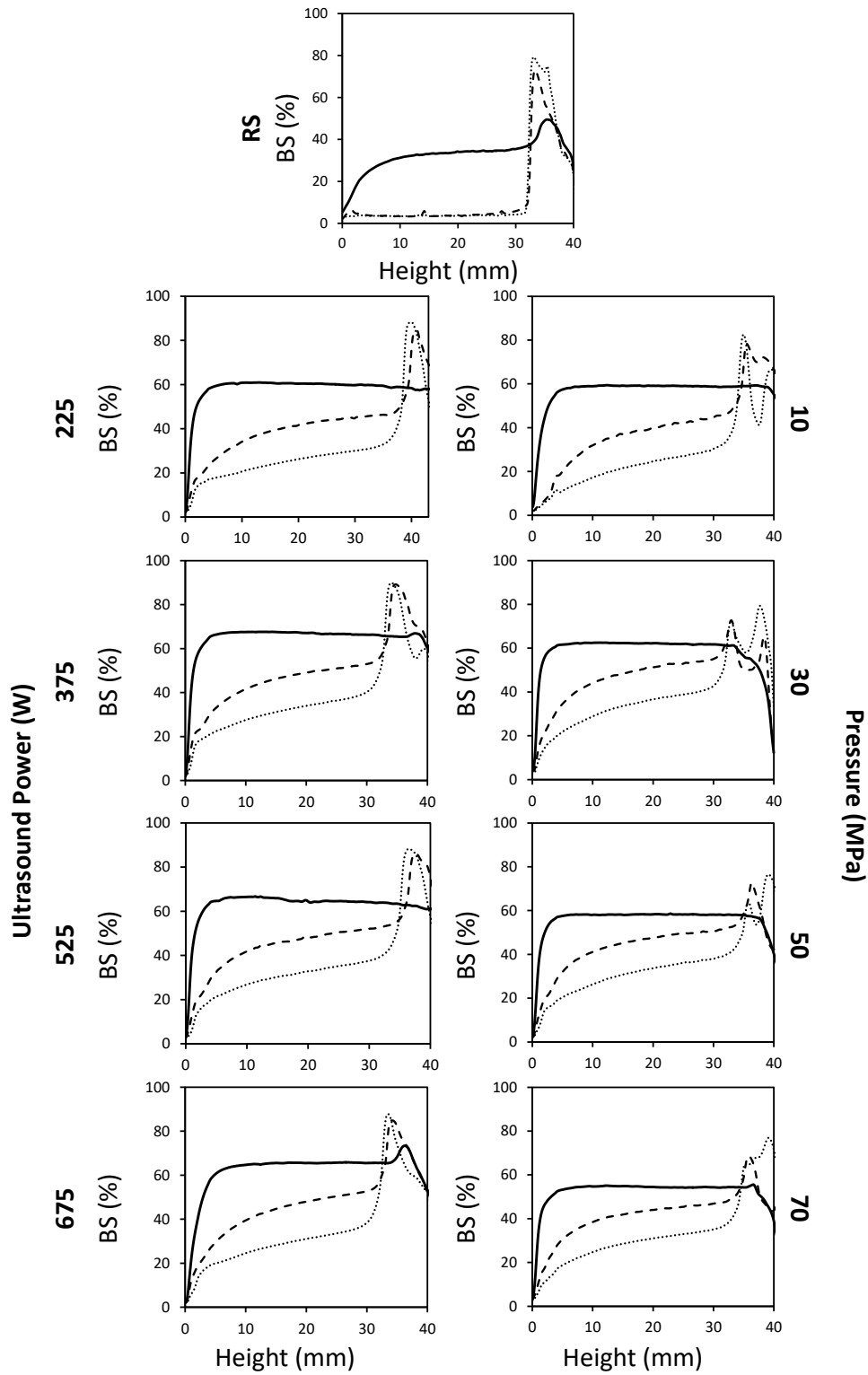
Conventional emulsifiers can decrease the interfacial tension between the oil-water phases favoring droplet breakup during the emulsification process and kinetic stability of the emulsions (Mwangi et al., 2016). Our results showed that the interfacial tension measurements between oil and CNFs aqueous suspensions were very close to water. The reduced ability of CNFs to decrease interfacial tension indicates that the mechanism for emulsion stabilization produced with these particles differs from conventional emulsifiers showing surface activity.

The effect of mechanical treatments on the hydrophobicity of CNFs was investigated by the contact angle between sunflower oil and CNFs films (Table 4.1). Despite of the hydrophilic nature of cellulose (Binks, 2002), our results showed a more pronounced affinity between the oil droplets and CNFs films once the contact angle values were very small varying between  $15^\circ$  and  $24^\circ$ . The lowest values were observed increasing the intensity of ultrasound power, as well as, at lower homogenization pressure. Hydrophobic domains could be formed after partial degradation of crystalline regions of CNFs mainly caused by the cavitation phenomenon promoted by ultrasound process.

#### 4.3.2. Properties of Pickering emulsions

Physical stability of systems was determined in the fresh emulsions and after 1 and 6 days of storage at  $25 \pm 2^\circ\text{C}$ . The multiple light scattering technique provides information about the changes associated with destabilization phenomena before the effective visualization of the phase separation. The backscattering (BS) profiles versus the height of the measurement

cell are shown in Figure 4.4a. The fresh emulsions produced using rotor-stator (RS) presented BS values around 20–40%, while the emulsions produced from ultrasound or high-pressure homogenizer showed values near 60%. After 1 and 6 days, all the profiles suggest the occurrence of creaming phenomenon of oil droplets since BS values decreased at the bottom of the measuring cell and the increase on the top can be attributed to an increase of the droplets concentration. In Pickering emulsions creaming indicate effectively the loss of stability only when the particles adsorption onto the droplets interface are not able to prevent the droplets coalescence and their redispersion by means of gentle stirring (Chevalier & Bolzinger, 2013). The highest phase separation (Figure 4.4b) was observed in emulsions prepared using RS since an abrupt increase in BS values indicates the presence of a defined interface (light and cream layer). During storage droplets that were initially distributed in the emulsified system were concentrated on the top of the measuring cell, so the BS values were higher than the fresh emulsion values (around 80%). A more gradual increase of BS values in emulsions produced using high-pressure homogenizer or ultrasound indicates a slower creaming rate. In addition the BS profiles were slightly affected by intensification of power ultrasound and homogenization pressure (Figure 4.4a). Formation of a thick creaming layer with a clear aqueous bottom phase was also observed in emulsions prepared using rotor-stator and stabilized with wood-based CNFs using rotor-stator. The authors associated creaming phenomenon with the droplets flocculation (droplet clusters) due to hydrophobic interactions and van der Waals forces between CNFs particles (Cunha, Mougél, Cathala, Berglund, & Capron, 2014; Gestranus, Stenius, Kontturi, Sjöblom, & Tammelin, 2017). Carboxymethyl cellulose (CMC), hydroxypropyl methylcellulose (HPMC) and microfibrillated bacterial cellulose (MBC) were used to stabilize emulsions produced by two methods, rotor-stator and ultrasound. MBC showed better emulsifying capacity compared to HPMC and CMC since the MBC fibrils became smaller when subjected to the ultrasonication process favoring their adsorption onto the droplet interface and formation of a network, which prevented droplet coalescence and reduced the rate of phase separation (Paximada et al., 2016). Our results suggest a slower creaming rate (Figure 4.4a) due to the formation of smaller oil droplets, which could also be associated with an easier accommodation of CNFs with a lower aspect ratio (Table 4.1) onto the droplets interface during emulsification using ultrasound and high-pressure homogenizer.



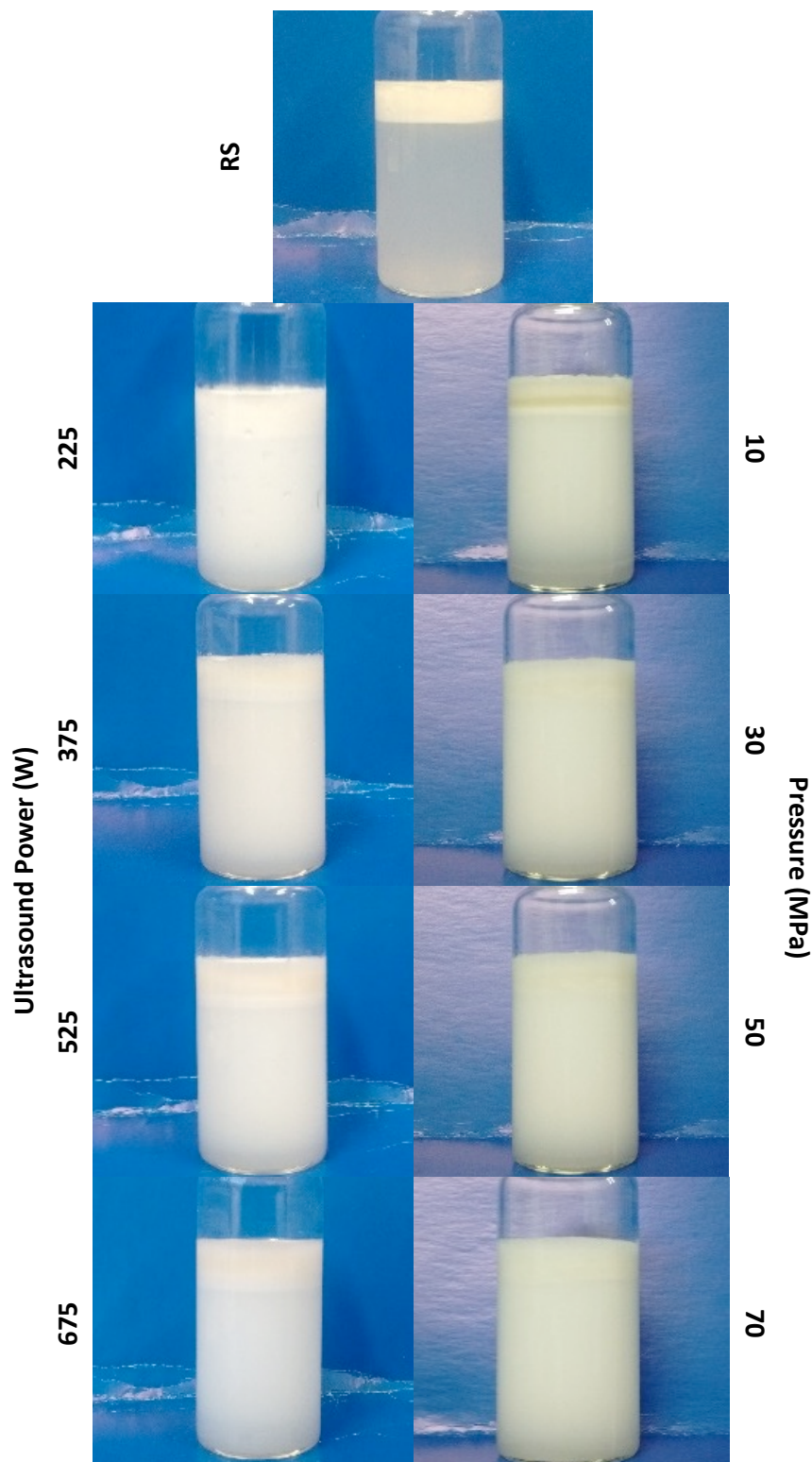


**Figure 4.4.** (a) Backscattering profiles (in fresh (—) and after 1 (---) and 6 (...) days of storage) of emulsions stabilized by cellulose nanofibers (0.01% w/w) obtained from ultrasound (W) and high-pressure processes (MPa). (b) Pictures of measuring cells containing emulsions stabilized by cellulose nanofibers (0.01% w/w) obtained from ultrasound (W) and high-pressure homogenizer (MPa) after 6 days of storage.

Rheological properties of CNFs-stabilized emulsions as a function of ultrasound power or pressure are presented in Table 4.2, showing that all fresh emulsions exhibited Newtonian fluid behavior. Viscosity increased in the emulsions produced using ultrasound, whereas a slight reduction was observed in those obtained under higher pressure (50 and 70 MPa). Viscosity increase could be associated with the intensification of cavitation phenomenon leading to extreme effects of heat, high pressure and high shear rates (Kaltsa, Michon, Yanniotis, & Mandala, 2013; Silva, Gomes, Hubinger, Cunha, & Meireles, 2015), which favored the formation of smaller droplets as well as changes on CNFs properties such as reduction of the length, aspect ratio and crystallinity index. The high-pressure homogenization also promotes cavitation and heating during emulsification, but the driving force prevailing to the droplet breakup is the strong mechanical shear stress exerted on the fluid flowing through the gap between the valve and the seat (Cortés-Muñoz, Chevalier-Lucia, & Dumay, 2009; Costa, Gomes, Andrade, & Cunha, 2017). Shear stress effect was less effective on the reduction of CNFs length and crystallinity index (Table 4.1) resulting in emulsions with the same or lowest viscosity than those obtained from RS. Thus, a high shear stress during high-pressure emulsification was relevant to the droplet breakup but not favored the increase of emulsion viscosity.

**Table 4.2.** Viscosity of emulsions stabilized by cellulose nanofibers (0.01% w/w) obtained from ultrasound (US) or high-pressure homogenizer (HP). Fresh emulsion and after 6 days of storage (6d).

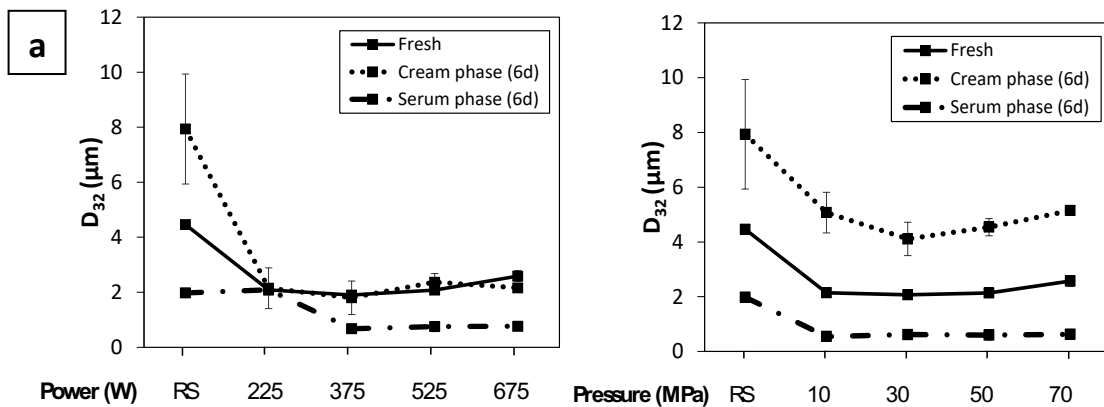
Treatment	Treatment Condition	$\eta$ - Fresh emulsion ( $\times 10^{-3}$ Pa.s)	$\eta$ - Serum phase (6days) ( $\times 10^{-3}$ Pa.s)
Untreated	RS	$1.96 \pm 0.01^{cA}$	$1.53 \pm 0.01^{bB}$
	10	$1.90 \pm 0.01^{cdA}$	$1.53 \pm 0.01^{abB}$
HP (MPa)	30	$1.86 \pm 0.01^{deA}$	$1.53 \pm 0.01^{abB}$
	50	$1.77 \pm 0.01^{eA}$	$1.54 \pm 0.01^{abB}$
	70	$1.77 \pm 0.01^{eA}$	$1.53 \pm 0.01^{abB}$
	225	$2.26 \pm 0.01^{aA}$	$1.53 \pm 0.01^{abB}$
US (W)	375	$2.21 \pm 0.01^{abA}$	$1.53 \pm 0.01^{abB}$
	525	$2.12 \pm 0.01^{bA}$	$1.54 \pm 0.01^{abB}$
	675	$2.23 \pm 0.01^{aA}$	$1.54 \pm 0.01^{aB}$

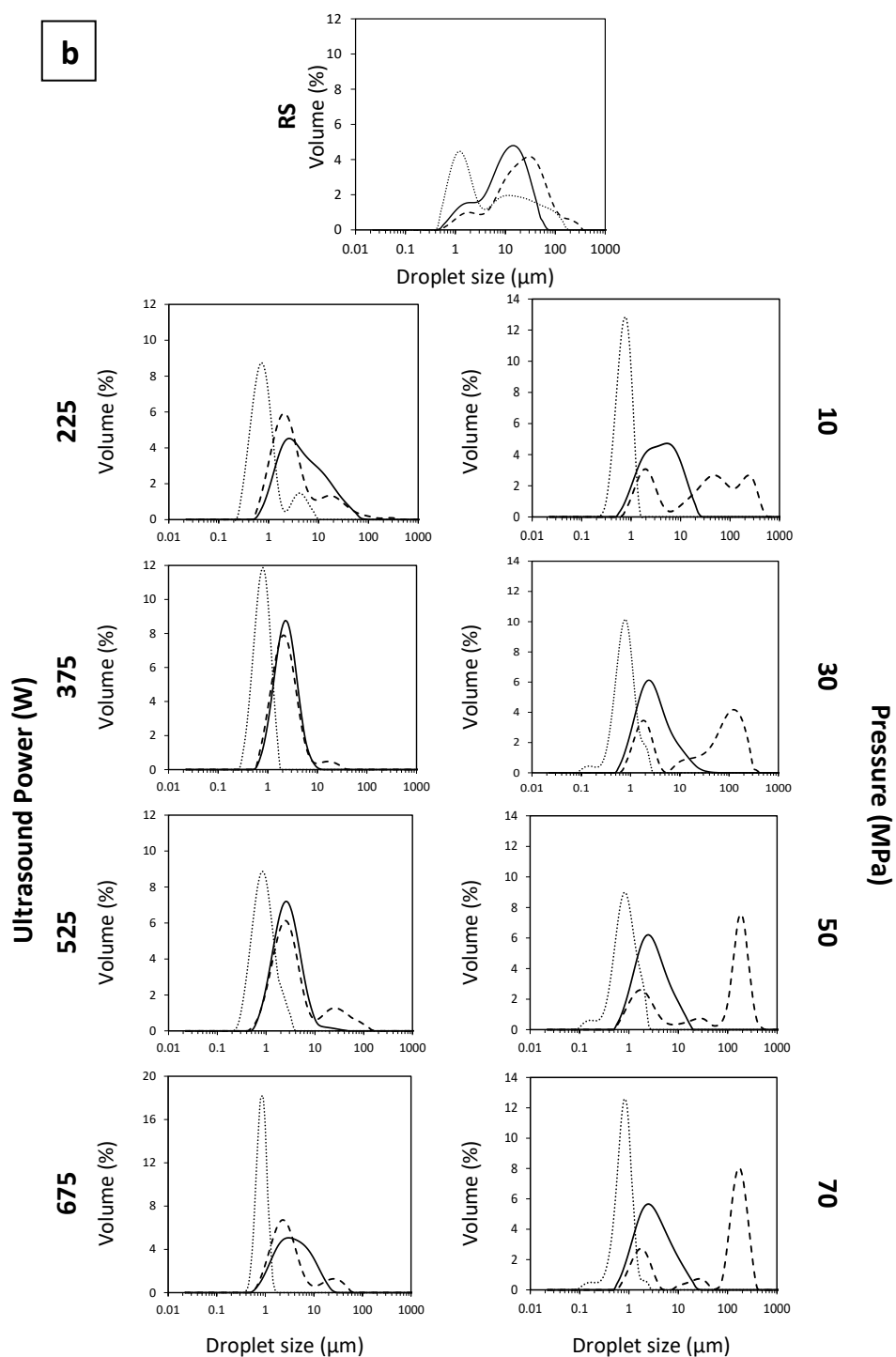
Mean values with the same letter do not differ statistically ( $p < 0.05$ ). Small letters: differences of viscosity between treatments in the same column. Capital letters: differences of viscosity of the fresh emulsion and after 6 days of storage in the same line.

Emulsions stabilized by microfibrillated cellulose (MFC) from mangosteen rind presented non-Newtonian behavior and a viscoelastic network, whereas cellulose nanofibers obtained from softwood fibers could stabilize emulsions by a cellulose network formed in the

continuous phase (Carrillo, Nypelö, & Rojas, 2015; Winuprasith & Suphantharika, 2013). A strongly entangled and disordered network structure was created due to the presence of residual hemicellulose and pectin in the MFC surface, which provide an important mechanism against to the emulsion creaming (Habibi et al., 2009; Winuprasith & Suphantharika, 2013). Formation of a viscoelastic network was not observed in our results, probably due to a low amount or absence of these materials. The alkaline pre-treatment partially removed the amorphous compounds of hemicellulose and lignin, as well as, other compounds present in CNFs, such as starch, pectin, and others polysaccharides (Tibolla et al., 2017). Despite the slight increase in emulsions viscosity produced from ultrasound, the viscosity values were very low in both emulsification processes indicating that creaming by droplets immobilization could not be hindered. As a consequence all the systems presented a similar serum phase viscosity (Table 4.2) and backscattering profiles (Figure 4.4) after 6 days of storage.

Therefore, the decrease of droplet size ( $D_{32}$ ) was the most important property influencing creaming rate of oil droplets of Pickering emulsions. Fresh emulsions produced using rotor-stator (RS) presented a wide bimodal size distribution. However, the width of the droplet size distribution decreased with the increase of ultrasound power or pressure until reach monomodal behavior (Figure 4.5b). As a consequence mean size ( $D_{32}$ ) values of the droplets emulsions was also reduced with the use of ultrasound or high-pressure homogenizer, from 4 to 2  $\mu\text{m}$ . However, no significant reduction in  $D_{32}$  was observed increasing both mechanical treatments intensity (Figure 4.5a). In general, a decrease of the  $D_{32}$  values is associated to an increase of the kinetic stability of emulsions reducing the effects of the gravitational phase separation, once the droplets velocity is proportional to the square of their radius (McClements, 2005).

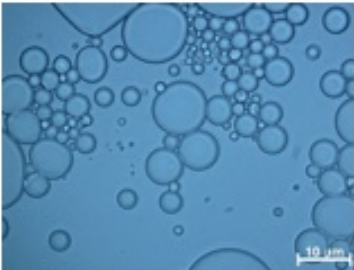
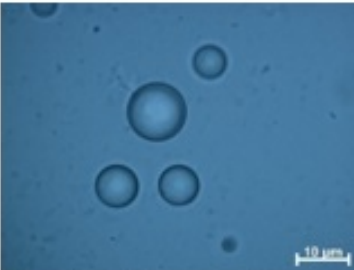
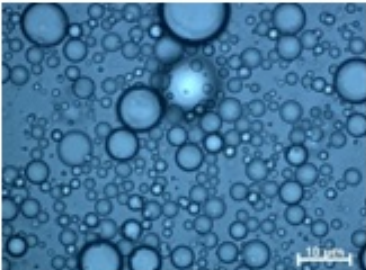
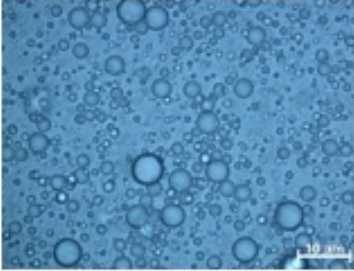
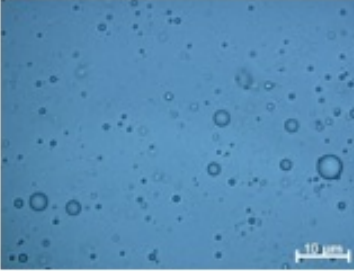
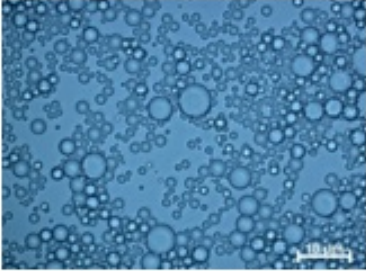
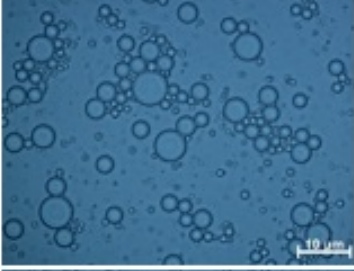
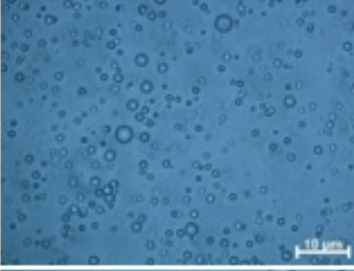
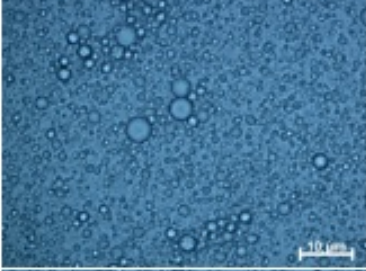
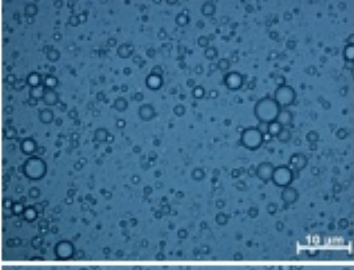
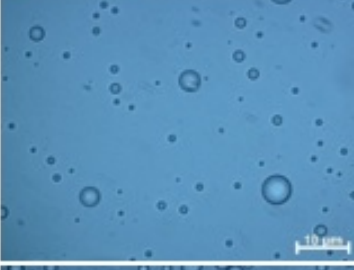
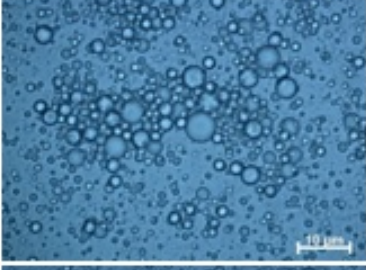
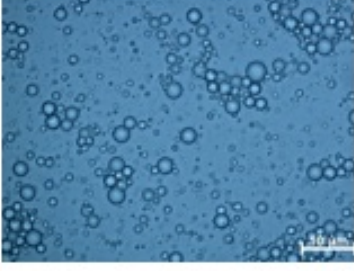
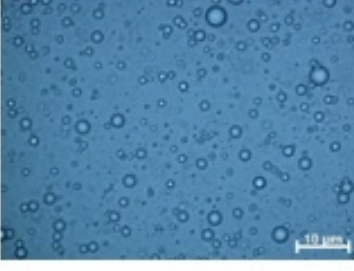
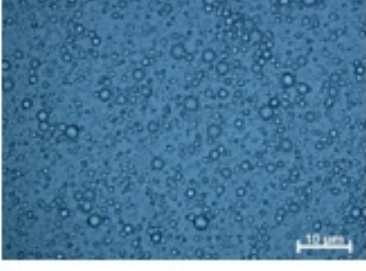


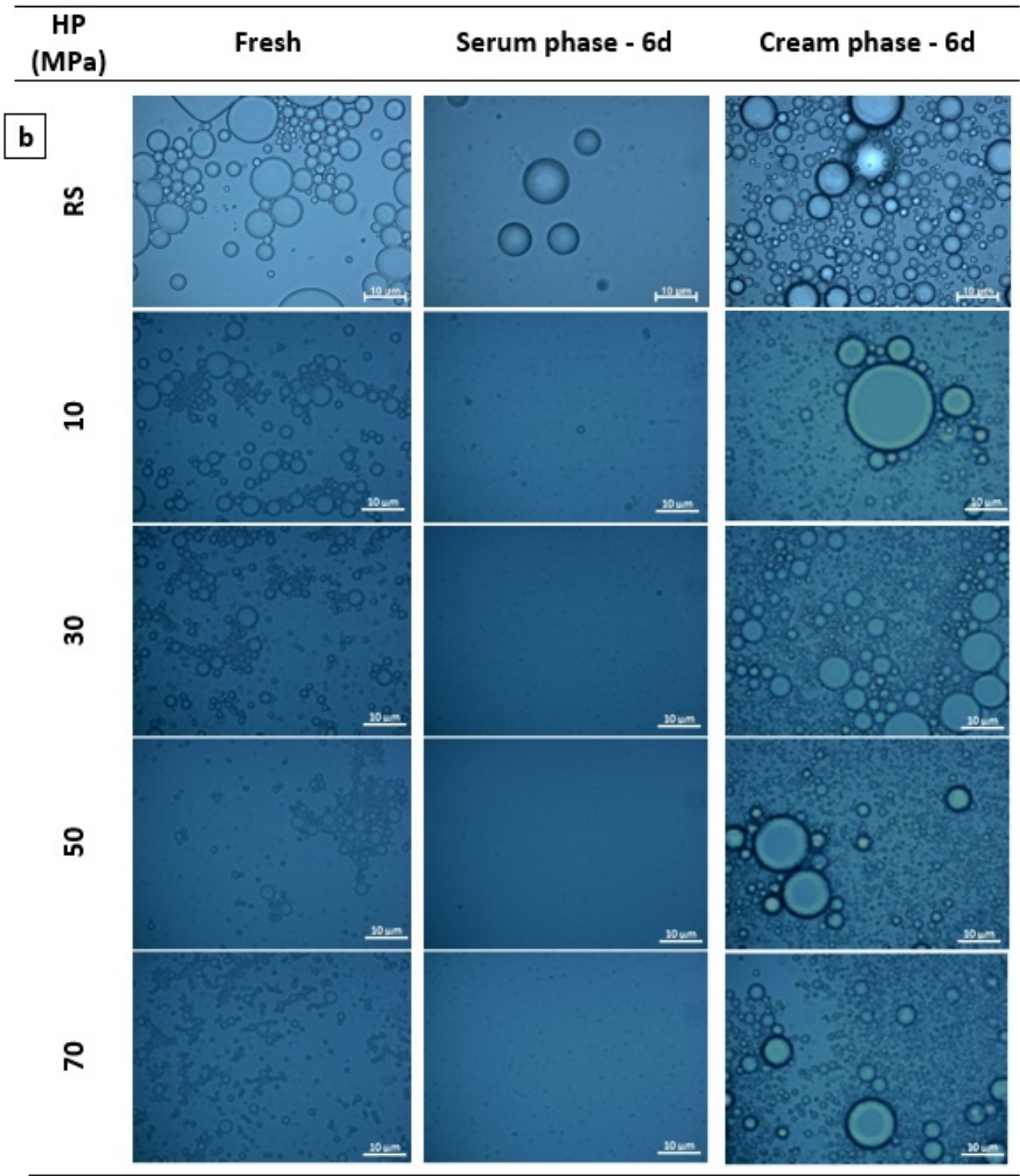


**Figure 4.5.** (a) Mean diameter ( $D_{32}$ ) and (b) size distribution of emulsions stabilized by cellulose nanofibers (0.01% w/w) obtained from ultrasound (W) or high-pressure homogenizer (MPa). Fresh emulsions (—) and after 6 days of storage (6d): (---) cream phase (...) serum phase.



Confocal micrographs revealed the deposition of CNFs (red color) onto the oil-water interface (Figure 4.6c and d), whereas optical micrographs of the emulsions confirmed the results obtained in the size distribution curves (Figure 4.6a and b). After 6 days, the emulsions produced using RS presented large droplets (6–8  $\mu\text{m}$ ) on the cream phase, whereas smaller droplets were observed (2  $\mu\text{m}$ ) in the serum phase. Similar behavior was observed for all emulsions prepared under other emulsification conditions. A narrower droplet size distribution and mean diameter around 1  $\mu\text{m}$  were observed in the serum phase of the emulsions after more intense mechanical treatments. However emulsions prepared using high-pressure homogenizer presented multimodal behavior with mean droplet size between 4 and 7  $\mu\text{m}$  on the cream phase indicating the occurrence of the coalescence phenomenon (Figure 4.5b), while the emulsions prepared using ultrasound showed bimodal behavior and mean droplet size around 2  $\mu\text{m}$ . In the latter case, the droplets were not higher than ones of the fresh emulsions indicating that the phase separation occurred due to flocculation of the droplets (Figure 4.5a). Flocculation is a mechanism, which two or more droplets associate with each other maintaining their individual droplet interface. In this physical process, the size and structure of the flocs exert a great influence on the creaming rate. At low or intermediate droplet concentration, flocculation tends to increase the creaming velocity because the flocs have a larger effective size than the individual droplets (McClements, 2005; Paximada et al., 2016).

P (W)		Fresh	Serum phase - 6d	Cream phase - 6d
a	RS			
	225			
	375			
	525			
	675			





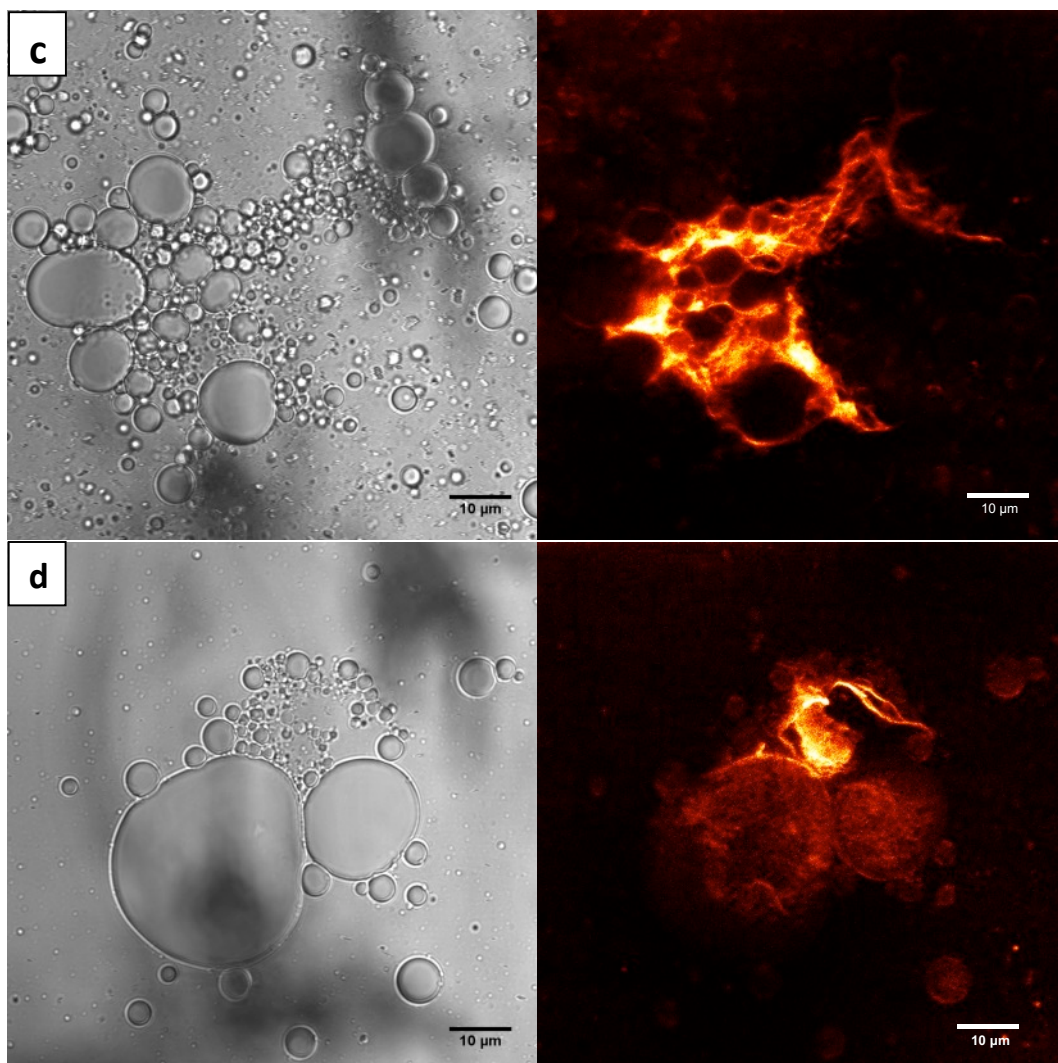


**Figure 4.6.** Optical micrograph emulsions stabilized by cellulose nanofibers (0.01% w/w) obtained from (a) ultrasound (P: power; W) or (b) high-pressure homogenizer (HP: pressure; MPa). Confocal micrograph of emulsion stabilized by cellulose nanofibers and stained with Congo red (red color). Process conditions in (c) ultrasound: 675 W and (d) high-pressure: 50 MPa. Scale bar: 10 µm.

All the emulsions stabilized using cellulose reported in literature showed bimodal or multimodal behavior (Carrillo et al., 2015; Paximada et al., 2016; Winuprasith & Suphantharika, 2015). Specifically, emulsions stabilized by microfibrillated cellulose (MFC) from mangosteen rind presented a slight displacement in the bimodal size distribution towards lower droplet sizes increasing the number of homogenization passes from 0 to 20 (Winuprasith & Suphantharika, 2013). Despite these results, cellulose particles-stabilized emulsions present

good stability against creaming over time. Overall, the kinetic stability of Pickering emulsions stabilized by cellulose particles was mainly due to the formation of a three-dimensional network between particles, whereas the droplet size had a smaller role against emulsion destabilization.

In this work, the low emulsions viscosity was not able to reduce the collision between droplets induced by Brownian motion and separation by gravitational effects (McClements, 2005). In addition, the high surface charge of the particles after the mechanical processes (between  $-49.2$  and  $-57.9$  mV) was not enough prevent the droplets aggregation (flocculation mechanism) by electrostatic repulsion. Therefore, droplets size distribution was an important parameter since, after the first droplets collision the increase of the droplets size can lead to higher creaming rate favoring even more the droplets collision (McClements, 2005). Coalescence phenomenon was observed in the emulsions produced using high-pressure homogenizer due to a slight decrease of the emulsions viscosity and lower amount of CNFs to accommodate and recover the oil droplets interface (higher CNFs length and aspect ratio as showed in Table 4.1). However, the coalescence stability was attained by emulsification using ultrasound, since the slight increase of viscosity reduced the droplets collision, whereas CNFs with smaller length, aspect ratio and crystallinity (Table 4.1) produced during the emulsification process could act onto the oil-water interface as an effective steric barrier against coalescence.

#### 4.4. Conclusion

The effects of emulsification process conditions by ultrasound or high-pressure homogenizer on the physicochemical properties of cellulose nanofibers (CNFs) obtained from banana peels and the use of these fibers to produce Pickering emulsions were studied. The ultrasonication power and pressure promoted a length reduction and changes on the crystallinity index of CNFs and emulsions viscosity. These changes were associated to the intense effects of cavitation phenomenon and shear forces promoted by ultrasound and high-pressure homogenizer, respectively. Emulsions produced using both emulsification processes presented creaming phenomenon of the oil droplets. Coalescence phenomenon was observed in the emulsions produced using high-pressure homogenizer due to a less pronounced effect of shear stress on the CNFs breakup and a reduced CNFs accommodation onto the oil droplet interface (higher length and aspect ratio). However, a higher reduction in the CNFs length and aspect ratio during the emulsification process using ultrasound allowed the formation of enough particles to recover the oil droplets interface preventing the coalescence phenomenon. It was clear that the kinetic stability of emulsions can still be improved by changes on the particle (such as on surface charge and hydrophobicity) and emulsions properties (such as a reduction in the droplets size and increase of viscosity). However our results could provide specific and

relevant findings about how different emulsification processes influence the mechanisms involved in the stability of CNFs-stabilized Pickering emulsions.

### Acknowledgments

The authors thank CAPES – Brazil (DEA/FEA/PROEX) and FAPESP – Brazil (FAPESP 2007/58017-5 and 2011/06083-0) for their financial support. Ana Letícia Rodrigues Costa Lelis thanks CNPq – Brazil (CNPq 140710/2015-9) and Andresa Gomes Brunassi thanks CNPq – Brazil (CNPq 140705/2015-5) for the fellowship; Rosiane Lopes Cunha thanks CNPq (CNPq 307168/2016-6) for the productivity grant. The authors also acknowledge the Prof. Paulo José do Amaral Sobral of Laboratory of Food Technology (FZEA/USP) for allocation of the FTIR equipment and the Brazilian Nanotechnology National Laboratory (LNNano) for allocation of the TEM apparatus.

### References

- Berton-Carabin, C. C., & Schroën, K. (2015). Pickering emulsions for food applications: Background, trends, and challenges. *Annual Review of Food Science and Technology*, 6, 263–297.
- Bhattacharya, S. S., Banerjee, S., Chowdhury, P., Ghosh, A., Hegde, R. R., & Mondal, R. (2013). *Colloids and Surfaces B: Biointerfaces*, 112, 483–491.
- Binks, B. P. (2002). Particles as surfactants-Similarities and differences. *Current Opinion in Colloid & Interface Science*, 7(1–2), 21–41.
- Bondeson, D., Mathew, A., & Oksman, K. (2006). Optimization of the isolation of nanocrystals from microcrystalline cellulose by acid hydrolysis. *Cellulose*, 13, 171.
- Carrillo, C. A., Nypelö, T. E., & Rojas, O. J. (2015). Cellulose nanofibrils for one-step stabilization of multiple emulsions (W/O/W) based on soybean oil. *Journal of Colloid and Interface Science*, 445, 166–173.
- Cherian, B. M., Pothan, L. A., Nguyen-Chung, T., Mennig, G., Kottaisamy, M., & Thomas, S. (2008). A Novel Method for the Synthesis of Cellulose Nanofibril Whiskers from Banana Fibers and Characterization. *Journal of Agricultural and Food Chemistry*, 56(14), 5617–5627.
- Chevalier, Y., & Bolzinger, M.-A. (2013). Emulsions stabilized with solid nanoparticles: Pickering emulsions. *Colloids and Surfaces A: Physicochemical and Engineering Aspects*, 439, 23–34.

- Cortés-Muñoz, M., Chevalier-Lucia, D., & Dumay, E. (2009). Characteristics of submicron emulsions prepared by ultra-high pressure homogenisation: Effect of chilled or frozen storage. *Food Hydrocolloids*, 23(3), 640–654.
- Costa, A. L. R., Gomes, A., Andrade, C. C. P.d., & Cunha, R. L. (2017). Emulsifier functionality and process engineering: Progress and challenges. *Food Hydrocolloids*, 68, 69–80.
- Cunha, A. G., Mougél, J.-B., Cathala, B., Berglund, L. A., & Capron, I. (2014). Preparation of double pickering emulsions stabilized by chemically tailored nanocelluloses. *Langmuir*, 30(31), 9327–9335.
- Dong, X. M., Revol, J. F., & Gray, D. G. (1998). Effect of microcrystallite preparation conditions on the formation of colloid crystals of cellulose. *Cellulose*, 5, 19.
- Dufresne, A., Dupeyre, D., & Vignon, M. R. (2000). Cellulose microfibrils from potato tuber cells: Processing and characterization of starch-cellulose microfibril composites. *Journal of Applied Polymer Science*, 76, 2080–2092.
- Gómez, H. C., Serpa, A., Velásquez-Cock, J., Gañán, P., Castro, C., Vélez, L., & Zuluaga, R. (2016). Vegetable nanocellulose in food science: A review. *Food Hydrocolloids*, 57, 178–186.
- Gestranius, M., Stenius, P., Kontturi, E., Sjöblom, J., & Tammelin, T. (2017). Phase behaviour and droplet size of oil-in-water Pickering emulsions stabilised with plantderived nanocellulosic materials. *Colloids and Surfaces A: Physicochemical and Engineering Aspects*, 519, 60–70.
- Habibi, Y., Mahrouz, M., & Vignon, M. R. (2009). Microfibrillated cellulose from the peel of prickly pear fruits. *Food Chemistry*, 115(2), 423–429.
- Hassan, M. L., Mathew, A. P., Hassan, E. A., & Oksman, K. (2010). Effect of pretreatment of bagasse pulp on properties of isolated nanofibers and nanopaper sheets. *Wood and Fiber Science*, 42(3), 362–376.
- Herrick, F. W., Casebier, R. L., Hamilton, J. K., & Sandberg, K. R. (1983). Microfibrillated cellulose: Morphology and accessibility. *Journal of Applied Polymer Science: Applied Polymer Symposiom*, 37, 797–813.
- Ho, K. W., Ooi, C. W., Mwangi, W. W., Leong, W. F., Tey, B. T., & Chan, E. S. (2016). Comparison of self-aggregated chitosan particles prepared with and without ultrasonication pretreatment as Pickering emulsifier. *Food Hydrocolloids*, 52, 827–837.

- Hubbe, M. A., Rojas, O. J., Lucia, L. A., & Sain, M. (2008). Cellulosic nanocomposites: A review. *BioResources*, 3, 929–980.
- Kalashnikova, I., Bizot, H., Cathala, B., & Capron, I. (2012). Modulation of cellulose nanocrystals amphiphilic properties to stabilize oil/water interface. *Biomacromolecules*, 13(1), 267–275.
- Kaltsa, O., Michon, C., Yanniotis, S., & Mandala, I. (2013). Ultrasonic energy input influence on the production of sub-micron o/w emulsions containing whey protein and common stabilizers. *Ultrasonics Sonochemistry*, 20(3), 881–891.
- Khawas, P., & Deka, S. C. (2016). Isolation and characterization of cellulose nanofibers from culinary banana peel using high-intensity ultrasonication combined with chemical treatment. *Carbohydrate Polymers*, 137, 608–616.
- Kim, J., Yun, S., & Ounaies, Z. (2006). Discovery of cellulose as a smart material. *Macromolecules*, 39(12), 4202–4206.
- Kitamura, Y., Okawa, O., Kato, T., & Sugawara, K. (2016). Effect of ultrasound intensity on the size and morphology of synthesized scorodite particles. *Advanced Powder Technology*, 27, 891–897.
- Lee, K.-Y., Aitomäki, Y., Berglund, L. A., Oksman, K., & Bismarck, A. (2014). On the use of nanocellulose as reinforcement in polymer matrix composites. *Composites Science and Technology*, 105, 15–27.
- Li, J., Wei, X., Wang, Q., Chen, J., Chang, G., Kong, L., ... Liu, Y. (2012). Homogeneous isolation of nanocellulose from sugarcane bagasse by high pressure homogenization. *Carbohydrate Polymers*, 90(4), 1609–1613.
- McClements, D. J. (2005). Food emulsions: Principles, practices, and techniques (2nd ed.). Boca Raton, FL: CRC Press.
- Meyabadi, T. F., & Dadashian, F. (2012). Optimization of enzymatic hydrolysis of waste cotton fibers for nanoparticles production using response surface methodology. *Fibers and Polymers*, 13(3), 313–321.
- Mikulcová, V., Bordes, R., & Kašpárková, V. (2016). On the preparation and antibacterial activity of emulsions stabilized with nanocellulose particles. *Food Hydrocolloids*, 61, 780–792.



- Mwangi, W. W., Ho, K.-W., Tey, B.-T., & Chan, E.-S. (2016). Effects of environmental factors on the physical stability of pickering-emulsions stabilized by chitosan particles. *Food Hydrocolloids*, 60, 543–550.
- Pääkko, M., Ankerfors, M., Kosonen, H., Nykänen, A., Ahola, S., Österberg, M., ... Lindström, T. (2007). Enzymatic hydrolysis combined with mechanical shearing and high-pressure homogenization for nanoscale cellulose fibrils and strong gels. *Biomacromolecules*, 8(6), 1934–1941.
- Paximada, P., Tsouko, E., Kopsahelis, N., Koutinas, A. A., & Mandala, I. (2016). Bacterial cellulose as stabilizer of o/w emulsions. *Food Hydrocolloids*, 53, 225–232.
- Pelissari, F. M., Andrade-Mahecha, M. M., Sobral, P. J.d. A., & Menegalli, F. C. (2012). Isolation and characterization of the flour and starch of plantain bananas (*Musa paradisiaca*). *Starch – Stärke*, 64(5), 382–391.
- Pelissari, F. M., Sobral, P. J.d. A., & Menegalli, F. C. (2014). Isolation and characterization of cellulose nanofibers from banana peels. *Cellulose*, 21(1), 417–432.
- Pickering, S. U. (1907). CXCVI. –Emulsions. *Journal of the Chemical Society, Transactions*, 91(0), 2001–2021.
- Pirani, S., & Hashaikeh, R. (2013). Nanocrystalline cellulose extraction process and utilization of the byproduct for biofuels production. *Carbohydrate Polymers*, 93(1), 357–363.
- Rosa, M. F., Medeiros, E. S., Malmonge, J. A., Gregorski, K. S., Wood, D. F., Mattoso, L. H. C., ... Imam, S. H. (2010). Cellulose nanowhiskers from coconut husk fibers: Effect of preparation conditions on their thermal and morphological behavior. *Carbohydrate Polymers*, 81(1), 83–92.
- Segal, L., Creely, J. J., Martin, A. E., & Conrad, C. M. (1959). An empirical method for estimating the degree of crystallinity of native cellulose using the X-ray diffractometer. *Textile Research Journal*, 29(10), 786–794.
- Silva, E. K., Gomes, M. T. M. S., Hubinger, M. D., Cunha, R. L., & Meireles, M. A. A. (2015). Ultrasound-assisted formation of annatto seed oil emulsions stabilized by biopolymers. *Food Hydrocolloids*, 47, 1–13.
- Siqueira, G., Bras, J., & Dufresne, A. (2010). Cellulosic bionanocomposites: A review of preparation, properties and applications. *Polymers*, 2(4).
- TAPPI (2011). Proposed new TAPPI standard: Standard terms and their definition for cellulose nanomaterial.

- Teixeira, E.d. M., Bondancia, T. J., Teodoro, K. B. R., Corrêa, A. C., Marconcini, J. M., & Mattoso, L. H. C. (2011). Sugarcane bagasse whiskers: Extraction and characterizations. *Industrial Crops and Products*, 33(1), 63–66.
- Tibolla, H., Pelissari, F. M., & Menegalli, F. C. (2014). Cellulose nanofibers produced from banana peel by chemical and enzymatic treatment. *LWT – Food Science and Technology*, 59(2P2), 1311–1318.
- Tibolla, H., Pelissari, F. M., Rodrigues, M. I., & Menegalli, F. C. (2017). Cellulose nanofibers produced from banana peel by enzymatic treatment: Study of process conditions. *Industrial Crops and Products*, 95, 664–674.
- Turbak, A. F., Snyder, F. W., & Sandberg, K. R. (1982). US 4.341.807. Washington, DC, US: Patent and Trademark Office.
- Turbak, A. F., Snyder, F. W., & Sandberg, K. R. (1983a). Microfibrillated cellulose, a new cellulose product: Properties, uses, and commercial potential. *Journal of Applied Polymer Science: Applied Polymer Symposiom*, 37, 815–827.
- Turbak, A. F., Snyder, F. W., & Sandberg, K. R. (1983b). US 4.378.381. Washington DC, US: Patent and Trademark Office.
- Turbak, A. F., Snyder, F. W., & Sandberg, K. R. (1984). US 4.487.634. Washington, DC, US: Patent and Trademark Office.
- Tzoumaki, M. V., Moschakis, T., Scholten, E., & Biliaderis, C. G. (2013). In vitro lipid digestion of chitin nanocrystal stabilized o/w emulsions. *Food and Function*, 4(1), 121–129.
- Van Soest, J. J. G., Hullemans, S. H. D., de Wit, D., & Vliegenthart, J. F. G. (1996). Changes in the mechanical properties of thermoplastic potato starch in relation with changes in B-type crystallinity. *Carbohydrate Polymers*, 29(3), 225–232.
- Vicentini, N. M., Dupuy, N., Leitzelman, M., Cereda, M. P., & Sobral, P. J. A. (2005). Prediction of cassava starch edible film properties by chemometric analysis of infrared spectra. *Spectroscopy Letters*, 38(6), 749–767.
- Wang, W., Du, G., Li, C., Zhang, H., Long, Y., & Ni, Y. (2016). Preparation of cellulose nanocrystals from asparagus (*Asparagus officinalis* L.) and their applications to palm oil/water Pickering emulsion. *Carbohydrate Polymers*, 151, 1–8.

- Winuprasith, T., & Supphantharika, M. (2013). Microfibrillated cellulose from mangosteen (*Garcinia mangostana* L.) rind: Preparation, characterization, and evaluation as an emulsion stabilizer. *Food Hydrocolloids*, 32(2), 383–394.
- Winuprasith, T., & Supphantharika, M. (2015). Properties and stability of oil-in-water emulsions stabilized by microfibrillated cellulose from mangosteen rind. *Food Hydrocolloids*, 43, 690–699.
- Xu, F., Sun, J.-X., Sun, R., Fowler, P., & Baird, M. S. (2006). Comparative study of organosolv lignins from wheat straw. *Industrial Crops and Products*, 23(2), 180–193.
- Zuluaga, R., Putaux, J. L., Cruz, J., Vélez, J., Mondragon, I., & Gañán, P. (2009). Cellulose microfibrils from banana rachis: Effect of alkaline treatments on structural and morphological features. *Carbohydrate Polymers*, 76(1), 51–59.

## CAPÍTULO V

---

Modulating *in vitro* digestibility of Pickering emulsions stabilized by food-grade polysaccharides particles

*Paper to be submitted to Carbohydrate Polymers*

## **Modulating *in vitro* digestibility of Pickering emulsions stabilized by food-grade polysaccharides particles**

Ana Letícia Rodrigues Costa<sup>1</sup>, Andresa Gomes<sup>1</sup>, Guilherme de Figueiredo Furtado<sup>1</sup>, Heloisa Tibolla<sup>1</sup>, Florencia Cecilia Menegalli<sup>1</sup>, Rosiane Lopes Cunha<sup>1</sup>

<sup>1</sup> Department of Food Engineering, Faculty of Food Engineering, University of Campinas (UNICAMP), 13083-862, Campinas, SP, Brazil.

### **Abstract**

An *in vitro* digestibility protocol was used to elucidate the role of different emulsifying polysaccharides particles on the lipid digestion rate of oil-in-water Pickering emulsions. Emulsions stabilized by cellulose crystals (CCrys), cellulose nanofibers (CNFs), chitosan particles and a conventional emulsifier (Tween 80) were evaluated concerning microstructure, droplet size, zeta potential and free fatty acids released during digestion. After gastric step, the high positive charge of chitosan-stabilized emulsions favored the droplets disaggregation resulting in a mild effect of bridging flocculation by particles sharing and displacement of the size curve distribution toward lower size. After passing through the intestinal condition, these emulsions presented few droplets and chitosan aggregates with a monomodal size distribution and high mean size ( $D_{4,3} = 197 \pm 8 \mu\text{m}$ ). On the other hand, Tween 80, CCrys and CNFs were able to inhibit lipid digestion and no changes on droplet mean size were observed following intestinal step. CNFs-stabilized emulsion showed the lowest lipid digestion, whereas the strong adherence of the CCrys particles onto the droplet interface became them resistant to displacement by surface-active components (*i.e.* bile salts and lipase enzyme). On the other hand, a slow lipid hydrolysis could be observed in chitosan-stabilized emulsions promoted by competition between chitosan aggregates and intestinal fluids by the oil droplet interface. Studying the emulsions stabilized using different polysaccharides particles on gastrointestinal conditions we could elucidate important features for their potential application as control systems of lipid digestion rate, as well as, as delivery systems of lipophilic compounds.

**Keywords:** cellulose, nanofibers, Pickering emulsion, free fat acids, lipid digestion

### **5.1. Introduction**

The use of natural and biocompatible ingredients has attracted a lot of attention of food industry considering the growing demand for safer and healthier products by health-conscious consumers. Emulsions stabilized by biopolymer particles, such as polysaccharides and proteins,

have been widely studied as an alternative for replacement of synthetic or semi-synthetic emulsifiers once some allergenic and cytotoxicity effects caused could be eliminated depending on particle nature (Chevalier & Bolzinger, 2013). In addition, a high physical and energy barrier promoted by particles adsorbed onto the droplet interface prevent droplets coalescence more efficiently than conventional emulsifiers (Berton-Carabin & Schroën, 2015; Pickering, 1907).

Lipid digestion is an interfacial process and consequently, the food-particle choice can play an important role on the rate and extent of lipid digestion (Tzoumaki et al, 2013; Yao et al, 2013). An irreversible adsorption (high desorption energy) of some particles onto the interface of oil-in-water emulsion (O/W) contributes to the control of the lipid digestibility restricting the access of bile salts and lipase to the lipid from the dispersed phase. This unique feature makes these systems suitable for the development of products presenting low lipid adsorption, promoting satiety and reducing obesity (Chevalier & Bolzinger, 2013; Sarkar et al, 2017; Tzoumaki et al, 2013).

In the present study, three polysaccharides and one conventional emulsifier were submitted to the simulated gastrointestinal tract system. Tween 80 is a semi-synthetic and non-ionic surfactant capable of promoting the kinetic stability of emulsions by steric hindrance. Recent studies have reported some changes in the emulsion properties stabilized using Tween 80 on gastrointestinal conditions, therefore it was chosen as a model emulsifier (Li et al, 2016; Yao et al, 2013). Chitosan is a cationic polysaccharide obtained from alkaline deacetylation of chitin consisting of repeated *D*-glucosamine and *N*-acetyl-*D*-glucosamine units linked via  $\beta(1\rightarrow4)$  glycosidic bonds (Mohammed et al, 2013). Free amino groups of chitosan are protonated in acid aqueous solution (below  $pK_a \approx 6.5$ ) conferring water solubility and positive charge to this polysaccharide, but low interfacial activity. Chitosan particles are formed when the free amino groups of chitosan chains are deprotonated ( $pK_a > 6.5$ ) and intermolecular attraction between acetyl units (*N*-acetyl-*D*-glucosamine), conferring hydrophobic character to the particles that act as effective biopolymer-emulsifier (Ho et al, 2016; Philippova & Korchagina, 2012). O/W emulsions stabilized by chitosan particles have shown to present high kinetic stability and changes on their properties depending on the pH of the continuous phase (Ho et al, 2016; Mwangi et al, 2016).

Cellulose is the main component of plant cell walls and a potential ingredient for the food industry considering its biocompatibility, biodegradability, renewability and sustainability (Kim et al, 2006). Cellulose nanofibers and crystals have been widely investigated due to their application in numerous areas including as emulsion stabilizers (Gestranus et al, 2017; Winuprasith & Supphantharika, 2015; Yan et al, 2017). Properties of cellulose based emulsifiers are mainly influenced by the shape and size of the particle, as well as, their wettability between

oily and aqueous phases (Hu et al, 2015). Therefore, both cellulose crystals (from cellulose microcrystalline) and cellulose nanofibers (from banana peels) were used to prepare emulsions. Cellulose fibers contain crystalline and amorphous domains with very large aspect ratio (defined as the ratio of fiber length to diameter). Low aspect ratio crystalline particles can be produced when the amorphous regions are removed (Carrillo et al, 2015). The high amount of cellulose-rich waste generated by banana during food processing (Rosa et al, 2010; Tibolla et al, 2014) supported our interest to use this biomass in order to obtain the cellulose nanofibers. On the other hand, the cellulose crystals obtained from microcrystalline cellulose ensure that there is no presence of amorphous groups influencing the adsorption of the particle onto the droplet interface. Cellulose particles have shown to enhance the emulsion stability due to strong interfacial adsorption and interactions between particles that prevents droplets collision and coalescence (Carrillo et al, 2015; Kalashnikova et al, 2011; Winuprasith & Suphantharika, 2015).

Therefore, the aim of this study was to obtain a better understanding of the role of polysaccharides particles as stabilizers of O/W emulsions under gastrointestinal conditions. Pickering emulsions were submitted to *in vitro* digestion protocol in order to evaluate physicochemical and structural changes during digestion process. Interfacial mechanisms involved in the lipid hydrolysis of sunflower oil droplet were investigated using three different polysaccharides (chitosan, CCrys and CNFs) and one conventional emulsifier (Tween 80) to stabilize O/W emulsions.

## 5.2. Material and Methods

### 5.2.1. Material

Low molecular chitosan with a deacetylation degree of 75–85%, cellulose microcrystalline (mean particle= 20µm), dialysis tubing cellulose membrane with 12–14 kDa molecular weight cut off, bile extract (B8631), pancreatin from porcine (P7545) and pepsin from porcine gastric mucosa (77160) were purchased from Sigma-Aldrich (USA). Banana was obtained from the southeastern region of Brazil and the crop was harvested in March 2013. Xylanase enzyme, kindly provided by Novozymes (Araucária – PR, Brazil), was used to produce CNFs by enzymatic hydrolysis. Polyoxyethylene sorbitan monooleate (Tween 80) was obtained from Dinamica Quimica Contemporanea Ltda (Diadema, Brazil). Sunflower oil (Bunge Alimentos, Brazil) was purchased in the local market and ultrapure water was obtained from a Milli-Q system (resistivity 18.2 MΩ/cm). All the chemicals used were of analytical grade.

## 5.2.2. Methods

### 5.2.2.1. Particles preparation

#### 5.2.2.2.1. Chitosan

Chitosan particles were synthesized according to the method previously described by Liu et al. (2012). Briefly, an acetic acid solution (4 M) was prepared, and then the chitosan powder was added to this solution. The mass ratio chitosan to acetic acid was fixed at 2:3. The acid-chitosan solution (0.8 % w/v) was gently stirred for 12 h before to be filtered using a Whatman paper (Grade 1). The chitosan particles were formed by *in situ* deprotonation of the amine groups after adjusting the pH value of the acid-chitosan solution (0.8 % w/v) from 3.3 to 6.9 using 4 M NaOH.

#### 5.2.2.2.2. Cellulose nanofibers (CNFs)

The bran was delignified to reduce the large amount of amorphous compounds contained in banana peels. An alkaline treatment was performed according to the method described by Tibolla et al (2014). This process was done using 5% w/v KOH alkaline solution and a bran/solution ratio of 1:20 under vigorous stirring at room temperature during 14 h. Then, the substrate was subjected to successive washings with deionized water and centrifuged after each washing (10,000 rpm, 5 °C, 15 min). This process removed hemicellulose and lignin improving the next step of enzymatic hydrolysis.

Enzymatic hydrolysis was conducted according to the method adapted from Tibolla et al (2014). Erlenmeyer flasks containing the substrate (banana peels bran at concentration of 15% w/v) and 0.1 M acetate buffer at pH 6.0 were placed in a thermostatic shaker at temperature of 35 °C for 10 min before enzyme addition. Then xylanase at concentration of 70 U/g of bran was added to the mixture and left at the same temperature for 24 h under agitation (150 rpm). After that the suspensions were placed in a thermostatic bath at 80 °C for 30 min to denature the enzyme. Next, the residual pulp was washed with deionized water, the solid was separated by centrifugation (15,317<sub>x</sub>g, 5 °C, 15 min) and suspended in deionized water. At the end of these procedures, a colloidal suspension of CNFs was obtained and stored at 4 °C in a sealed container.

#### 5.2.2.2.3. Cellulose crystals (CCrys)

Cellulose crystals were prepared from cellulose microcrystalline by acid hydrolysis. 1 g of microcrystalline cellulose was added to 35 ml of hydrochloric acid aqueous solution (HCl,



4M) at 80 °C during 3h 45min under vigorous mechanical stirring. The hydrolysis was stopped with the addition of equal volume of ice from deionized water and the excess of hydrochloric acid was removed with 3 centrifugation cycles (15,317<sub>x</sub>g/15 min). After the centrifugation process, the cellulose crystal dispersion was dialyzed against deionized water until dispersion reached pH 6. This process took around 12 h (Araki et al, 1998).

#### 5.2.2.2. Preparation of Pickering emulsions

Oil-in-water emulsions stabilized by Tween 80, chitosan, CCrys and CNFs particles were prepared by homogenizing the oily (10% w/w) and aqueous phases (90% w/w) in rotor-stator (Ultra Turrax T18, IKA, Germany) at 10,000 rpm for 2 min. After pre-emulsification, the emulsions were subjected to an emulsification process in a QR 750 W ultrasonic probe (Ultronique, Campinas) with a 13 mm diameter titanium probe and a frequency of 20 kHz. The emulsification process was carried out into a jacketed vessel attached to a thermostatic bath (Quimis, Brasil) at  $10 \pm 2$  °C, in order to avoid emulsions overheating. Table 5.1 shows the emulsifier/particle concentration in aqueous phase and emulsification process conditions (ultrasound power (P) and time (t)) in high-intensity ultrasound for each emulsifier/particle type. Particle concentrations and emulsification process conditions were defined previously in order to obtain emulsions kinetically stable and oil droplets with similar initial volume mean diameter ( $D_{4,3}$ ), polydispersity and size distribution curves, considering particle composition, size, aspect ratio and shape.

**Table 5.1.** Particle/emulsifier concentration and emulsification process conditions in high-intensity ultrasound

Emulsifier/particle type	Emulsifier/particle concentration	Process conditions: ultrasound power (W)/time (min)
Tween 80	1.0 % (w/w)	150/2
Chitosan	0.6 % (w/v)	675/5
Cellulose crystals (CCrys)	1.0 % (w/w)	225/5
Cellulose nanofibers (CNFs)	0.01 % (w/w)	225/5

#### 5.2.2.3. *In vitro* digestion of the emulsions and free fatty acids release

Emulsions were digested by subjecting them to sequential incubation in simulated gastric fluid and simulated intestinal fluid using the slightly modified *in vitro* digestion protocol of Minekus et al (2014), where according to the authors the mouth step can be eliminated for liquid samples. The samples were placed in a stirred (100 rpm) double jacketed reaction vessel maintained at  $37 \pm 1$  °C (Mun et al, 2016). Then, 60 mL of each sample was incubated for 2 hours

with 60 mL of gastric fluid at pH 3. The gastric fluid contained 6.9 mmol L<sup>-1</sup> of KCl, 0.9 mmol L<sup>-1</sup> KH<sub>2</sub>PO<sub>4</sub>, 25.0 mmol L<sup>-1</sup> NaHCO<sub>3</sub>, 47.2 mmol L<sup>-1</sup> NaCl, 0.1 mmol L<sup>-1</sup> MgCl<sub>2</sub>(H<sub>2</sub>O)<sub>6</sub>, 0.5 mmol L<sup>-1</sup> (NH<sub>4</sub>)<sub>2</sub>CO<sub>3</sub>, 0.15 mmol L<sup>-1</sup> CaCl<sub>2</sub>(H<sub>2</sub>O)<sub>2</sub> and 9.6 mL of freshly prepared pepsin dispersion (25,000 U mL<sup>-1</sup>). After 2 hours of incubation in gastric fluid, 20 mL of sample was collected for immediate characterization (Section 5.2.2.4). Then sample + gastric fluid was mixed with intestinal fluid (1:1). The temperature was adjusted to 37±1°C and pH was adjusted to 7 with 1M NaOH. The intestinal fluid contained 6.8 mmol L<sup>-1</sup> KCl, 0.8 mmol L<sup>-1</sup> KH<sub>2</sub>PO<sub>4</sub>, 85.0 mmol L<sup>-1</sup> NaHCO<sub>3</sub>, 38.42 mmol L<sup>-1</sup> NaCl, 0.33 mmol L<sup>-1</sup> MgCl<sub>2</sub>(H<sub>2</sub>O)<sub>6</sub>, 0.6 mmol L<sup>-1</sup> CaCl<sub>2</sub>(H<sub>2</sub>O)<sub>2</sub>, 70.72 g L<sup>-1</sup> of bile salts and 25 mL of freshly prepared pancreatin dispersion (800 U mL<sup>-1</sup> based on trypsin activity).

During intestinal digestion, the pH was maintained at 7.0 by the addition of 1 M NaOH, through an automatic titration unit (pH-stat T50 titrator, Metler Toledo, Mississauga, Canada). The measurements were taken every 1 minute. The volume of NaOH added to the samples was used to calculate the concentration of free fatty acids (FFA) released in the reaction vessel. FFA released were calculated using Equation 5.1, taking into account the number of moles of NaOH required to neutralize the FFA that could be produced from the triacylglycerols if they were completely digested (assuming the generation of 2 FFAs per triacylglycerol molecule by the action of lipase) (Li & McClements, 2010). After 2 hours of incubation in SIF, samples were taken for structural characterization (Section 5.2.2.4).

$$\%FFA = 100 \cdot \frac{V_{NaOH} \cdot M_{NaOH} \cdot MW_{lipid}}{2 \cdot W_{lipid}} \quad (5.1)$$

where  $V_{NaOH}$  is the volume of NaOH,  $M_{NaOH}$  is the molarity of NaOH,  $MW_{lipid}$  is the average molecular weight of the oil and  $W_{lipid}$  is the weight of lipid initially added in the reaction vessel.

#### 5.2.2.4. Characterization of Pickering emulsions

##### 5.2.2.4.1. Particle size distribution

The droplet size distribution was determined by laser diffraction using a Mastersizer 2000 (Malvern Instruments Ltd, Malvern, UK) and water was used as dispersant. Ultrasound was applied for 2 min in order to avoid the presence of bubbles and the rotational velocity was 1,750 rpm. The droplet size was expressed as the volume mean diameter ( $D_{4,3}$ ), calculated

according to Equation (5.2) and polydispersity index (*Span*) was calculated according to Equation (5.3).

$$D_{4,3} = \frac{\sum n_i D_i^4}{\sum n_i D_i^3} \quad (5.2)$$

$$Span = \frac{d_{(90)} - d_{(10)}}{d_{(50)}} \quad (5.3)$$

where  $n_i$  is the droplets number with diameter  $d_i$  and  $d_{10}$ ,  $d_{50}$  and  $d_{90}$  are the diameters at 10%, 50% and 90% of cumulative volume, respectively.

#### 5.2.2.4.2. Optical microscopy

The emulsion microstructure was observed by an optical microscope (Axio Scope.A1, Carl Zeiss, Germany) with 100x oil immersion objective lens. The images were captured with the software AxioVision Rel. 4.8 (Carl Zeiss, Germany).

#### 5.2.2.4.3. Zeta potential

Zeta potential of the emulsions was determined using a ZetaSizer Nano Series (Malvern Instruments, Worcestershire, UK). Samples were diluted in MilliQ water (0.001 vol %) and then equilibrated for 120 s into the instrument before data collection over 5 continuous readings.

#### 5.2.2.4.4. Statistical analysis

All experiments were performed in duplicate, with at least three measurements being made per sample. The results were reported as the average and the standard deviation of these measurements.

### 5.3. Results and discussion

#### 5.3.1. Characterizing Pickering emulsions in gastric step

Figures 5.1a and b show the effect of each stage of the *in vitro* digestion on the mean diameter ( $D_{4,3}$ ) and droplet size distribution of Pickering emulsions. The  $D_{4,3}$  values ( $D_{4,3}$ = 13  $\mu$ m), polydispersity (*span*= around 2.5%) and size distribution curves (bimodal behavior) of oil droplets were similar for all initial emulsions stabilized by Tween 80 and polysaccharide particles. After the gastric step, the Tween 80 and CCrys-stabilized emulsions presented a slight increase in the  $D_{4,3}$  about of 21  $\mu$ m and 16  $\mu$ m, respectively and almost no change in size

distribution curves. These results indicate the high emulsion stability against droplets coalescence. Microscopies confirmed that the microstructure of Tween 80 and CCrys-stabilized emulsions remained similar after gastric step compared to the initial emulsions before the *in vitro* digestion (Figure 5.2). On the other hand, a substantial increase on droplet mean size ( $D_{4,3} = 87 \mu\text{m}$ ) and shifting of size distribution curve toward higher sizes (multimodal distribution) indicated initially, a partial displacement of the CNFs onto the oil droplets interface by pepsin and/or others gastric fluids components, which could result in the occurrence of droplets coalescence.

Changes in the surface charge of oil droplets due to the emulsifier type and *in vitro* digestion stages were evaluated through zeta potential measurements (Figure 5.3). Initial emulsions stabilized using Tween 80, CCrys and CNFs presented negative charge, whereas chitosan particles-stabilized emulsions showed positive charge. These results are in agreement with previous works (Espinal-Ruiz et al, 2014; Tzoumaki et al, 2013). After gastric step there was a reduction in the magnitude of negative charge of Tween 80, CCrys and CNFs-stabilized emulsions. It was associated to the effects of charge neutralization with salts addition from gastric fluid and pH reduction (pH=3.0). Reduction of negative charge was more pronounced in the CNFs-stabilized emulsions. A lower electrostatic repulsion effect between particles led to the formation of an unstable CNFs layer onto the droplet interface that induced droplets aggregation by non-covalent interactions between particles and creaming phenomenon. Thus, only CNFs systems presented phases separation after gastric step, however, oil layer was not observed on the top phase (Figure 5.4). This instability is related to the occurrence of droplets flocculation, in which two or more droplets were associated each other maintaining their individual droplet interface (Figure 5.2). Droplets flocculation tends to increase the creaming velocity because the flocs have a larger effective size than the individual droplets (Paximada et al, 2016; McClements, 2005). Optical microscopy of the CNFs-stabilized emulsions confirmed the results noticed in the micrographs and size distribution curves, once both a high amount of smaller droplets in flocculated state and a low amount of larger droplets (coalescence phenomenon) were observed (Figure 5.2).

On the other hand, chitosan-stabilized emulsions presented size curve distribution shifted toward lower size resulting in a decrease on droplet mean diameter ( $D_{4,3} = 6 \mu\text{m}$ ) after gastric step (Figure 5.1). Therefore, aggregate state of the oil droplets observed in the initial emulsion was associated to the sharing effects between adsorbed chitosan particles onto the droplets interface (bridging flocculation) (Liu & Tang, 2016; Costa et al, 2018). After passing through the gastric condition, the oil droplets were distributed throughout the gastric fluid and the

sharing of chitosan particles between them was not more observed (Figure 5.2). An increase in the zeta potential ( $\approx +43$  mV) of chitosan-stabilized emulsions suggested an exposition of amino groups after the reduction of emulsion pH from 6.9 to 3 (Figure 5.3). The amino groups of chitosan are protonated below the pKa ( $pK_a \approx 6.7$ ), which confers a high positive surface charge to this polysaccharide (Arrascue et al, 2003). Thus, electrostatic repulsion between chitosan chains favored the droplets disaggregation resulting in a reduced effect of bridging flocculation (by particles sharing) between oil droplets.

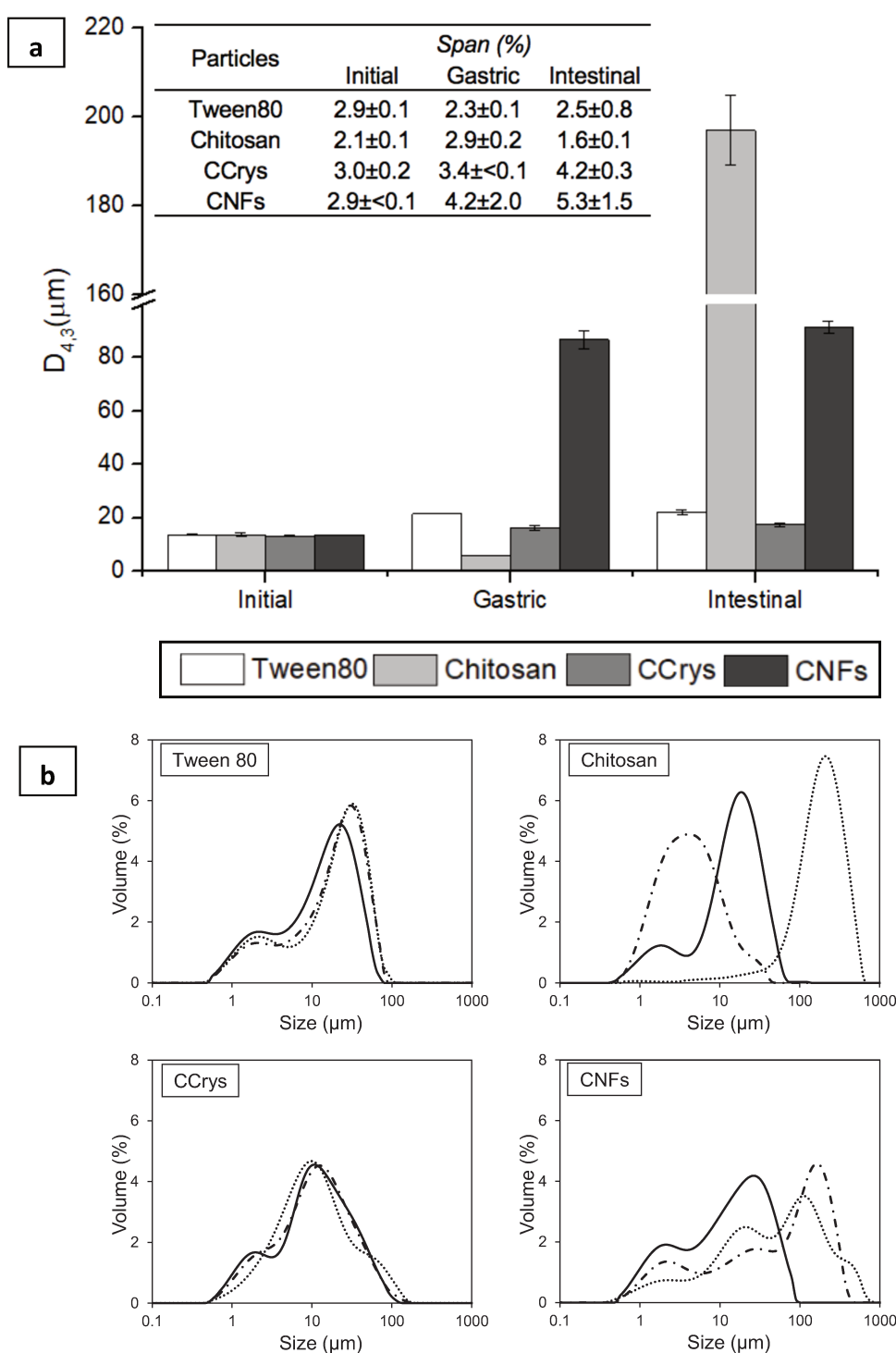


**Figure 5.1.** a) Mean droplet size ( $D_{4,3}$ ) and b) volume size distribution of the Pickering emulsions before digestion (initial or full line) and after gastric (dashed line) and intestinal (dotted line) steps.

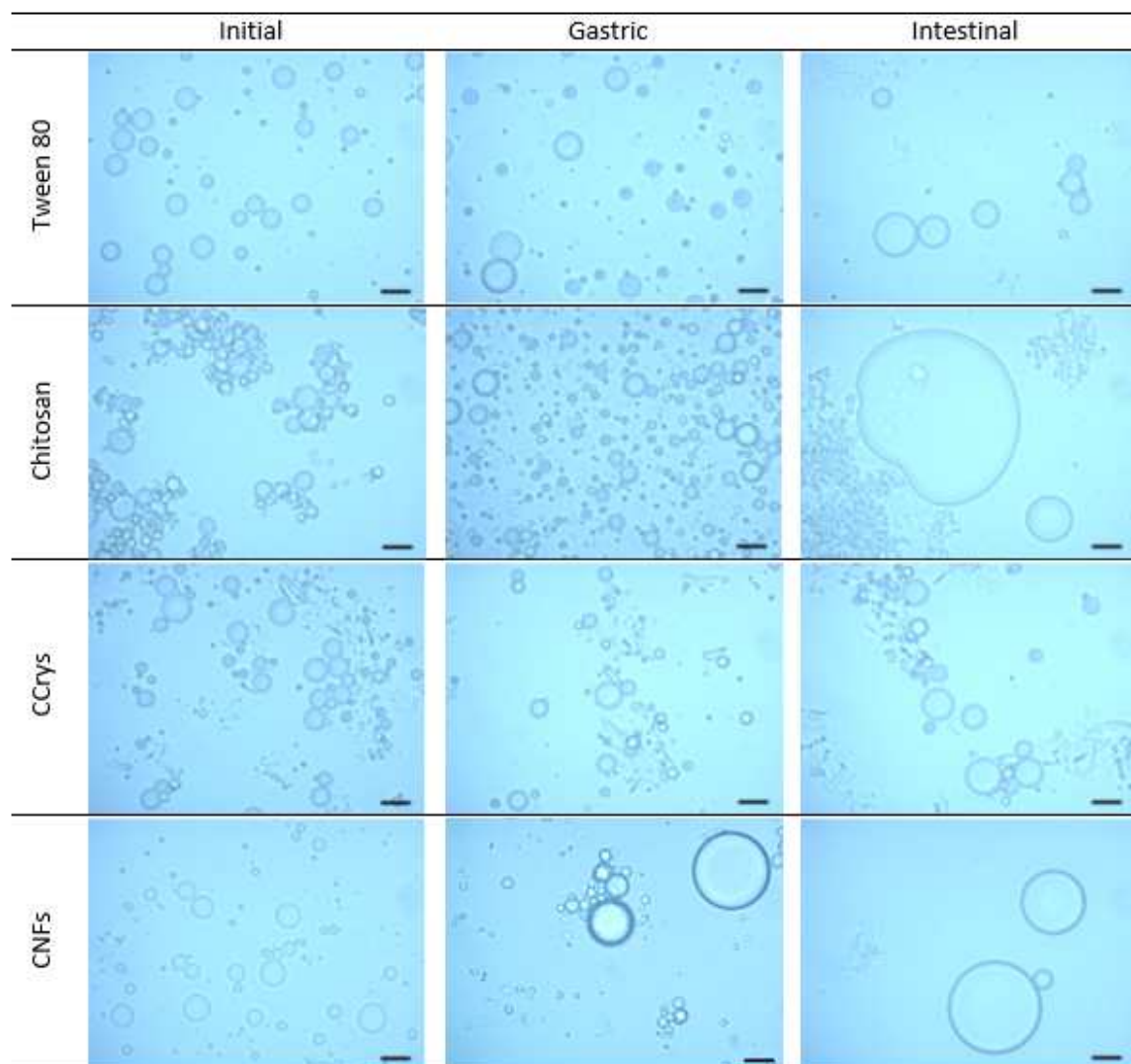


**Figure 5.2.** Microscopy of the Pickering emulsions before digestion (initial) and after gastric and intestinal steps. Scale bar: 10  $\mu\text{m}$ .

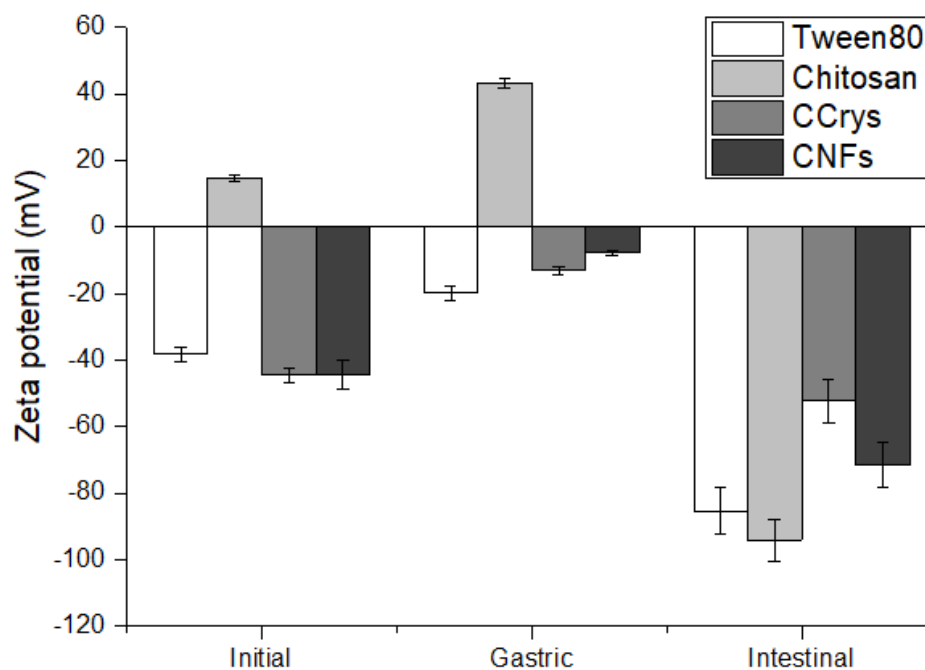


**Figure 5.3.** Zeta potential values of Pickering emulsions before digestion (initial) and after gastric and intestinal steps.

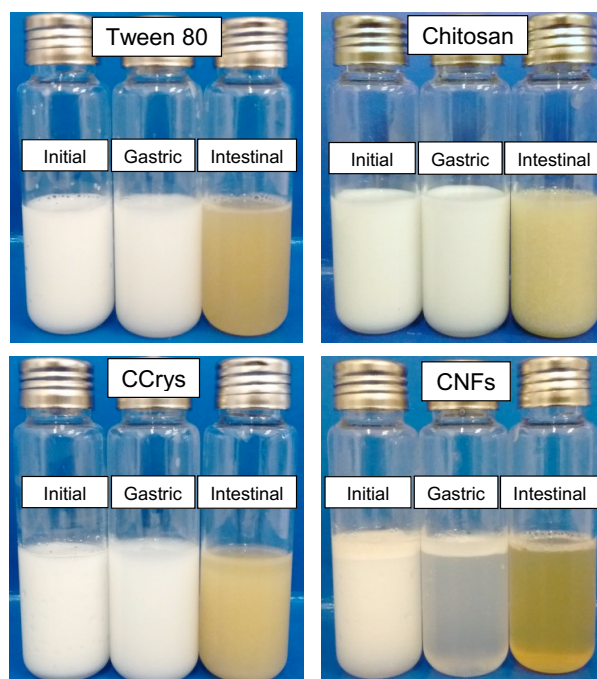


**Figure 5.4.** Visual aspect of the Pickering emulsions before digestion (initial) and after gastric and intestinal steps.

### 5.3.2. Characterizing Pickering emulsions in intestinal step

The intense yellow color of all systems was attributed to the addition of bile salts and no indicative of phase separation was noticed (Figure 5.4). After passing through the intestinal condition, emulsions stabilized by chitosan particles showed a substantial increase in the droplet mean size ( $D_{4,3} = 197 \mu\text{m}$ ) and monomodal distribution with a high mode value (Figure 5.1). Microscopy showed the presence of few droplets and large aggregates, possibly due to almost complete lipid hydrolysis and network formation between chitosan aggregates (Figure 5.2). These results are consistent with the visual observation since an oil layer was not observed, but some aggregation state could be hardly observed once both chitosan aggregates and intestinal fluid were optically opaque. Tween 80 and CCrys systems showed no changes in droplet mean size and microstructure following the intestinal step. A predominance of the coalescence phenomenon between oil droplets was noticed in the CNFs-stabilized emulsions, although no changes on the  $D_{4,3}$  values were observed between gastric and intestinal steps (Figure 5.2). All systems, included chitosan particles-stabilized emulsions, presented an enhance of the negative surface charge after incubation in the intestinal phase (Figure 5.3), which was attributed to the addition of pancreatic lipase, bile salts and other intestinal fluid components, as well as, the formation of lipid digestion products, such as free fatty acids (Sarkar et al, 2010; Zhang et al, 2015).

In the presence of bile salts, the lipase enzyme can adsorb onto the oil droplet interface promoting the hydrolysis of lipids, after that, lipolysis products (mainly free fatty acids) can be absorbed by human body (Bauer et al, 2005; Mun et al, 2007; Yao et al, 2013). Thus, the role of Tween 80 and particles type on the rate and extent of lipid digestion was determined by the amount of free fatty acids (FFAs) released from the oil droplets under intestinal condition (Figure 5.5). The initial rate of FFAs release was faster for emulsions stabilized by chitosan than Tween 80, CCrys and CNFs. In addition, only for Tween 80, CCrys and CNFs- stabilized emulsions, a low (2-5 wt. %) and constant percentage (plateau region) of FFAs release was reached after a certain time (about 15-20 min) whereas this region was not observed for chitosan-stabilized emulsion even after 2 hours under intestinal condition (Figure 5.5). The plateau region corresponds to the maximum concentration of fatty acids released even though all of the lipids had not been digested. This plateau can be reached (or not) depending on some physicochemical effects that prevent the lipase from accessing the undigested lipid (Yao et al, 2013).



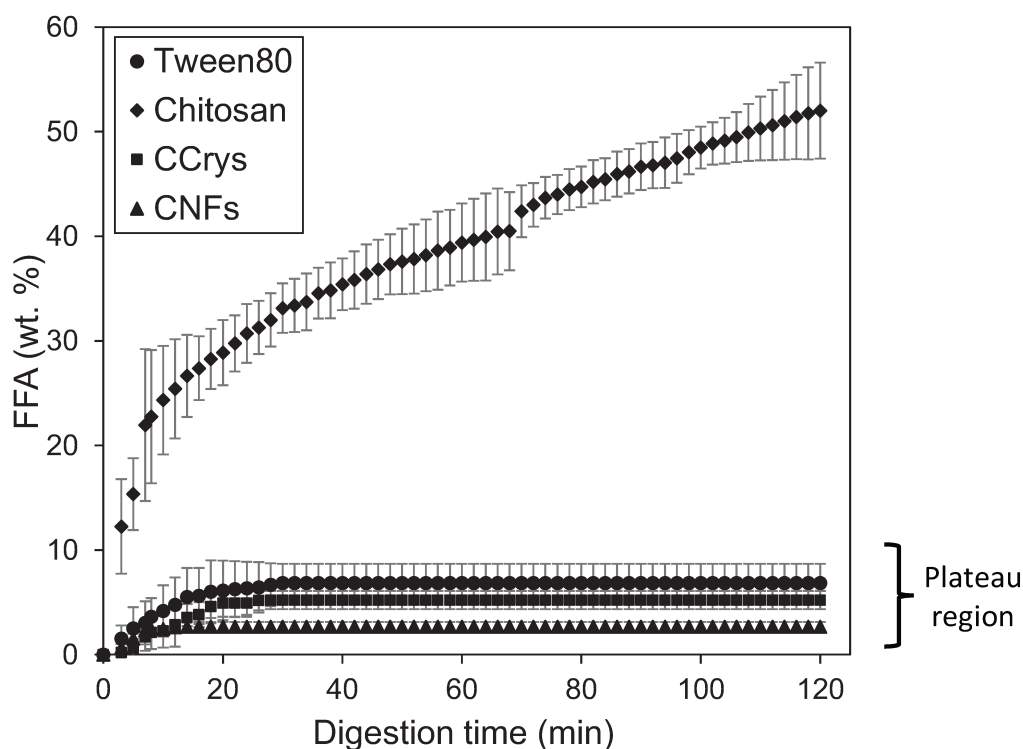


**Figure 5.5.** Kinetics of free fat acids (FFA) release under simulated intestinal conditions.

In particular, our results suggest that Tween 80, CCrys and CNFs were able to inhibit lipid digestion, which may be explained by the occurrence of different physicochemical phenomena associated to the droplet interfacial composition (emulsifier nature) and emulsion properties (Golding & Wooster, 2010). Initially, differences found in the lipid digestion profiles of emulsions could be related to the droplet mean size and size distribution curves after gastric condition. The rate of lipid digestion has been shown to increase with decreasing droplet size (higher interfacial area) once a high number of triacylglycerol chains are exposed to the lipase action (Tzoumaki et al, 2013; Yao et al, 2013). CNFs-stabilized emulsion showed the biggest oil droplets (by coalescence or flocculation) after gastric step and the lowest lipid digestion confirming the more difficult access of lipase to hydrolyze triacylglycerol chains. An opposite result was obtained for chitosan-stabilized systems, which presented the smallest droplet mean size leading to the highest lipid digestion during the intestinal step. In addition, an aggregation state of chitosan was observed since amine groups were neutralized (pH=7-intestinal condition) displacing this polysaccharide from the interface of oil droplets. At the same time, surface-active compounds of the intestinal fluid such as bile salts and phospholipids, as well as, lipase enzyme could adsorb onto the droplet interface promoting the triacylglycerol hydrolysis. Previous study reported the fast and almost complete digestion of oil (about 90 wt.%) in the absence of this polysaccharide (Espinal-Ruiz et al, 2014; Klinkesorn & McClements, 2009). However, we could observe a delayed lipid hydrolysis (about 60 wt.%) promoted by

competition between chitosan aggregates and compounds of the intestinal fluids onto the oil droplets interface, as well as, increasing interactions between chitosan chains due to the exposition of hydrophobic groups at pH=7.0. Since droplet size and zeta potential of Tween 80 and CCrys-stabilized systems have shown similar values after the gastric step, the influence of emulsifier type on lipid hydrolysis was further explored. Emulsions stabilized using high concentrations of Tween 80 (Tween 80 > 0.4%) have shown to be resistant to lipase action and droplet coalescence under *in vitro* digestion conditions. This result has been associated to the presence of free Tween 80 micelles in the aqueous phase that could interact with the bile acids and lipase enzyme, avoiding their adsorption onto the oil droplet interface (Yao et al, 2013). On the other hand, the similar stability of CCrys-stabilized emulsions to the lipid digestion process was associated to the strong adherence of CCrys onto the droplet interface forming a steric layer resistant that can be hardly displaced by surface-active compounds and hindering the lipase action on triglycerides (Tzoumaki et al, 2013). Indeed wheat fiber and microcrystalline cellulose can not practically interact with bile acids (Dongowski, 2007) confirming differences between stabilization mechanisms of particles and conventional emulsifiers. Therefore we assumed that both effects of increasing the surface area of CNFs-stabilized emulsions and the non-displacement of the CCrys particles from the oil droplet interface by surface-active compounds prevented lipid digestion.

Our results indicate that emulsions stability during *in vitro* digestion is modulated according to the properties of emulsifiers. Figure 5.6 shows a schematic representation of the possible physicochemical mechanisms involved in the *in vitro* digestion steps of each emulsifier/particles- stabilized emulsions. We highlight the physicochemical effects discussed throughout this study, as the important role of changes on surface charge and oil droplet size, as well as the differences between mechanisms involved in reducing the lipid digestion rate of conventional emulsifiers and particles-stabilized emulsions.

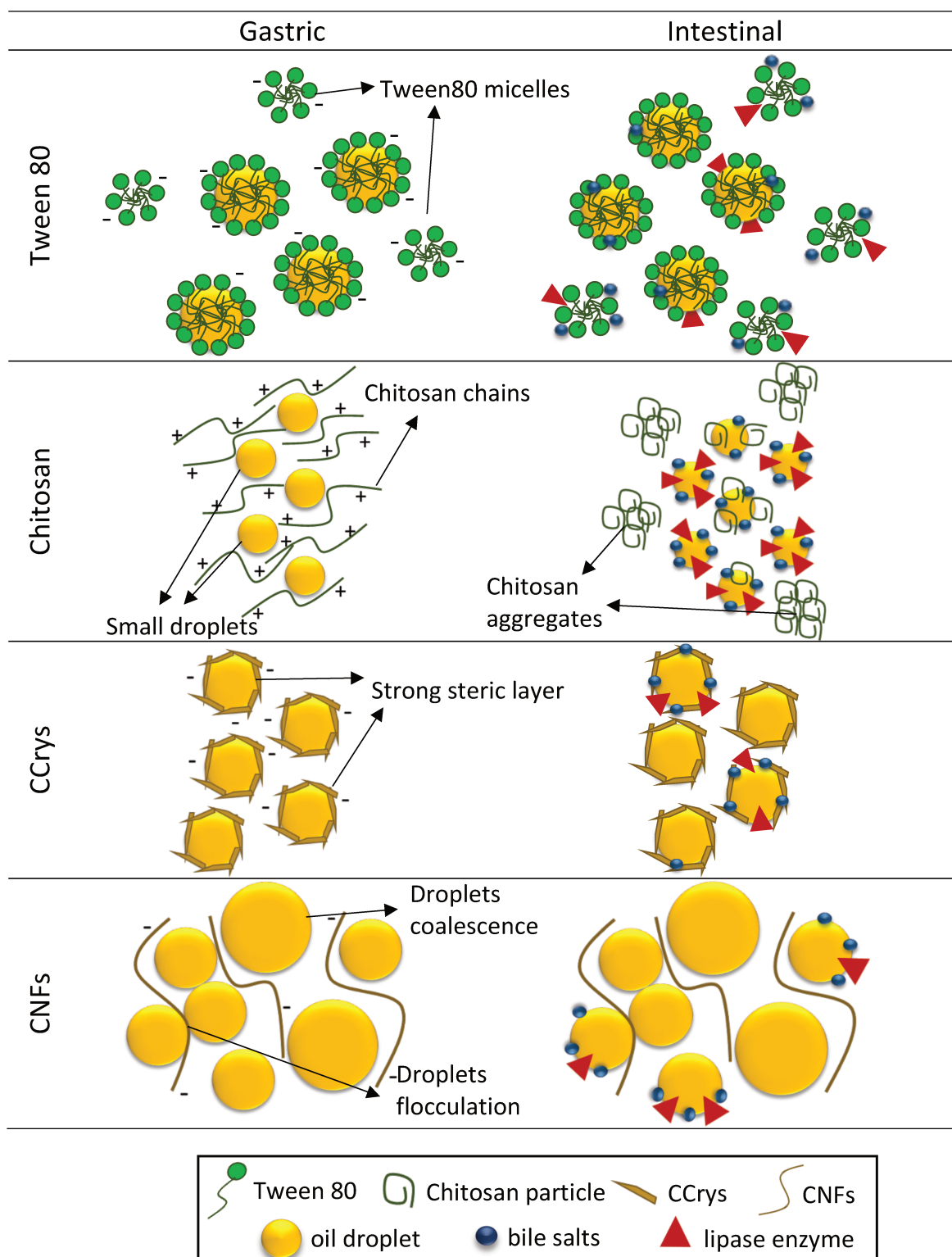


**Figure 5.6.** Schematic representation of the physicochemical mechanism involved in the in vitro digestion steps of each emulsifier/particles- stabilized emulsions.

## 5.4. Conclusion

The choice of different emulsifying polysaccharides particles affected the physicochemical properties of the Pickering emulsions, as well as, the lipid hydrolysis during the simulated *in vitro* digestion. After gastric condition, changes on zeta potential affected the aggregation state of oil droplets resulting in the formation of more or less stable emulsions depending on the nature of the emulsifier. CCrys and CNFs particles were able to inhibit lipid digestion by the strong particle adsorption onto the oil droplet interface and due to the presence of larger oil droplets that reduced the number of triacylglycerol molecules exposed to the lipase action, respectively. Moreover, we also observed a delayed lipid hydrolysis promoted by competition between chitosan aggregates and compounds of the intestinal fluids onto the oil droplets interface, as well as, increasing interactions between chitosan chains due to the exposition of hydrophobic groups at neutral pH. Despite these results, it was clear that stabilization mechanisms during *in vitro* digestion are still not completely understood. However, relevant aspects were provided about the interfacial design of food emulsions using particles as stabilizing systems in order to use these emulsions as delivery systems of active compounds, such as chitosan particles or as lipid digestion inhibitor systems, such as cellulose particles.

## Acknowledgments

The authors thank CAPES – Brazil (DEA/FEA/PROEX) and FAPESP – Brazil (FAPESP 2007/58017-5 and 2011/06083-0) for their financial support. Ana Letícia Rodrigues Costa Lelis thanks CNPq – Brazil (CNPq 140710/2015-9) and Andresa Gomes Brunassi thanks CNPq – Brazil (CNPq 140705/2015-5) for the fellowship; Rosiane Lopes Cunha thanks CNPq (CNPq 307168/2016-6) for the productivity grant.

## References

- Araki, J., Wada, M., Kuga, S. & Okano, T. (1998) Flow properties of microcrystalline cellulose suspension prepared by acid treatment of native cellulose. *Colloids and Surfaces A: Physicochemical and Engineering Aspects*, 142(1), 75-82.
- Arrascue, M. L., Garcia, H. M., Horna, O. & Guibal, E. (2003) Gold sorption on chitosan derivatives. *Hydrometallurgy*, 71(1-2), 191-200.
- Bauer, E., Jakob, S. & Mosenthin, R. (2005) Principles of Physiology of Lipid Digestion. *Asian-Australas J Anim Sci*, 18(2), 282-295.

- Berton-Carabin, C. C. & Schroën, K. (2015) Pickering emulsions for food applications: Background, trends, and challenges. *Annual Review of Food Science and Technology*, 6, 263-297.
- Carrillo, C. A., Nypelö, T. E. & Rojas, O. J. (2015) Cellulose nanofibrils for one-step stabilization of multiple emulsions (W/O/W) based on soybean oil. *Journal of Colloid and Interface Science*, 445, 166-173.
- Chevalier, Y. & Bolzinger, M.-A. (2013) Emulsions stabilized with solid nanoparticles: Pickering emulsions. *Colloids and Surfaces A: Physicochemical and Engineering Aspects*, 439, 23-34.
- Costa, A. L. R., Gomes, A., Cunha, R. L., 2018. One-step ultrasound producing O/W emulsions stabilized by chitosan particles. *Food Research International* 107, 717-725.
- Dongowski, G. (2007) Interactions between dietary fibre-rich preparations and glycoconjugated bile acids in vitro. *Food Chemistry*, 104(1), 390-397.
- Espinal-Ruiz, M., Parada-Alfonso, F., Restrepo-Sanchez, L.-P., Narvaez-Cuenca, C.-E. & McClements, D. J. (2014) Impact of dietary fibers [methyl cellulose, chitosan, and pectin] on digestion of lipids under simulated gastrointestinal conditions. *Food & Function*, 5(12), 3083-3095.
- Gestranius, M., Stenius, P., Kontturi, E., Sjöblom, J. & Tammelin, T. (2017) Phase behaviour and droplet size of oil-in-water Pickering emulsions stabilised with plant-derived nanocellulosic materials. *Colloids and Surfaces A: Physicochemical and Engineering Aspects*, 519(Supplement C), 60-70.
- Golding, M. & Wooster, T. J. (2010) The influence of emulsion structure and stability on lipid digestion. *Current Opinion in Colloid & Interface Science*, 15(1–2), 90-101.
- Ho, K. W., Ooi, C. W., Mwangi, W. W., Leong, W. F., Tey, B. T. & Chan, E. S. (2016) Comparison of self-aggregated chitosan particles prepared with and without ultrasonication pretreatment as Pickering emulsifier. *Food Hydrocolloids*, 52, 827-837.
- Hu, Z., Ballinger, S., Pelton, R. & Cranston, E. D. (2015) Surfactant-enhanced cellulose nanocrystal Pickering emulsions. *Journal of Colloid and Interface Science*, 439, 139-148.
- Kalashnikova, I., Bizot, H., Cathala, B. & Capron, I. (2011) New pickering emulsions stabilized by bacterial cellulose nanocrystals. *Langmuir*, 27(12), 7471-7479.
- Kim, J., Yun, S. & Ounaies, Z. (2006) Discovery of Cellulose as a Smart Material. *Macromolecules*, 39(12), 4202-4206.

- Klinkesorn, U. & McClements, D. J. (2009) Influence of chitosan on stability and lipase digestibility of lecithin-stabilized tuna oil-in-water emulsions. *Food Chemistry*, 114(4), 1308-1315.
- Li, J., Hwang, I.-C., Chen, X. & Park, H. J. (2016) Effects of chitosan coating on curcumin loaded nano-emulsion: Study on stability and in vitro digestibility. *Food Hydrocolloids*, 60(Supplement C), 138-147.
- Li, Y. & McClements, D. J. (2010) New Mathematical Model for Interpreting pH-Stat Digestion Profiles: Impact of Lipid Droplet Characteristics on in Vitro Digestibility. *Journal of Agricultural and Food Chemistry*, 58(13), 8085-8092.
- Liu, F. & Tang, C.-H. (2016) Soy glycinin as food-grade Pickering stabilizers: Part. I. Structural characteristics, emulsifying properties and adsorption/arrangement at interface. *Food Hydrocolloids*, 60, 606-619.
- Liu, H., Wang, C., Zou, S., Wei, Z. & Tong, Z. (2012) Simple, reversible emulsion system switched by pH on the basis of chitosan without any hydrophobic modification. *Langmuir*, 28(30), 11017-11024.
- McClements, D. J. (2005). *Food Emulsions: Principles, Practices, and Techniques*, 2nd edition. CRC Press, Boca Raton, FL.
- Minekus, M., Alming, M., Alvito, P., Ballance, S., Bohn, T., Bourlieu, C., Carriere, F., Boutrou, R., Corredig, M., Dupont, D., Dufour, C., Egger, L., Golding, M., Karakaya, S., Kirkhus, B., Le Feunteun, S., Lesmes, U., Macierzanka, A., Mackie, A., Marze, S., McClements, D. J., Menard, O., Recio, I., Santos, C. N., Singh, R. P., Vegarud, G. E., Wickham, M. S. J., Weitschies, W. & Brodtkorb, A. (2014) A standardised static in vitro digestion method suitable for food - an international consensus. *Food & Function*, 5(6), 1113-1124.
- Mohammed, M. H., Williams, P. A. & Tverezovskaya, O. (2013) Extraction of chitin from prawn shells and conversion to low molecular mass chitosan. *Food Hydrocolloids*, 31(2), 166-171.
- Mun, S., Decker, E. A. & McClements, D. J. (2007) Influence of emulsifier type on in vitro digestibility of lipid droplets by pancreatic lipase. *Food Research International*, 40(6), 770-781.
- Mun, S., Park, S., Kim, Y.-R. & McClements, D. J. (2016) Influence of methylcellulose on attributes of  $\beta$ -carotene fortified starch-based filled hydrogels: Optical, rheological,

- structural, digestibility, and bioaccessibility properties. *Food Research International*, 87, 18-24.
- Mwangi, W. W., Ho, K.-W., Tey, B.-T. & Chan, E.-S. (2016) Effects of environmental factors on the physical stability of pickering-emulsions stabilized by chitosan particles. *Food Hydrocolloids*, 60, 543-550.
- Paximada, P., Tsouko, E., Kopsahelis, N., Koutinas, A. A. & Mandala, I. (2016) Bacterial cellulose as stabilizer of o/w emulsions. *Food Hydrocolloids*, 53, 225-232.
- Philippova, O. E. & Korchagina, E. V. (2012) Chitosan and its hydrophobic derivatives: Preparation and aggregation in dilute aqueous solutions. *Polymer Science - Series A*, 54(7), 552-572.
- Pickering, S. U. (1907) CXCVI.-Emulsions. *Journal of the Chemical Society, Transactions*, 91(0), 2001-2021.
- Rosa, M. F., Medeiros, E. S., Malmonge, J. A., Gregorski, K. S., Wood, D. F., Mattoso, L. H. C., Glenn, G., Orts, W. J. & Imam, S. H. (2010) Cellulose nanowhiskers from coconut husk fibers: Effect of preparation conditions on their thermal and morphological behavior. *Carbohydrate Polymers*, 81(1), 83-92.
- Sarkar, A., Horne, D. S. & Singh, H. (2010) Interactions of milk protein-stabilized oil-in-water emulsions with bile salts in a simulated upper intestinal model. *Food Hydrocolloids*, 24(2), 142-151.
- Sarkar, A., Zhang, S., Murray, B., Russell, J. A. & Boxal, S. (2017) Modulating in vitro gastric digestion of emulsions using composite whey protein-cellulose nanocrystal interfaces. *Colloids and Surfaces B: Biointerfaces*, 158(Supplement C), 137-146.
- Tibolla, H., Pelissari, F. M. & Menegalli, F. C. (2014) Cellulose nanofibers produced from banana peel by chemical and enzymatic treatment. *LWT - Food Science and Technology*, 59(2P2), 1311-1318.
- Tzoumaki, M. V., Moschakis, T., Scholten, E. & Biliaderis, C. G. (2013) In vitro lipid digestion of chitin nanocrystal stabilized o/w emulsions. *Food and Function*, 4(1), 121-129.
- Winuprasith, T. & Supphantharika, M. (2015) Properties and stability of oil-in-water emulsions stabilized by microfibrillated cellulose from mangosteen rind. *Food Hydrocolloids*, 43, 690-699.
- Yan, H., Chen, X., Song, H., Li, J., Feng, Y., Shi, Z., Wang, X. & Lin, Q. (2017) Synthesis of bacterial cellulose and bacterial cellulose nanocrystals for their applications in the

stabilization of olive oil pickering emulsion. *Food Hydrocolloids*, 72(Supplement C), 127-135.

Yao, X., Wang, N., Fang, Y., Phillips, G. O., Jiang, F., Hu, J., Lu, J., Xu, Q. & Tian, D. (2013) Impact of surfactants on the lipase digestibility of gum arabic-stabilized O/W emulsions. *Food Hydrocolloids*, 33(2), 393-401.

Zhang, R., Zhang, Z., Zhang, H., Decker, E. A. & McClements, D. J. (2015) Influence of emulsifier type on gastrointestinal fate of oil-in-water emulsions containing anionic dietary fiber (pectin). *Food Hydrocolloids*, 45, 175-185.



## CAPÍTULO VI

---

Microfluidic approach of production and stability of O/W Pickering emulsions  
stabilized by cellulose nanocrystals

*Paper to be submitted to Food Hydrocolloids*

## **Microfluidic approach of production and stability of O/W Pickering emulsions stabilized by cellulose nanocrystals**

Ana Letícia Rodrigues Costa<sup>1</sup>, Weixia Zhang<sup>2</sup>, David A. Weitz<sup>2</sup>, Rosiane Lopes Cunha<sup>1</sup>

<sup>1</sup>Department of Food Engineering, Faculty of Food Engineering, University of Campinas (UNICAMP), 13083-862 Campinas, SP, Brazil

<sup>2</sup>Department of Physics and School of Engineering and Applied Sciences, Harvard University, Cambridge, Massachusetts, USA.

### **Abstract**

Cellulose nanoparticles have shown potential to act as food-grade particle stabilizer of oil-in-water (O/W) Pickering emulsions. In this work, the formation and stability of oil droplets in the presence of cellulose nanocrystals was studied using a microcapillary device. Microfluidic technique was a powerful tool to observe discrete events during the droplet breakup and coalescence as a function of particles concentration and process conditions. Monodisperse oil droplets and stable emulsions over time could be produced from a balance between droplets generation time and particles adsorption. Large oil droplets and less stable emulsions were obtained after coalescence events inside the microchannel using low particles concentration and high disperse phase flow rate. On the other hand, at high particles concentration, viscosity increasing led to the jetting regime disfavoring the controlled formation of oil droplets. Discrete changes on the droplet size distribution and coefficient of variation could be clearly observed in the Pickering emulsions after 7 days of storage. Microfluid approach contributed to a better understanding of the dynamic conditions of formation and stabilization inside and outside the microchannels revealing the relevance of discrete events that are usually hidden in emulsions produced by conventional emulsification methods.

**Keywords:** nanoparticle, microchannel, coalescence, flow rate, jetting regime

### **6.1. Introduction**

Many of the daily use food products have particulate material that accumulates on the interface between immiscible liquids, as oil and water, contributing to the colloidal stabilization of emulsions. Margarines are example of these food systems, which are water-in-oil (W/O) emulsions stabilized by triglyceride crystals. Emulsions droplets coated and stabilized by a layer of solid particles adsorbed onto the oil-water interface are called Pickering emulsions

(Dickinson, 2010). One of the most important features of the particle-stabilized emulsions is the high physical and energy barrier preventing droplets coalescence more efficiently than conventional emulsifiers, which could eliminate appearance problems and consumer acceptability (Berton-Carabin & Schroën, 2015; Pickering, 1907). Irreversible adsorption of particles from the fluids interface also contributes to the control of the lipid digestibility, making these systems suitable for the development of products presenting low lipid adsorption promoting satiety and reducing obesity (Chevalier & Bolzinger, 2013; Tzoumaki, Moschakis, Scholten, & Biliaderis, 2013).

High-energy emulsification techniques have been used to prepare emulsions stabilized by food-grade particles (Costa et al., 2018a, Costa et al., 2018b, Tzoumaki, Moschakis, Kiosseoglou, & Biliaderis, 2011; Wang et al., 2016). Shear and cavitation forces are responsible by droplet breakup and faster displacement of particles from the continuous phase to the droplets interface. In some emulsions, the energy provided by mechanical treatments associated with the excess of particles in the continuous phase are also responsible by increasing the viscosity of the system (Costa et al., 2018a; Liu & Tang, 2016). Adsorption rate, droplets size and network formation are the main factors influencing the formation and stability of Pickering emulsions as promoted by conventional emulsifiers. However, understanding the stabilization mechanisms of an emulsion stabilized by food particles remains a challenge once some stabilization events, as droplet breakup/coalescence and particles adsorption, are hidden in the early stages of the emulsion production using conventional emulsification methods.

In microfluidics technique, the droplets are generated individually, allowing high control of the emulsification process and reduction of the coefficient of variation or droplets with low polydispersity (Shah et al., 2008, Zhao, 2013). Inorganic, monodisperse and spherical silica nanoparticles are widely used to study the effects of particle deposition, droplet coverage surface and particle size on the formation and properties of Pickering emulsions produced using microfluidic devices (Xu et al., 2005; Yuan et al., 2010; Priest et al., 2011). However, this model system has limited applicability in biocompatible systems since silica particles differ significantly from food particles, especially on properties related to polydispersity, shape, inhomogeneous composition and structure (Kutuzov et al., 2007; Tcholakova et al., 2008). For example, monodisperse spherical particles can penetrate without deforming the interface around droplets, whereas non-spherical particles must distort the interface to maintain a constant contact angle resulting in capillary forces between the particles (McGorty et al., 2010).

Microfluidic methods enable the *in-situ* study of flowing emulsions and droplet interactions from the individual generation of droplets using a high-speed camera and optical microscopy with a high time resolution (Krebs et al., 2012). Thus, we aimed to visualize discrete events in the first stages of droplet breaking and coalescence within the microchannels as a function of cellulose nanocrystals concentration and process conditions (disperse phase flow rate). The stability of the Pickering emulsion stabilized by cellulose nanocrystals (CNC) was also evaluated in order to determine the necessary conditions to form stable systems outside the channel.

## 6.2. Material and Methods

### 6.2.1. Material

Corn oil (Mazola, 100% pure, USA) purchased in the local market was used as oily phase for the preparation of the oil-water (O/W) emulsion. Cellulose nanocrystals with average diameter of  $4.3 \pm 0.4$  nm and length of  $91.66 \pm 25.26$  nm (CelluForce NCC™, Montreal, QC, Canada) were dispersed in deionized water ( $18.2 \text{ M}\Omega \text{ cm}^{-1}$ , Millipore Milli-Q system) using a magnetic stir bar and then sonicated using an ultrasonic processor (20 kHz, 600 W with 37% amplitude) for 2 min (Figure 6.1). This aqueous dispersion of nanoparticles was used to cover the surface of oil droplets through adsorption onto the O/W interface.

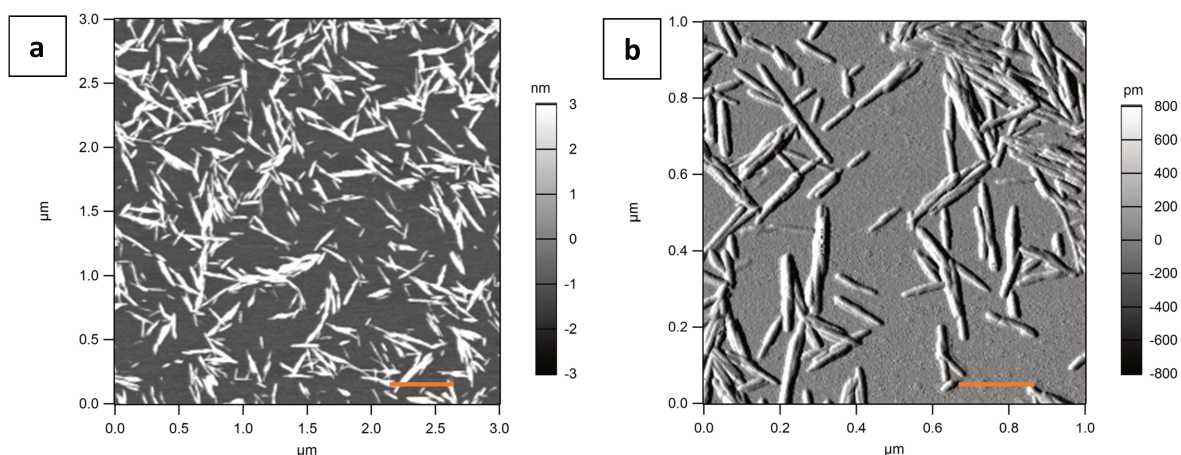


**Figure 6.1.** AFM image of cellulose nanocrystals. a) Scanning area  $3.0 \mu\text{m} \times 3.0 \mu\text{m}$ , scale bar = 500 nm and b) scanning area  $1.0 \mu\text{m} \times 1.0 \mu\text{m}$ , scale bar = 200 nm.

### 6.2.2. Glass microfluidic device

Combining co-flow and flow-focusing within the glass capillary device enable the preparation of emulsions from more complex and viscous materials (Utada et al., 2005). Thus, the device used in this work consisted of two circular capillaries, one for the inner fluid and the other one for collection of the prepared emulsions, arranged end-to-end within a square capillary (Figure 6.2). The inner diameter of the square capillary was about 1.05 mm and the outer diameter of the circular capillaries was 1 mm. We align these capillaries under an optical microscope to achieve coaxial configuration of them. The tapered cylindrical tube was produced by axial heating of the end of a 0.58 mm inner diameter capillary tube (World Precision Instruments, Sarasota, FL, USA) using a micropipette puller (Model P-97 Flaming/Brown puller, Sutter Instrument, Novato, CA, USA). The tip diameters of the collection tube and the inner capillary were 160  $\mu\text{m}$  and 80  $\mu\text{m}$  respectively, and the distance between the capillaries was 80  $\mu\text{m}$ . Collection tube was coated with the hydrophilic coating 2-[methoxy(polymethyleneoxy) propyl]-9-12 trimethoxysilane (Gelest Inc., Netherlands).

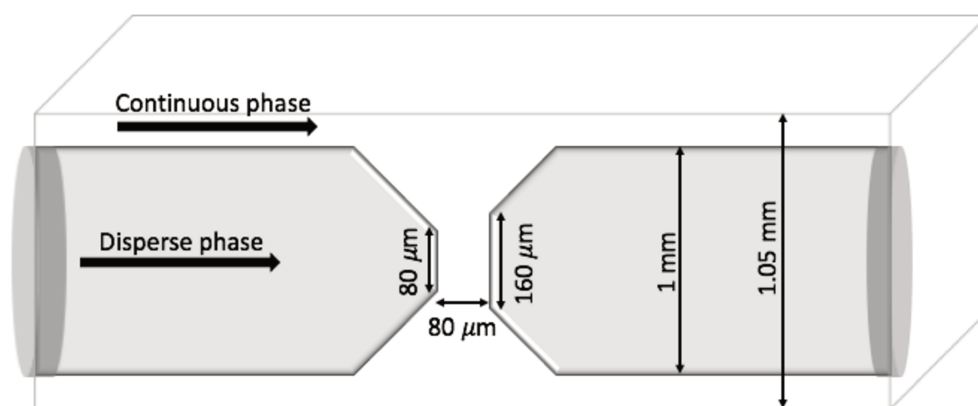


**Figure 6.2.** Schematic of the co-flow and flow-focusing microfluidic device used for production of Pickering emulsions.

Emulsion phases were pumped into the glass capillary devices using syringes pumps (Harvard Apparatus Holliston, USA). Syringes were attached to the inlets of the glass capillary device with plastic tubing (PE5 0.86  $\times$  1.32 mm, Scientific Commodities Inc., USA). The concentration of particles in the outer aqueous phase and the inner fluid flow rate were adjusted to control the particle coverage on the surface of droplets exiting the collection tube. The continuous phase flow rate flowed at the rate of 200  $\mu\text{L}/\text{min}$  and the disperse phase flow rate was adjusted within the range of 10-30  $\mu\text{L}/\text{min}$ , whereas the concentration of cellulose

nanocrystals in the aqueous phase varied between 0.5 and 3.0% (w/w). The formation of O/W emulsions were visualized using a high-speed camera (Phantom V5, Vision Research) connected to an inverted microscope (DM-IRB; Leica, New York, USA).

### **6.2.3. Physical properties of the phases and emulsion characterization**

The interfacial tension between the oily and aqueous phases (cellulose nanocrystals dispersions) was measured by the pendant drop method with droplet volume of  $12.8 \pm 0.5 \mu\text{L}$ . Rheological measurements were performed in a stress-controlled rheometer (Physica MCR301, Anton Paar, Austria). Flow curves of oily and aqueous phases were obtained using a double concentric cylinders geometry consisting of an inner cylinder (outer radius = 17.53 mm, inner radius = 16.02 mm) and an outside cup (outer radius = 18.45 mm, inner radius = 15.10 mm). Shear rate varied between 0 and  $1000 \text{ s}^{-1}$  and the flow curves were obtained in a sequential three flow steps: up-down-up cycles. Data obtained from the third flow curve were fitted to Newton or power-law equations. All measurements were performed at  $22^\circ\text{C}$  in duplicate.

Oil droplets formed in the glass microfluidic devices were collected and stored in glass bottles (14 cm height; 1.6 cm diameter) at  $22^\circ\text{C}$ . The droplets freshly prepared and after 7 days of storage were deposited in glass slides for observation in an optical microscope under transmitted light (model SMZ800, Nikon Instruments Inc., United States). Six images of each emulsion were obtained, and the droplet size distribution was evaluated using a custom-written image processing routine in MATLAB (R2016b, Mathworks). From the droplet size distribution, the mean droplet size and polydispersity index (as coefficient of variance) of the emulsion were calculated for given operating conditions. To quantify the percentage of coalescence events, the number of droplets formed at the channel junction was compared with the number of individual droplets merging with each other.

## **6.3. Results and discussion**

### **6.3.1. Events inside the microchannel**

At low particles concentrations (0.5 and 1.0% w/w), oil droplets were produced in the dripping regime with droplet formation times ranging from 8,000; 6,000 and  $4,000 \pm 250 \mu\text{s}$  depending on the disperse phase flow rate, 10; 20 and  $30 \mu\text{L}/\text{min}$ , respectively and regardless particles concentration (Supplementary Figure S1). The droplets traveled along the collection tube, and the droplet surface coverage was determined by particles concentration. Coalescence events inside the microchannel occurred only at lower particles concentration and they were

more pronounced increasing the disperse phase flow rate, as a result of the highest probability of droplet collision due to shorter droplet formation time (Figure 6.2). Closer droplets with lower surface coverage exhibited unprotected sites on the surface that favored the coalescence. Oil droplets produced at 0.5% (w/w) were not stable outside channel indicating that more coalescence events occurred out of the field of view, probably inside the collection plastic tubing. On the other hand, oil droplets produced at 1.0% w/w could be collected even after the coalescence events inside channel, indicating that more intense coalescence was prevented by late adsorption of the particles onto the droplet interface (Supplementary Figure S2).

We could observe that different from conventional surfactants that show fast adsorption, a certain time is necessary for particles to anchor on the oil-water interface. High-energy levels are provided for breaking droplets in conventional emulsification mechanisms, following a top-down design. However, due to turbulent flow conditions, droplets collision followed by coalescence can happen quickly if a minimum particle concentration is not adequately defined. Thus, microfluidic technique can also be a tool to determine the particle concentration able to prevent the early coalescence events during the emulsification process (Figure 6.3).

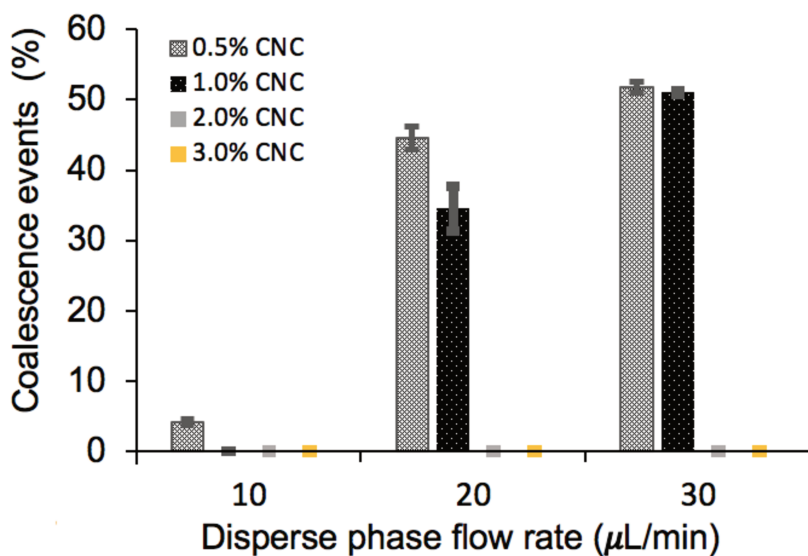


**Figure 6.3.** Coalescence events (%) of oil droplets as a function of the disperse phase flow rate (μL/min) and cellulose nanocrystals (CNC) dispersion concentration (% w/w). Continuous phase flow rate= 200 μL/min.

At higher particles concentration (2.0 and 3.0% w/w), coalescence events were not observed even at shorter droplet formation times ( $6,000$  and  $4,000 \pm 250$  μs at 10 and 20 μL/min, respectively). However, a transition from dripping to jetting regime occurred increasing the

disperse phase flow rate (Supplementary Figure S3). The dripping regime is characterized by the breakup of the dispersed phase at the orifice whereas, in the jetting regime, breakup occurs after the dispersed phase forms a long neck, downstream of the orifice (Tarchichi et al., 2013). This transition involves a balance between the viscous force that pulls on the droplet and the interfacial tension force that holds the droplet during the formation process (Umbanhowar et al., 2000).

Conventional emulsifiers can decrease the interfacial tension between the oil-water phases favoring droplet breakup during the droplet formation and kinetic stability of the emulsions (Mwangi et al., 2016). However, our results showed that the interfacial tension values between oil and CNC aqueous dispersions did not present significant reduction compared to the value of interfacial tension between water and corn oil ( $\gamma = 24.24 \pm 1.73$  mN/m), indicating that the droplet formation mechanism and emulsion stabilization by these particles differs from conventional emulsifiers (Table 6.1). On the other hand, highest viscosity values at 2.0 and 3.0% w/w of CNC indicate that the particles can interact with each other leading the system to a shear-thinning behavior (Table 6.1). In complex systems, viscosity ratio ( $\alpha = \eta_d/\eta_c$ , where  $\eta_c = 51.58 \pm 0.01$  mPa.s) between aqueous and oil phases decreasing means that the viscous forces can easier overcome the interfacial ones (Costa et al., 2017) inducing formation of smaller droplets. However, at the highest disperse phase flow rate (30  $\mu\text{L}/\text{min}$ ) the inertial forces effects became more relevant than viscous forces disfavoring the controlled droplets formation and leading to the jetting regime.

**Table 6.1.** Viscosity or apparent viscosity at  $1000 \text{ s}^{-1}$  ( $\eta$ ) and rheological parameters (k and n) of the cellulose nanocrystals (CNC) aqueous dispersion (% w/w). Viscosity ratio ( $\alpha$ ) and interfacial tension ( $\gamma$ ) between CNC aqueous dispersion (% w/w) and corn oil.

CNC concentration (% w/w)	n	k ( $\cdot 10^{-3}$ ) (Pa.s <sup>n</sup> )	$\eta$ at $1000 \text{ s}^{-1}$ (mPa.s)	$\alpha$	$\gamma$ (mN/m)
0.5	-	-	$1.63 \pm 0.01^a$	$31.64 \pm 0.01^a$	$24.06 \pm 1.61^a$
1.0	$0.89 \pm 0.01$	$4.90 \pm 0.01$	$2.33 \pm 0.01^b$	$22.14 \pm 0.01^b$	$24.23 \pm 2.54^a$
2.0	$0.79 \pm 0.01$	$18.14 \pm 0.01$	$4.14 \pm 0.01^c$	$12.46 \pm 0.01^c$	$21.88 \pm 2.62^a$
3.0	$0.69 \pm 0.01$	$64.04 \pm 0.01$	$7.48 \pm 0.01^d$	$6.90 \pm 0.01^d$	$20.18 \pm 1.97^a$

Means with the same letters in the same column do not differ statistically ( $p < 0.05$ ).

### 6.3.2. Pickering emulsions outside the microchannel

Results presented above could be confirmed from mean diameter,  $\bar{D}$ , and CV values (Table 6.2). At 10  $\mu\text{L}/\text{min}$  of disperse phase flow rate the droplets became significantly smaller



decreasing the viscosity ratio between phases from 31.6 to 6.89 (Table 6.1) or increasing particles concentration on aqueous phase (Table 6.2). At 1.0% w/w of CNC, small and monodisperse ( $CV < 5\%$ ) droplets could be obtained outside the microchannel at the lowest disperse phase flow rate, whereas large droplets and high  $CV$  values were a consequence of coalescence events inside the microchannels at lower droplet formation times ( $6,000$  and  $4,000 \pm 250 \mu s$ ). The higher distance between two adjacent droplets due to the highest droplet formation time ( $8,000 \pm 250 \mu s$ ) was the most important parameter in order to avoid the coalescence events until CNC particles could be anchored onto the droplets interface. At 2.0 and 3.0% w/w of CNC, larger droplets and high  $CV$  values were obtained from droplets generated by jetting regime ( $Q_d=30 \mu L/min$ ), whereas even at lower droplet formation times ( $6,000$  and  $4,000 \pm 250 \mu s$ ), small and monodisperse ( $CV < 7\%$ ) droplets could be formed by dripping regime ( $Q_d=10$  and  $20 \mu L/min$ ). At higher particle concentrations there was a large amount of CNC particles surrounding the newly generated droplets promoting a faster stabilization. In these conditions, the effects of droplet formation time and coalescence events became less important, and the properties of aqueous and oily phases as well as forces involved in the droplet formation process were responsible for controlling the oil droplets size.

**Table 6.2.** Mean diameter ( $\bar{D}$ ;  $\mu m$ ) and coefficient of variation ( $CV$ ; %) of O/W Pickering emulsions stabilized by cellulose nanocrystals (CNC).

CNC concentration (% w/w)	Days of storage	Disperse phase flow rate ( $\mu L/min$ )					
		10		20		30	
		$\bar{D}$	$CV$	$\bar{D}$	$CV$	$\bar{D}$	$CV$
1.0	0	133.70 $\pm$ 6.19 <sup>aA</sup>	4.63	144.98 $\pm$ 17.24 <sup>aA</sup>	11.89	208.70 $\pm$ 36.70 <sup>aA</sup>	17.59
	7	132.18 $\pm$ 7.40 <sup>aA</sup>	5.60	140.07 $\pm$ 13.92 <sup>aA</sup>	9.94	203.88 $\pm$ 38.13 <sup>aA</sup>	18.70
2.0	0	127.02 $\pm$ 4.70 <sup>abA</sup>	3.70	130.71 $\pm$ 5.32 <sup>aA</sup>	4.07	200.94 $\pm$ 15.93 <sup>aA</sup>	7.93
	7	125.40 $\pm$ 5.63 <sup>aA</sup>	4.48	131.24 $\pm$ 5.43 <sup>aA</sup>	4.13	197.33 $\pm$ 28.04 <sup>aA</sup>	14.21
3.0	0	118.65 $\pm$ 6.84 <sup>bA</sup>	5.77	125.09 $\pm$ 6.34 <sup>aA</sup>	5.07	209.46 $\pm$ 21.33 <sup>aA</sup>	10.19
	7	119.09 $\pm$ 14.79 <sup>aA</sup>	12.42	122.68 $\pm$ 5.01 <sup>aA</sup>	4.08	203.72 $\pm$ 26.30 <sup>aA</sup>	12.91

Means with the same letters in the same column do not differ statistically ( $p < 0.05$ ). Small letters: differences between CNC concentrations at a fixed disperse phase flow rate and days of storage. Capital letters: differences between days of storage at a fixed disperse phase flow rate and CNC concentration.

The oil droplets of the collected emulsion quickly creamed due to the big droplets size and low density of corn oil as compared to water (Supplementary Figure S4). Large oil droplets ( $\bar{D}$  varying between 118 and 209  $\mu m$ ) were generated due to a limitation associated to the glass microchannels dimensions and nanoparticles size since the later needed to be at least one

magnitude smaller than the droplets to form an effective layer around the droplet the particles (Dickinson, 2012). Thus, most of Pickering emulsions with large droplets can exhibit high stability towards coalescence, but creaming or sedimentation can occur (Linke & Drusch, 2017). No significative changes in the  $\bar{D}$  values were observed after 7 days of storage indicating high stability of emulsions stabilized by CNC particles against the coalescence process. Unlike surfactants, solid particles are generally irreversibly adsorbed onto the water-oil interface providing long-term stability of emulsions by steric hindrance (Binks, 2002; Dickinson, 2010). However, small changes in the droplet size distribution curves and microscopies were observed in emulsions that presented coalescence events inside microchannels or produced by the jetting regime (Figure 6.4). The high polydispersity of droplet size distribution (high initial CV values) led to the changes in the droplets size of these emulsions since small droplets can diffuse through the continuous phase toward larger droplets (Oswald ripening mechanism) (Walstra, 2005).

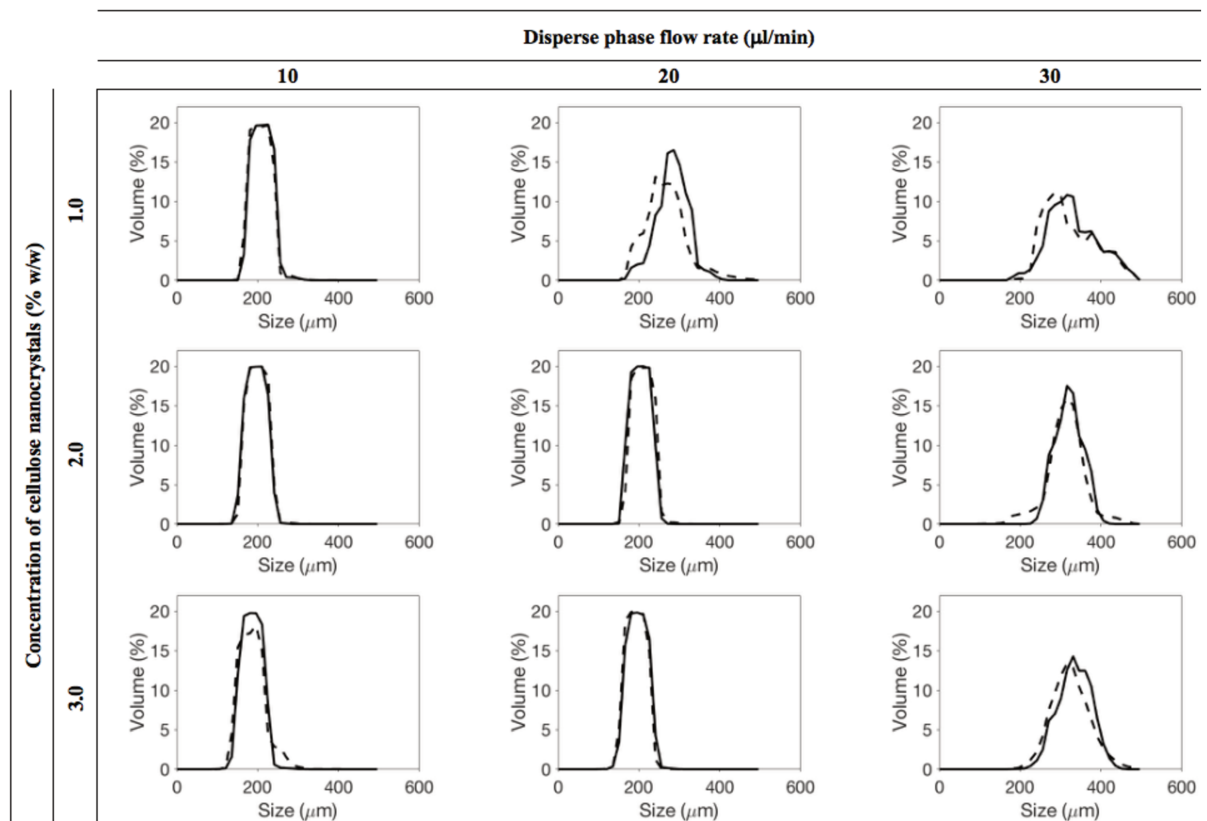


**Figure 6.4.** Particles (droplets) size distribution of O/W Pickering emulsions stabilized by cellulose nanocrystals. Fresh emulsions (solid line) and after 7 days of storage (dashed line).

Surprisingly, emulsions produced at 3.0% w/w of CNC and 10  $\mu\text{L}/\text{min}$  also presented coalescence events outside microchannel after 7 days of storage even at lower initial  $CV$  value ( $CV= 5.77\%$ ). These events were evidenced from microscopy, size distribution curve and  $CV$  value increasing ( $CV= 12.42\%$ ). It was associated with the excess of particles in the water once coalescence events were at least partly suppressed increasing the dispersed phase volume fraction to 0.1 and 0.15 at  $Q_d=20$  and 30  $\mu\text{L}/\text{min}$ , respectively (Figure 6.5).

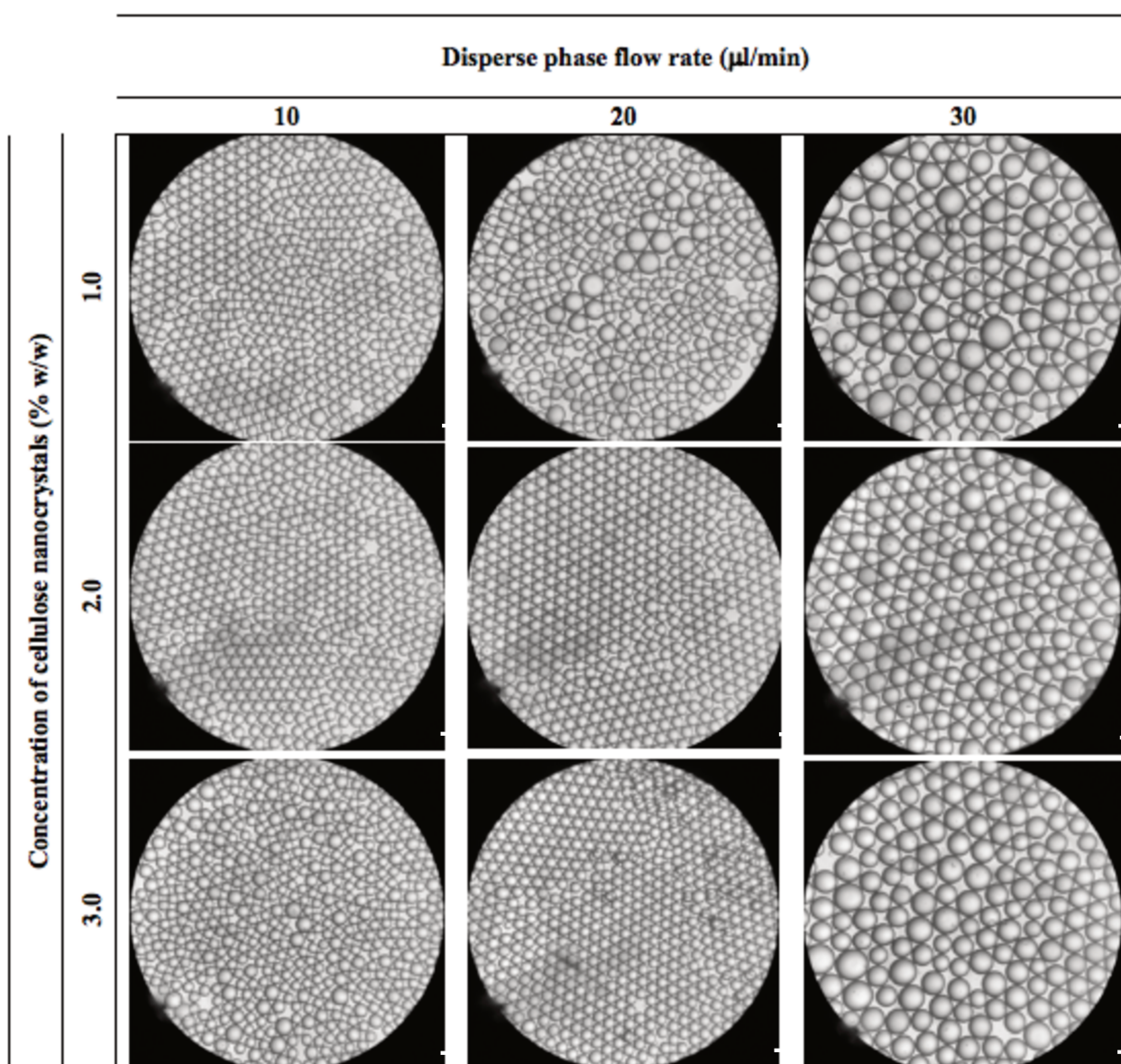


**Figure 6.5.** Optical micrograph of O/W Pickering emulsions stabilized by cellulose nanocrystals after 7 days of storage. Scale bar: 200  $\mu\text{m}$ .

Several experiments have shown that unadsorbed conventional surfactants dispersed in water can cause further desorption of surfactants from the oil droplet interface, thus destabilizing emulsion (Dickinson et al., 2003; Dickinson and Ritzoulis, 2000). This effect has not been observed in emulsions stabilized by solid particles. Pickering emulsions prepared by conventional emulsification process (rotor-stator, ultrasound, and high-pressure homogenizer) have shown increased stability by the excess of particles in water. Unadsorbed particles in continuous phase hinder the creaming and coalescence events by increasing the viscosity of emulsion and gel-like behavior (Carrillo et al., 2005; Wen et al., 2014; Pandey et al., 2018; Costa et al., 2018a). However, low-energy emulsification technique does not provide enough energy (by shear or cavitation forces) to the system to promote strong particles interactions and formation of a three-dimensional network. Thus, we assumed that the depletion attraction between the oil droplets interfaces was mediated by the weak interactions between the coverage of particles onto the interface and aggregated particles in the continuous phase. These interactions led to the formation of free-particles interface due to the discrete displacement of particles from the oil droplets interface increasing the probability of coalescence events outside the microchannel. In order to evaluate the effect of particle concentration on the emulsion stability, we collected the emulsions produced at 3.0% w/w of CNC and disperse phase flow rate of 10  $\mu\text{L}/\text{min}$  in tubes containing water (collected emulsion/water ratio of 2:1). At lower particle concentration, the higher distance between them reduced the interaction with each other (less particles aggregation) leading to the formation of stable droplet coverage and no change on the droplet size distribution after 7 days of storage (Figure 6.6).

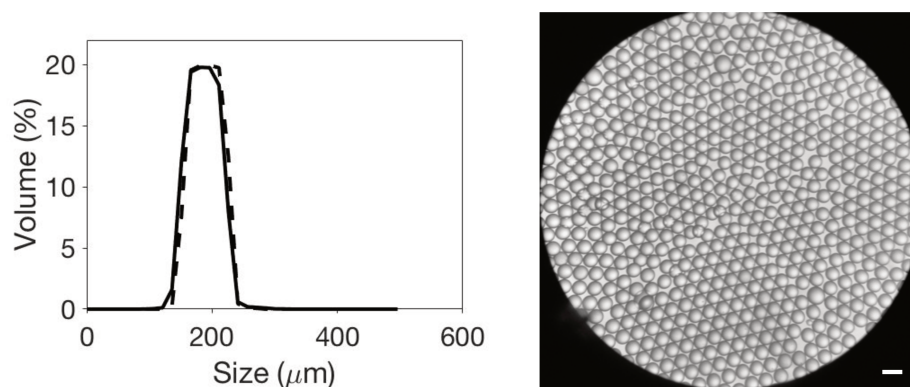


**Figure 6.6.** Size distribution (fresh emulsions: solid line and after 7 days of storage: dashed line) and optical micrograph (after 7 days of storage) of Pickering emulsions produced at 3.0% w/w of cellulose nanocrystals and disperse phase flow rate of 10  $\mu\text{L}/\text{min}$  and collected in tubes with water. Scale bar: 200  $\mu\text{m}$ .

The early stages of oil droplet generation and changes on  $\bar{D}$  and  $CV$  after 7 days of storage could only be observed because they occurred from highly monodisperse emulsions produced by microfluidic techniques. Coalescence events inside microchannels and even changes observed outside channels are discrete events that are usually hidden within the conventional emulsification process once high polydispersity of droplet size is characteristic of these processes. Therefore microfluidics allows defining a balance between the phases flow rate and particles concentration that can lead to emulsions highly stable and monodisperse.

#### 6.4. Conclusion

Oil-in-water emulsions stabilized by cellulose nanocrystals were produced through microfluidic techniques. Discrete events of stabilization and destabilization could be clearly observed inside and outside the microchannels, from the individual generation of highly monodisperse oil droplets. At low particles concentration, coalescence events were observed in the early stages of emulsification depending on the disperse phase flow rate, which led the formation of large oil droplets and less stable emulsions. However, monodisperse oil droplets and stable emulsions over time were produced from a balance between droplets generation time and particles adsorption. At high particles concentration, coalescence events were prevented by higher amount of particles around newly generated droplets and quicker particles adsorption. However properties of aqueous and oily phases and also the forces involved in the droplet formation process are important variables on the control of the oil droplets size at high disperse flow rate. Microfluidics allowed observing coalescence discrete events that are usually hidden in emulsion produced by conventional methods, contributing to a better understanding of the dynamic conditions of emulsions stabilization by food-grade particles.

#### Acknowledgments

The authors thank CAPES – Brazil (DEA/FEA/PROEX) and FAPESP – Brazil (FAPESP 2007/58017-5 and 2011/06083-0) for their financial support. Ana Leticia Rodrigues Costa Lelis thanks CNPq – Brazil (CNPq 204109/2017-5) for the fellowship; Rosiane Lopes Cunha thanks CNPq (CNPq 307168/2016-6) for the productivity grant.

## References

- Berton-Carabin, C. C., Schroën, K., 2015. Pickering emulsions for food applications: Background, trends, and challenges. *Annual Review of Food Science and Technology* 6, 263-297.
- Binks, B.P., (2002). Particles as surfactants—similarities and differences, *Current Opinion in Colloid & Interface Science* 7, 21–41.
- Carrillo, C. A., Nypelö, T. E., & Rojas, O. J. (2015). Cellulose nanofibrils for one-step stabilization of multiple emulsions (W/O/W) based on soybean oil. *Journal of Colloid and Interface Science*, 445, 166–173.
- Chevalier, Y., Bolzinger, M.-A., 2013. Emulsions stabilized with solid nanoparticles: Pickering emulsions. *Colloids and Surfaces A: Physicochemical and Engineering Aspects* 439, 23–34.
- Costa, A. L. R., Gomes, A., Cunha, R. L., 2017. Studies of droplets formation regime and actual flow rate of liquid-liquid flows in flow-focusing microfluidic devices. *Experimental Thermal and Fluid Science* 85, 167-175
- Costa, A. L. R., Gomes, A., Cunha, R. L., 2018a. One-step ultrasound producing O/W emulsions stabilized by chitosan particles. *Food Research International* 107, 717-725.
- Costa, A. L. R., Gomes, A., Tibolla, H., Menegalli, F. C., Cunha, R. L., 2018b. Cellulose nanofibers from banana peels as a Pickering emulsifier: High-energy emulsification processes. *Carbohydrate Polymers* 194, 122-131.
- Dickinson, E., 2010. Food emulsions and foams: stabilization by particles, *Current Opinion in Colloid & Interface Science* 15, 40–49.
- Dickinson, E., 2010. Food emulsions and foams: Stabilization by particles. *Current Opinion in Colloid & Interface Science* 15 (1-2), 40-49.
- Dickinson, E., Radford, S. J., Golding, M., 2003. Stability and Rheology of Emulsions Containing Sodium Caseinate: Combined Effects of Ionic Calcium and Non-ionic Surfactant. *Food Hydrocolloids*, 17, 211-220.
- Dickinson, E., Ritzoulis, C., 2000. Creaming and Rheology of Oil-in-Water Emulsions Containing Sodium Dodecyl Sulfate and Sodium Caseinate. *Journal of Colloid and Interface Science* 224, 148-154.



- Krebs, T., Schroën, K., Boomb, R., 2012. Coalescence dynamics of surfactant-stabilized emulsions studied with microfluidics. *Soft Matter* 8, 10650–10657.
- Kutuzov, S., He, J., Tangirala, R., Emrick, T., Russell, T.P., Böker, A., 2007. On the kinetics of nanoparticle self-assembly at liquid/liquid interfaces. *Physical Chemistry Chemical Physics* 9, 6351–6358.
- Linke, C., Drusch, S., 2017. Pickering emulsions in foods - opportunities and limitations. *Journal Critical Reviews in Food Science and Nutrition* 58, 1971-1985.
- Liu, F., Tang, C.-H., 2016. Soy glycinin as food-grade Pickering stabilizers: Part. I. Structural characteristics, emulsifying properties and adsorption/arrangement at interface. *Food Hydrocolloids* 60, 606–619.
- McGorty, R., Fung, J., Kaz, D., Manoharan, V.N., 2010. Colloidal self-assembly at an interface. *Materials Today* 13, 34–42.
- Mwangi, W. W., Ho, K.-W., Tey, B.-T., Chan, E.-S., 2016. Effects of environmental factors on the physical stability of Pickering-emulsions stabilized by chitosan particles. *Food Hydrocolloids* 60, 543–550.
- Pandey, A., Derakhshandeh, M., Kedzior, S.A., Pilapil, B., Shomrat, N., Segal-Peretz, T., Bryant, S. L., Trifkovic, M., 2018. Role of interparticle interactions on microstructural and rheological properties of cellulose nanocrystal stabilized emulsions. *Journal of Colloid and Interface Science* 532, 808-818.
- Pickering, S. U., 1907. CXCVI.-emulsions. *Journal of the Chemical Society, Transactions* 91(0), 2001–2021.
- Priest, C.; Reid, M. D.; Whitby, C. P., 2011 Formation and stability of nanoparticle- stabilized oil-in-water emulsions in a microfluidic chip. *Journal of Colloid and Interface Science* 363 (1), 301-306.
- Shah, R. K., Shum, H. C., Rowat, A. C., Lee, D., Agresti, J. J, Utada, A. S., Chu, L. -Y., Kim, J. -W., Fernandez-Nieves, A., Martinez, C. J., Weitz, D. A., 2008. Designer emulsions using microfluidics. *Materials Today*, 11 (4), 18-27.
- Tarchichi, N., Chollet, F., Manceau, J.F., 2013. New regime of droplet generation in a T-shape microfluidic junction. *Microfluidic Nanofluidic* 14, 45–51.
- Tcholakova, S., Denkov, N.D., Lips, A., 2008. Comparison of solid particles, globular proteins and surfactants as emulsifiers. *Physical Chemistry Chemical Physics* 10, 1608–1627.

- Tzoumaki, M. V., Moschakis, T., Kiosseoglou, V., Biliaderis, C. G., 2011. Oil-in-water emulsions stabilized by chitin nanocrystal particles. *Food Hydrocolloids* 25(6), 1521–1529.
- Tzoumaki, M. V., Moschakis, T., Scholten, E., Biliaderis, C. G., 2013. In vitro lipid digestion of chitin nanocrystal stabilized o/w emulsions. *Food and Function* 4, 121-129.
- Umbanhowar, P., Prasad, V., Weitz, D.A., 2000. Monodisperse emulsion generation via drop break off in a coflowing stream. *Langmuir* 16, 347–351.
- Utada, A. S., Lorenceau, E., Link, D. R., Kaplan, P. D., Stone, H. A., Weitz, D. A., 2005. Monodisperse double emulsions generated from a microcapillary device. *Science* 308 (5721), 537-541.
- Walstra, P., 2005. Emulsions, *Fundamentals of Interface and Colloid Science* 5, 8.1-8.94.
- Wang, W., Du, G., Li, C., Zhang, H., Long, Y., Ni, Y., 2016. Preparation of cellulose nanocrystals from asparagus (*Asparagus officinalis* L.) and their applications to palm oil/water Pickering emulsion. *Carbohydrate Polymers* 151, 1–8.
- Wen, C., Yuan, Q., Liang, H., Vriesekoop, F., 2014. Preparation and stabilization of d-limonene Pickering emulsions by cellulose nanocrystals. *Carbohydrate Polymers* 112, 695-700.
- Xu, Q. Y.; Nakajima, M.; Binks, B. P., 2005. Preparation of particle-stabilized oil-in-water emulsions with the microchannel emulsification method. *Colloids and Surfaces A: Physicochemical and Engineering Aspects* 262 (1–3), 94-100.
- Yuan, Q.; Cayre, O. J.; Manga, M.; Williams, R. A.; Biggs, S., 2010. Preparation of particle-stabilized emulsions using membrane emulsification. *Soft Matter* 6 (7), 1580-1588.
- Zhao, C. X., 2013. Multiphase flow microfluidics for the production of single or multiple emulsions for drug delivery. *Advanced Drug Delivery Reviews* 65 (11-12), 1420-1446.



## Supplementary Figure S1

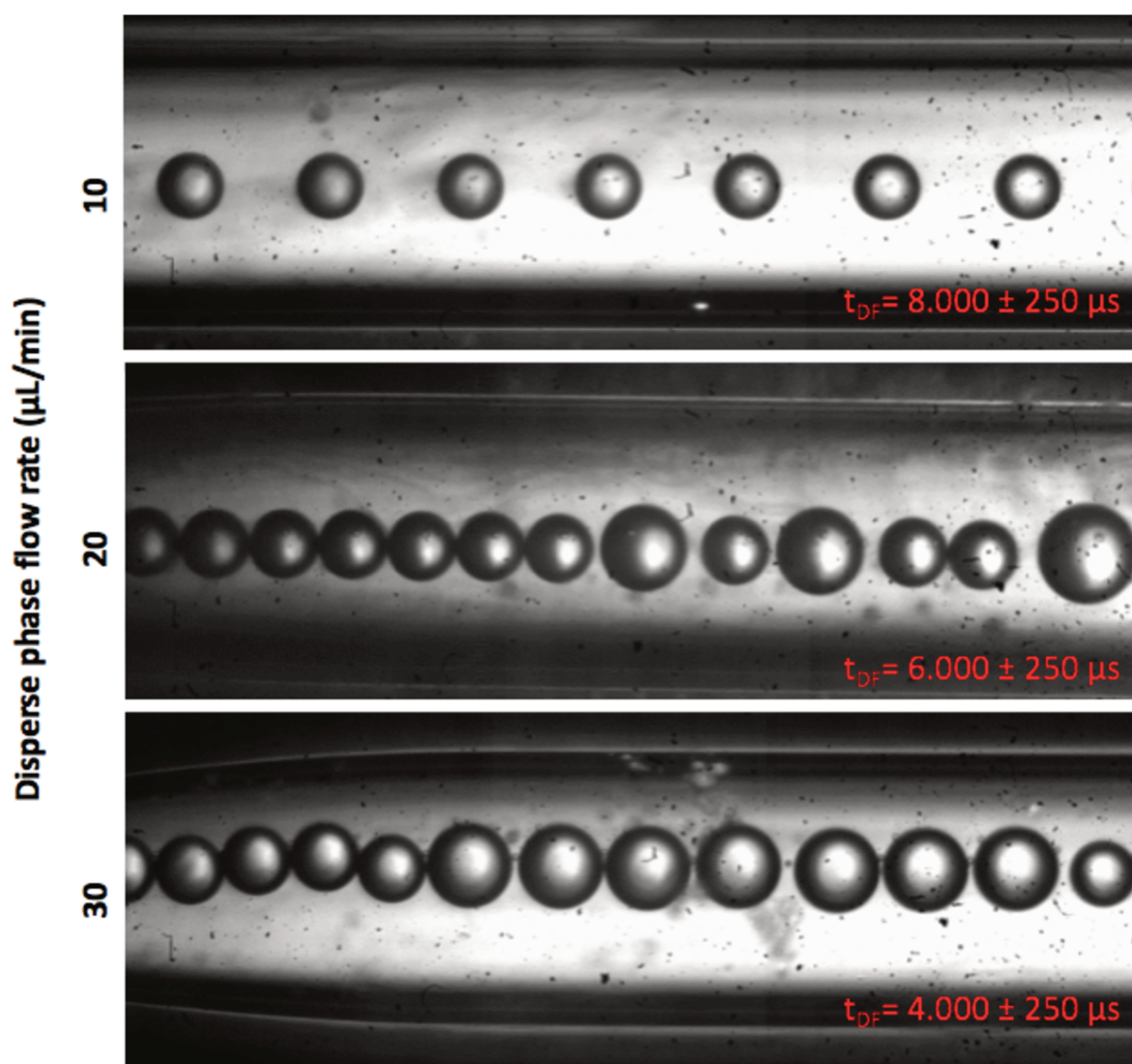


**Figure S1.** Coalescence events of oil droplets stabilized by cellulose nanocrystals (CNC) inside the microchannels.  $t_{DF}$ =droplet formation time. CNC concentration= 1.0% w/w and continuous phase flow rate= 200 μL/min.

## Supplementary Figure S2

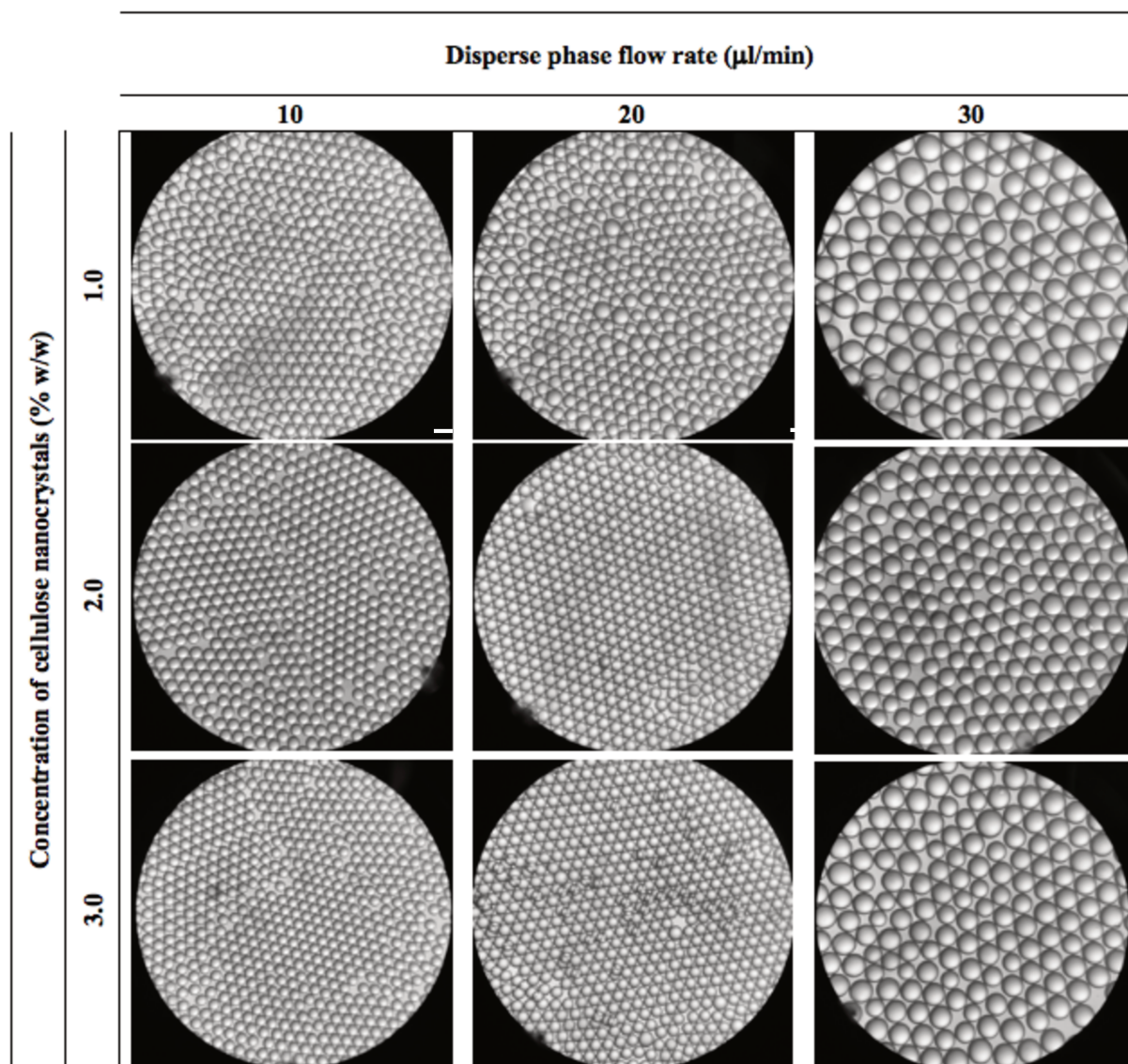


**Figure S2.** Optical micrograph of Pickering emulsions stabilized by cellulose nanocrystals freshly prepared. Scale bar: 200  $\mu\text{m}$ .

## Supplementary Figure S3

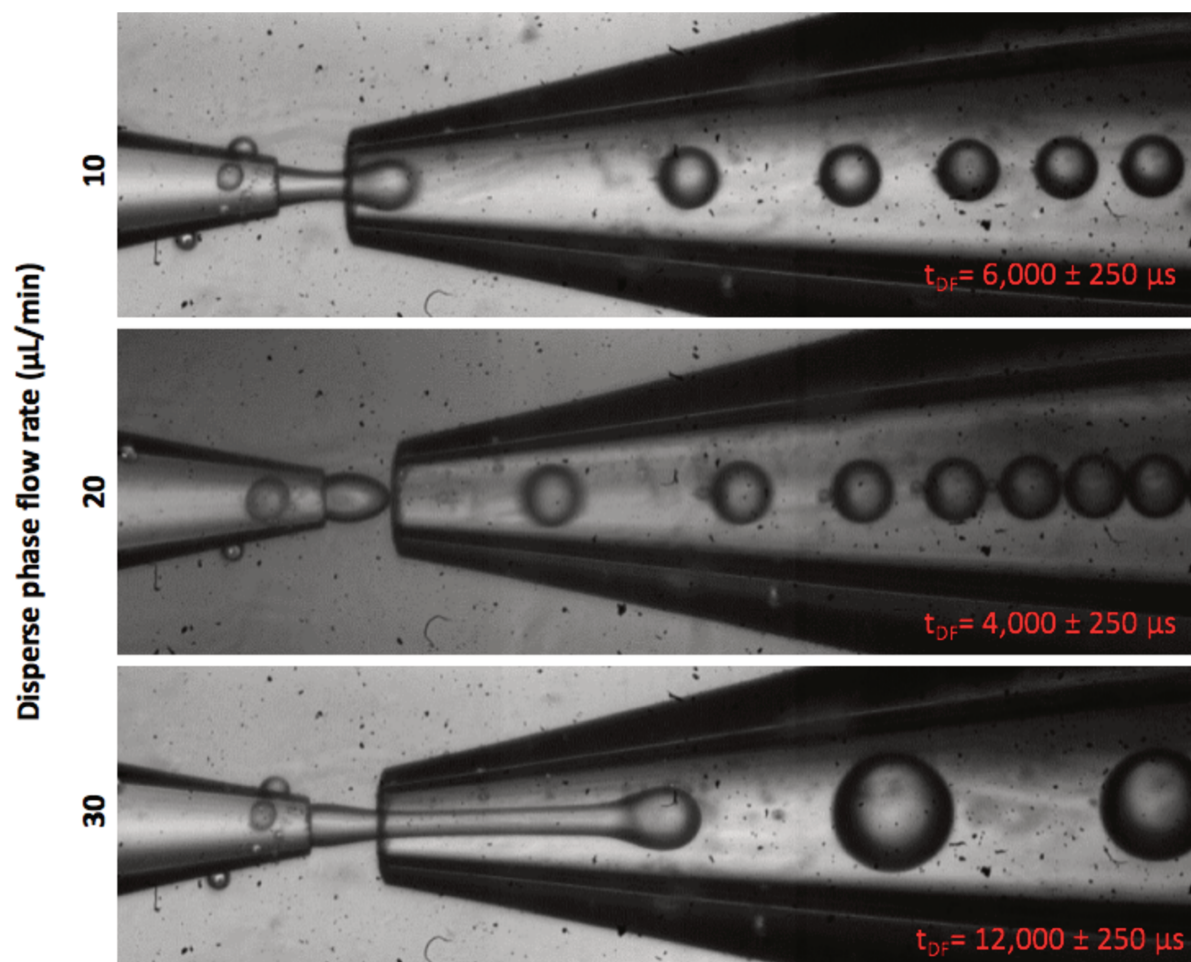


**Figure S3.** Droplet formation process of Pickering emulsions stabilized by cellulose nanocrystals (CNC) inside the microchannels.  $t_{\text{DF}}$ =droplet formation time. Continuous phase flow rate= 200  $\mu\text{L}/\text{min}$  and CNC concentration= 3.0% w/w.



Supplementary Figure S4

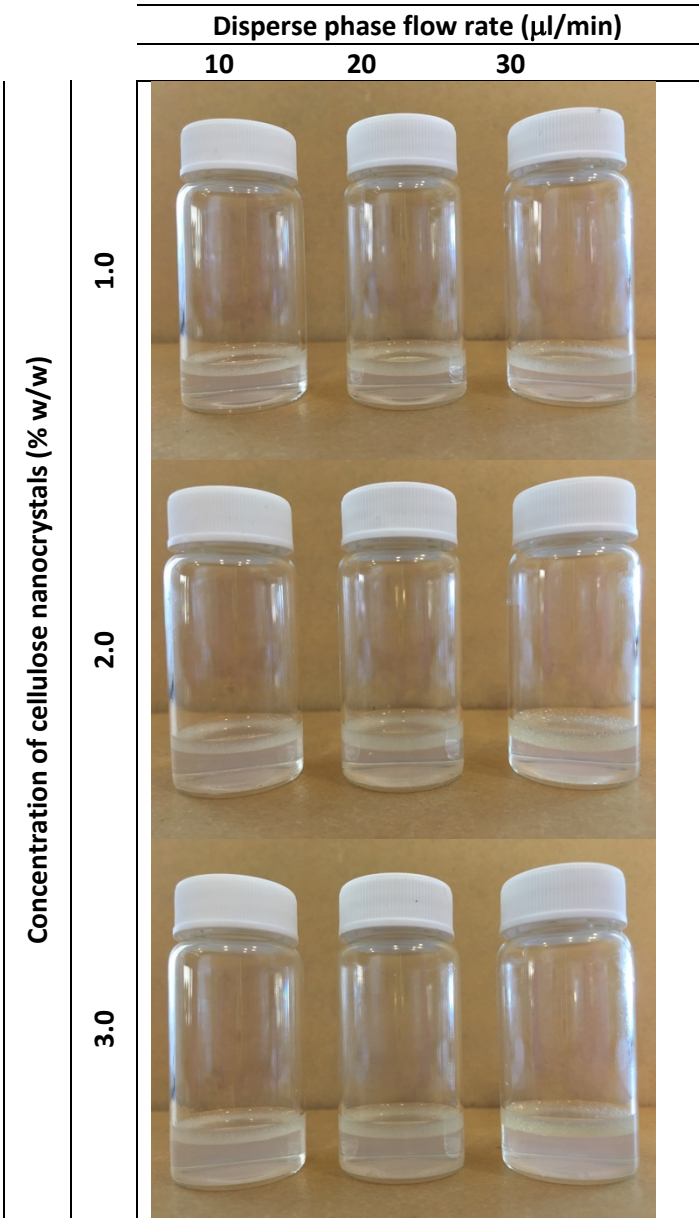


**Figure S4.** Pictures of Pickering emulsions stabilized by cellulose nanocrystals freshly prepared.

## CAPÍTULO VII

---

- DISCUSSÃO GERAL

### 7.1. Discussão Geral

Nanopartículas de quitosana foram produzidas e caracterizadas quanto aos efeitos da variação da potência aplicada e tempo de processamento sobre a estabilidade destas partículas e das emulsões produzidas simultaneamente em ultrassom de alta intensidade (resultados apresentados no Capítulo III). A atividade superficial das partículas de quitosana foi evidenciada com a redução da tensão interfacial entre o óleo e a água. Este resultado foi atribuído à capacidade dos grupos hidrofóbicos (*N*-acetil-*D*-glucosamina) de atuar na interface óleo-água após a formação da quitosana auto-agregada com características hidrofílicas e hidrofóbicas. Além disso, a intensificação combinada do tempo e potência de ultrassom também levou a um aumento da hidrofobicidade e polidispersidade, mudanças nos valores de potencial zeta e redução no tamanho das partículas de quitosana. A alta estabilidade das emulsões durante os 6 dias de armazenamento foi associada aos intensos efeitos de cavitação gerados com altas potências de ultrassom capazes de quebrar as gotas de óleo em menores tamanhos promovendo a formação de uma rede tridimensional devido ao compartilhamento das partículas adsorvidas na interface das gotas. Essa adsorção foi associada à maior capacidade dos grupos hidrofóbicos em atuar na interface durante a quebra das gotas (aumento da hidrofobicidade das partículas de quitosana) e às interações não-covalentes entre as gotas de óleo (fenômeno de floculação). Além disso, o aumento do fenômeno de floculação das gotas alterou a viscosidade das emulsões levando à formação de uma estrutura semelhante a gel que também proporcionou um aumento na estabilidade da emulsão Pickering. Por fim, foi possível elucidar os mecanismos de estabilização de emulsões por partículas de quitosana desprotonadas e propor um método de emulsificação em uma etapa que gasta menos tempo e energia de processo, mas que pode produzir simultaneamente partículas de quitosana e emulsões cineticamente estáveis.

No Capítulo IV foram apresentados os resultados referentes ao estudo dos efeitos das condições de emulsificação usando ultrassom e homogenizador a alta pressão sobre as propriedades das nanofibras de celulose (CNFs) obtidas da casca da banana e emulsões estabilizadas por essas partículas. A potência de processamento e as altas pressões promoveram redução no comprimento e alterações no índice de cristalinidade das CNFs e um aumento na viscosidade das emulsões. Essas alterações foram associadas aos intensos efeitos de cavitação e forças de cisalhamento promovidas pelo ultrassom e homogeneizador a alta pressão, respectivamente. O fenômeno de cremação ocorreu nas emulsões produzidas por ambos os processos de emulsificação. A coalescência das gotas foi observada nas emulsões produzidas usando homogeneizador a alta pressão devido a um efeito menos pronunciado da tensão de

cisalhamento sobre a quebra das CNFs e uma menor acomodação das CNFs na interface da gota de óleo (maior comprimento e razão de aspecto). No entanto, uma maior redução no comprimento e na razão de aspecto das CNFs durante o processo de emulsificação utilizando ultrassom permitiu a formação de partículas suficientes para recobrir a interface de gotas de óleo, evitando o fenômeno de coalescência. Está claro que a estabilidade cinética das emulsões ainda pode ser melhorada através de mudanças nas pr

opriedades das partículas e emulsões. Entretanto, nossos resultados forneceram relevantes descobertas sobre como os diferentes processos de emulsificação influenciam os mecanismos envolvidos na estabilidade de emulsões Pickering estabilizadas com CNFs.

Um trabalho considerável tem sido feito para compreender os fenômenos de estabilização de emulsões tipo Pickering, mas pouco tinha sido feito para aplicar esses conhecimentos na potencialização do desempenho funcional dessas emulsões. A deposição de determinadas partículas na interface das gotas contribui para o controle da digestibilidade lipídica, sendo estas emulsões adequadas no desenvolvimento de produtos que promovem a saciedade e combatem a obesidade. Esse desafio tecnológico impulsionou os estudos apresentados no Capítulo V. O protocolo de digestibilidade *in vitro* utilizado elucidou o papel das partículas (quitosana, nanofibras; CNFs e cristais de celulose; CCrys) na taxa de digestão lipídica de emulsões Pickering óleo-em-água. A escolha de diferentes partículas de polissacarídeos emulsionantes afetou as propriedades físico-químicas das emulsões Pickering, bem como a hidrólise lipídica durante a digestão simulada *in vitro*. Após a etapa gástrica, a alta carga positiva das emulsões estabilizadas com partículas de quitosana favoreceu a desagregação das gotas, resultando em um efeito moderado de floculação entre as gotas devido ao compartilhamento de partículas e deslocamento da distribuição da curva de tamanho para menores valores. Após a passagem pela condição intestinal, essas emulsões apresentaram uma distribuição monomodal com um tamanho médio elevado ( $D_{4,3} = 197 \pm 8 \mu\text{m}$ ) com a presença de poucas gotas e grandes agregados. Partículas CCrys e CNFs foram capazes de inibir a digestão lipídica pela forte adsorção das partículas na interface das gotas de óleo e devido à presença de maiores gotas de óleo que reduziram o número de moléculas de triacilglicerol expostas à ação da lipase, respectivamente. Além disso, também observamos uma hidrólise retardada de lipídios (cerca de 60% em massa) promovida pela competição entre agregados de quitosana e compostos dos fluidos intestinais na interface de gotas de óleo, bem como, o aumento das interações entre as cadeias de quitosana devido à exposição dos grupos hidrofóbicos em pH 7. Nesta etapa, foram fornecidos aspectos relevantes sobre o projeto interfacial de emulsões Pickering usando partículas de grau-alimentício como sistemas estabilizadores visando a

utilização dessas emulsões como sistemas de entrega de compostos ativos ou como sistemas inibidores de digestão lipídica.

Os métodos microfluídicos permitem a avaliação *in situ* do escoamento e interações das gotas de emulsão a partir da geração individual de gotas. Este fato nos levou a produzir emulsões óleo-em-água estabilizadas por nanocristais de celulose usando dispositivos microcapilares de vidro afim de estudar eventos discretos de estabilização e coalescência de gotas como função da concentração de partículas e condições do processo (resultados apresentados no Capítulo VI). Nas baixas concentrações de partículas e altas vazões da fase dispersa, eventos de coalescência foram observados nos estágios iniciais da emulsificação dentro dos microcanais, o que levou à obtenção de grandes gotas de óleo e emulsões menos estáveis na saída do dispositivo microfluídico. No entanto, gotas de óleo monodispersas e emulsões estáveis ao longo do tempo foram produzidas a partir do balanço entre o tempo de geração das gotas e a adsorção das partículas na interface. Nas altas concentrações de partículas, os eventos de coalescência dentro dos microcanais foram evitados pela maior quantidade de partículas ao redor das gotas recém-geradas e adsorção mais rápida das partículas na interface óleo-água. No entanto, o aumento da viscosidade da fase dispersa levou ao regime de jateamento, desfavorecendo a formação controlada das gotas de óleo. Assim, as propriedades das fases aquosa e oleosa e as forças envolvidas no processo de formação de gotas tornaram-se variáveis importantes no controle do tamanho das gotas de óleo nas altas vazões de fase dispersa. A partir da geração individual de gotículas altamente monodispersas produzidas por técnicas microfluídicas, mudanças discretas na distribuição do tamanho das gotas e no coeficiente de variação puderam ser claramente observadas nas emulsões Pickering após 7 dias de armazenamento. A abordagem microfluídica contribuiu para uma melhor compreensão das condições dinâmicas de estabilização de emulsões Pickering e também permitiu a observação de eventos discretos que geralmente não podem ser observados em métodos convencionais de emulsificação.



## CAPÍTULO VIII

---

- CONCLUSÃO GERAL

### 8.1. Conclusão Geral

Emulsões Pickering estabilizadas com partícula de grau-alimentício foram produzidas com sucesso usando métodos de emulsificação de alta e baixa energia. A alta estabilidade das emulsões Pickering estabilizadas por partículas de quitosana foi associada à redução da tensão interfacial entre o óleo e a água e aos intensos efeitos de cavitação gerados com altas potências de ultrassom capazes de quebrar e aumentar a hidrofobicidade dessas partículas e as gotas de óleo em menores tamanhos promovendo a formação de uma rede tridimensional entre as gotas. Além disso, a emulsificação em apenas uma etapa permitiu produzir simultaneamente menores partículas e emulsões mais estáveis cineticamente usando menos energia e tempo de processo.

As emulsões Pickering estabilizadas por nanofibras de celulose e produzidas usando ultrassom e homogeneizador a alta pressão apresentaram desestabilização devido à cremeação das gotas de óleo. O fenômeno de coalescência foi observado nas emulsões produzidas no homogeneizador a alta pressão, enquanto que a floculação das gotas ocorreu naquelas obtidas em ultrassom de alta intensidade. Nesta última, a estabilidade à coalescência foi associada com o ligeiro aumento da viscosidade da emulsão devido aos efeitos da cavitação, bem como com o rompimento das nanofibras de celulose durante o processo de emulsificação em ultrassom de alta intensidade. Assim, as menores gotas geradas durante o processo de emulsificação puderam ser recobertas pelas nanopartículas que agiram como uma efetiva barreira contra a coalescência das gotas.

Esses resultados nos levam a concluir que as forças de cisalhamento e cavitação em processos de emulsificação de alta energia foram responsáveis pela quebra das gotas e partículas simultaneamente, bem como, pelo rápido deslocamento das partículas da fase contínua para a interface de gotas. Além disso, a energia fornecida pelos tratamentos mecânicos, associados ao excesso de partículas na fase contínua também foram responsáveis pelo aumento da viscosidade dos sistemas.

O protocolo de digestibilidade *in vitro* nos permitiu avaliar com sucesso o papel das partículas (partículas de celulose, nanofibras e cristais de celulose) comparado a um surfactante comercial (Tween 80) na taxa de digestão lipídica de emulsões óleo-em-água. A alta carga positiva das emulsões estabilizadas por quitosana levou à desagregação das gotas após a etapa gástrica, o que favoreceu a maior porcentagem de digestão lipídica na etapa intestinal. Por outro lado, Tween 80, cristais de celulose e nanofibras de celulose foram capazes de inibir a digestão lipídica e nenhuma alteração no tamanho médio das gotas foi observada após a etapa intestinal. A emulsão estabilizada com nanofibras de celulose apresentou menor digestão lipídica,

enquanto que a forte aderência das partículas de cristais de celulose na interface das gotas tornou-as resistentes ao deslocamento por componentes tensoativos. Esses resultados nos proporcionaram elucidar importantes características da aplicação das emulsões Pickering de grau alimentício como sistemas de controle da taxa de digestão lipídica ou como sistemas de entrega de compostos lipofílicos.

Gotas de óleo estabilizadas com nanocristais de celulose altamente monodispersas e emulsões cineticamente estáveis foram produzidas em dispositivos microcapilares de vidro a partir do balanço entre o tempo de geração das gotas e adsorção das partículas. Por outro lado, grandes gotas de óleo e emulsões menos estáveis foram obtidas após a ocorrência de eventos de coalescência dentro do microcanal ou devido ao aumento da viscosidade da fase dispersa que levou ao regime de jateamento desfavorecendo a formação controlada de gotículas de óleo. A partir da geração individual de gotas altamente monodispersas produzidas por técnicas microfluídicas, mudanças discretas na distribuição do tamanho de gotas e coeficiente de variação puderam ser claramente observadas nas emulsões Pickering ao longo do tempo. A abordagem microfluídica contribuiu para uma melhor compreensão das condições dinâmicas de estabilização e desestabilização das emulsões Pickering dentro e fora dos microcanais revelando eventos discretos que geralmente não podem ser observados em emulsões produzidas por métodos convencionais de emulsificação.

## REFERÊNCIAS

---

-REFERÊNCIAS BIBLIOGRÁFICAS GERAIS

- Alemдар, A., & Sain, M. (2008). Isolation and characterization of nanofibers from agricultural residues – Wheat straw and soy hulls. *Bioresource Technology*, 99(6), 1664-1671.
- Amiji, M. M. (1995). Pyrene fluorescence study of chitosan association in aqueous solution. *Carbohydrate Polymers*, 26, 211–213.
- Anton, N., Benoit, J.-P., & Saulnier, P. (2008). Design and production of nanoparticles formulated from nano-emulsion templates-A review. *Journal of Controlled Release*, 128(3), 185-199.
- Araki, J., Wada, M., Kuga, S. & Okano, T. (1998) Flow properties of microcrystalline cellulose suspension prepared by acid treatment of native cellulose. *Colloids and Surfaces A: Physicochemical and Engineering Aspects*, 142(1), 75-82.
- Arrascue, M. L., Garcia, H. M., Horna, O., & Guibal, E. (2003). Gold sorption on chitosan derivatives. *Hydrometallurgy*, 71(1–2), 191–200.
- Atkinson, P. J. et al. (1995). Neutron reflectivity of adsorbed  $\beta$ -casein and  $\beta$ -lactoglobulin at the air/water interface. *Journal of the Chemical Society*, 91(17), 2847-2854.
- Aveyard, R., Binks, B. P., & Clint, J. H. (2003). Emulsions stabilised solely by colloidal particles. *Advances in Colloid and Interface Science*, 100, 503-546.
- Bauer, E., Jakob, S. & Mosenthin, R. (2005) Principles of Physiology of Lipid Digestion. *Asian-Australasian Journal of Animal Sciences*, 18(2), 282-295.
- Baxter, S., Zivanovic, S., & Weiss, J. (2005). Molecular weight and degree of acetylation of high-intensity ultrasonicated chitosan. *Food Hydrocolloids*, 19(5), 821–830.
- Beck-Candanedo, S., Roman, M., & Gray, D. G. (2005). Effect of Reaction Conditions on the Properties and Behavior of Wood Cellulose Nanocrystal Suspensions. *Biomacromolecules*, 6(2), 1048-1054.
- Berton-Carabin, C. C., & Schroën, K. (2015). Pickering emulsions for food applications: Background, trends, and challenges. *Annual Review of Food Science and Technology*, 6, 263-297.
- Bhattacharya, S. S., Banerjee, S., Chowdhury, P., Ghosh, A., Hegde, R. R., & Mondal, R. (2013). *Colloids and Surfaces B: Biointerfaces*, 112, 483–491.
- Binks, B. P. (2002). Particles as surfactants-similarities and differences. *Current Opinion in Colloid & Interface Science*, 7(1-2), 21-41.
- Binks, B. P., & Lumsdon, S. O. (2001). Pickering Emulsions Stabilized by Monodisperse Latex Particles: Effects of Particle Size. *Langmuir*, 17(15), 4540-4547.

- Bondeson, D., Mathew, A., & Oksman, K. (2006). Optimization of the isolation of nanocrystals from microcrystalline cellulose by acid hydrolysis. *Cellulose*, 13, 171.
- Borel, T., & Sabliov, C. M. (2014). Nanodelivery of Bioactive components for food applications: Types of delivery systems, properties, and their effect on ADME profiles and toxicity of nanoparticles. *Annual Review of Food Science and Technology*, 5(1), 197-213.
- Bos, M. A., & Van Vliet, T. (2001). Interfacial rheological properties of adsorbed protein layers and surfactants: A review. *Advances in Colloid and Interface Science*, 91(3), 437-471.
- Carrillo, C. A., Nypelö, T. E., & Rojas, O. J. (2015). Cellulose nanofibrils for one-step stabilization of multiple emulsions (W/O/W) based on soybean oil. *Journal of Colloid and Interface Science*, 445, 166–173.
- Chemat, F., & Khan, M. K. (2011). Applications of ultrasound in food technology: Processing, preservation and extraction. *Ultrasonics Sonochemistry*, 18, 813–835.
- Cherian, B. M., Pothan, L. A., Nguyen-Chung, T., Mennig, G., Kottaisamy, M., & Thomas, S. (2008). A Novel Method for the Synthesis of Cellulose Nanofibril Whiskers from Banana Fibers and Characterization. *Journal of Agricultural and Food Chemistry*, 56(14), 5617–5627.
- Chevalier, Y., & Bolzinger, M.-A. (2013). Emulsions stabilized with solid nanoparticles: Pickering emulsions. *Colloids and Surfaces A: Physicochemical and Engineering Aspects*, 439, 23-34.
- Claesson, P. M. et al. (2003). Surface Forces and Emulsion Stability. In: Friberg, S., Larsson, K., & Sjöblom, J. *Food Emulsions*. Ed. CRC Press, 900.
- Cortés-Muñoz, M., Chevalier-Lucia, D., & Dumay, E. (2009). Characteristics of submicron emulsions prepared by ultra-high pressure homogenisation: Effect of chilled or frozen storage. *Food Hydrocolloids*, 23(3), 640–654.
- Costa, A. L. R., Gomes, A., Andrade, C. C. P.d., & Cunha, R. L. (2017). Emulsifier functionality and process engineering: Progress and challenges. *Food Hydrocolloids*, 68, 69–80.
- Costa, A. L. R., Gomes, A., Cunha, R. L. (2017). Studies of droplets formation regime and actual flow rate of liquid-liquid flows in flow-focusing microfluidic devices. *Experimental Thermal and Fluid Science*, 85, 167-175

- Costa, A. L. R., Gomes, A., Cunha, R. L. (2018). One-step ultrasound producing O/W emulsions stabilized by chitosan particles. *Food Research International*, 107, 717-725.
- Costa, A. L. R., Gomes, A., Tibolla, H., Menegalli, F. C., Cunha, R. L. (2018). Cellulose nanofibers from banana peels as a Pickering emulsifier: High-energy emulsification processes. *Carbohydrate Polymers*, 194, 122-131.
- Cunha, A. G., Mougél, J.-B., Cathala, B., Berglund, L. A., & Capron, I. (2014). Preparation of double pickering emulsions stabilized by chemically tailored nanocelluloses. *Langmuir*, 30(31), 9327–9335.
- de Folter, J. W. J., van Ruijven, M. W. M., & Velikov, K. P. (2012). Oil-in-water Pickering emulsions stabilized by colloidal particles from the water-insoluble protein zein. *Soft Matter*, 8(25), 6807-6815.
- Destribats, M., Wolfs, M., Pinaud, F., Lapeyre, V., Sellier, E., Schmitt, V., & Ravaine, V. (2013). Pickering emulsions stabilized by soft microgels: Influence of the emulsification process on particle interfacial organization and emulsion properties. *Langmuir*, 29(40), 12367–12374.
- Dickinson, E. (1992). An introduction to food colloids. *Oxford University Press*, 4(1), 26-27.
- Dickinson, E. (2006). Interfacial Particles in Food Emulsions and Foams, Colloidal Particles at Liquid Interfaces. Ed. Bernard P. Binks and Tommy S. Horozov. 1st ed. Cambridge: Cambridge University Press, 298-327.
- Dickinson, E. (2009). Hydrocolloids as emulsifiers and emulsion stabilizers. *Food Hydrocolloids*, 23(6), 1473-1482.
- Dickinson, E. (2010). Food emulsions and foams: Stabilization by particles. *Current Opinion in Colloid & Interface Science*, 15 (1–2), 40-49.
- Dickinson, E. (2012). Use of nanoparticles and microparticles in the formation and stabilization of food emulsions. *Trends in Food Science & Technology*, 24 (1), 4-12.
- Dickinson, E., Radford, S. J., Golding, M. (2003). Stability and Rheology of Emulsions Containing Sodium Caseinate: Combined Effects of Ionic Calcium and Non-ionic Surfactant. *Food Hydrocolloids*, 17, 211-220.
- Dickinson, E., Ritzoulis, C. (2000). Creaming and Rheology of Oil-in-Water Emulsions Containing Sodium Dodecyl Sulfate and Sodium Caseinate. *Journal of Colloid and Interface Science*, 224, 148-154.

- Dokić, L., Krstonošić, V., & Nikolić, I. (2012). Physicochemical characteristics and stability of oil-in-water emulsions stabilized by OSA starch. *Food Hydrocolloids*, 29(1), 185–192.
- Domian, E., Brynda-Kopytowska, A., & Oleksza, K. (2015). Rheological properties and physical stability of o/w emulsions stabilized by OSA starch with trehalose. *Food Hydrocolloids*, 44, 49–58.
- Dong, X. M., Revol, J. F., & Gray, D. G. (1998). Effect of microcrystallite preparation conditions on the formation of colloid crystals of cellulose. *Cellulose*, 5, 19.
- Dongowski, G. (2007) Interactions between dietary fibre-rich preparations and glycoconjugated bile acids in vitro. *Food Chemistry*, 104(1), 390-397.
- Duffus, L. J., Norton, J. E., Smith, P., Norton, I. T., & Spyropoulos, F. (2016). A comparative study on the capacity of a range of food-grade particles to form stable O/W and W/O Pickering emulsions. *Journal of Colloid and Interface Science*, 473, 9–21.
- Dufresne, A., Dupeyre, D., & Vignon, M. R. (2000). Cellulose microfibrils from potato tuber cells: Processing and characterization of starch-cellulose microfibril composites. *Journal of Applied Polymer Science*, 76, 2080–2092.
- Elsabee, M. Z., Morsi, R. E., & Al-Sabagh, A. M. (2009). Surface active properties of chitosan and its derivatives. *Colloids and Surfaces B: Biointerfaces*, 74(1), 1–16.
- Espinal-Ruiz, M., Parada-Alfonso, F., Restrepo-Sanchez, L.-P., Narvaez-Cuenca, C.-E. & McClements, D. J. (2014) Impact of dietary fibers [methyl cellulose, chitosan, and pectin] on digestion of lipids under simulated gastrointestinal conditions. *Food & Function*, 5(12), 3083-3095.
- Estrada-Fernández, A. G., Román-Guerrero, A., Jiménez-Alvarado, R., Lobato-Calleros, C., Alvarez-Ramirez, J., & Vernon-Carter, E. J. (2018). Stabilization of oil-in-water-in-oil (O1/W/O2). Pickering double emulsions by soluble and insoluble whey protein concentrate-gum Arabic complexes used as inner and outer interfaces. *Journal of Food Engineering*, 221, 35–44.
- EU (2011). Commission Regulation (EU) No 53/2011 of 21 January 2011 amending Regulation (EC) No 606/2009 laying down certain detailed rules for implementing Council Regulations (EC) No 479/2008 as regards the categories of grapevine products, oenological practices and the applicable restrictions. <http://eur-lex.europa.eu/LexUriServ/LexUriServ.do?uri=OJ:L:2011:019:0001:0006:EN:PDF>, Accessed date: 2 October 2018.



- EU (2012). Commission Regulations (EU) No 432/2012 of 16 May 2012, establishing a list of permitted health claims made on foods, other than those referring to the reduction of disease risk and to children's development and health. <http://eur-lex.europa.eu/LexUriServ/LexUriServ.do?uri=OJ:L:2012:136:0001:0040:EN:PDF>, Accessed date: 2 October 2018.
- FDA (2011). Agency response letter GRAS notice no. GRN 000397. <https://www.fda.gov/Food/IngredientsPackagingLabeling/GRAS/NoticeInventory/ucm287638.htm>, Accessed date: 2 October 2018.
- FSANZ (2013). Food standards Australia New Zealand (FSANZ). Approval report - Application A1077. Fungal chitosan as a processing aid. <https://www.foodstandards.gov.au/code/applications/Documents/A1077-ChitosanAppR.pdf>, Accessed date: 2 October 2018.
- Gaikwad, S. G., & Pandit, A. B. (2008). Ultrasound emulsification: Effect of ultrasonic and physicochemical properties on dispersed phase volume and droplet size. *Ultrasonics Sonochemistry*, 15(4), 554–563.
- Gao, Z. M., Yang, X. Q., Wu, N. N., Wang, L. J., Wang, J. M., Guo, J., & Yin, S. W. (2014). Protein- based pickering emulsion and oil gel prepared by complexes of zein colloidal particles and stearate. *Journal of Agricultural and Food Chemistry*, 62(12), 2672–2678.
- Gestranius, M., Stenius, P., Kontturi, E., Sjöblom, J., & Tammelin, T. (2017). Phase behaviour and droplet size of oil-in-water Pickering emulsions stabilised with plantderived nanocellulosic materials. *Colloids and Surfaces A: Physicochemical and Engineering Aspects*, 519, 60–70.
- Golding, M. & Wooster, T. J. (2010) The influence of emulsion structure and stability on lipid digestion. *Current Opinion in Colloid & Interface Science*, 15(1–2), 90–101.
- Gómez, H. C., Serpa, A., Velásquez-Cock, J., Gañán, P., Castro, C., Vélez, L., & Zuluaga, R. (2016). Vegetable nanocellulose in food science: A review. *Food Hydrocolloids*, 57, 178–186.
- Gould, J., Vieira, J., & Wolf, B. (2013). Cocoa particles for food emulsion stabilisation. *Food & Function*, 4(9), 1369–1375.
- Gupta, R., & Rousseau, D. (2012). Surface-active solid lipid nanoparticles as Pickering stabilizers for oil-in-water emulsions. *Food & Function*, 3(3), 302–311.

- Habibi, Y., Mahrouz, M., & Vignon, M. R. (2009). Microfibrillated cellulose from the peel of prickly pear fruits. *Food Chemistry*, 115(2), 423–429.
- Hassan, M. L., Mathew, A. P., Hassan, E. A., & Oksman, K. (2010). Effect of pretreatment of bagasse pulp on properties of isolated nanofibers and nanopaper sheets. *Wood and Fiber Science*, 42(3), 362–376.
- Henriksson, M., Henriksson, G., Berglund, L. A., & Lindström, T. (2007). An environmentally friendly method for enzyme-assisted preparation of microfibrillated cellulose (MFC) nanofibers. *European Polymer Journal*, 43(8), 3434–3441.
- Herrick, F. W., Casebier, R. L., Hamilton, J. K., & Sandberg, K. R. (1983). Microfibrillated cellulose: Morphology and accessibility. *Journal of Applied Polymer Science: Applied Polymer Symposium*, 37, 797–813.
- Ho, K. W., Ooi, C. W., Mwangi, W. W., Leong, W. F., Tey, B. T., & Chan, E. S. (2016). Comparison of self-aggregated chitosan particles prepared with and without ultrasonication pretreatment as Pickering emulsifier. *Food Hydrocolloids*, 52, 827–837.
- Hu, Z., Ballinger, S., Pelton, R. & Cranston, E. D. (2015) Surfactant-enhanced cellulose nanocrystal Pickering emulsions. *Journal of Colloid and Interface Science*, 439, 139–148.
- Hubbe, M. A., Rojas, O. J., Lucia, L. A., & Sain, M. (2008). Cellulosic nanocomposites: A review. *BioResources*, 3, 929–980.
- Hur, S. J., Decker, E. A., & McClements, D. J. (2009). Influence of initial emulsifier type on microstructural changes occurring in emulsified lipids during in vitro digestion. *Food Chemistry*, 114(1), 253–262.
- Jafari, S. M., Assadpoor, E., He, Y., & Bhandari, B. (2008). Re-coalescence of emulsion droplets during high-energy emulsification. *Food Hydrocolloids*, 22(7), 1191–1202.
- JFCRF (2014). Japan food chemical research foundation. List of existing food additives. [http://www.ffcr.or.jp/zaidan/FFCRHOME.nsf/7bd44c20b0dc562649256502001b65e9/346b67d78f8905324925685c0027a6e0/\\$FILE/En2014.1.30.pdf](http://www.ffcr.or.jp/zaidan/FFCRHOME.nsf/7bd44c20b0dc562649256502001b65e9/346b67d78f8905324925685c0027a6e0/$FILE/En2014.1.30.pdf), Accessed date: 2 October 2018.
- Kalashnikova, I., Bizot, H., Cathala, B., & Capron, I. (2011). New pickering emulsions stabilized by bacterial cellulose nanocrystals. *Langmuir*, 27(12), 7471–7479.
- Kalashnikova, I., Bizot, H., Cathala, B., & Capron, I. (2012). Modulation of cellulose nanocrystals amphiphilic properties to stabilize oil/water interface. *Biomacromolecules*, 13(1), 267–275.

- Kaltsa, O., Michon, C., Yanniotis, S., & Mandala, I. (2013). Ultrasonic energy input influence on the production of sub-micron o/w emulsions containing whey protein and common stabilizers. *Ultrasonics Sonochemistry*, 20(3), 881–891.
- Kargar, M., Fayazmanesh, K., Alavi, M., Spyropoulos, F., & Norton, I. T. (2012). Investigation into the potential ability of Pickering emulsions (food-grade particles) to enhance the oxidative stability of oil-in-water emulsions. *Journal of Colloid and Interface Science*, 366(1), 209–215.
- Kaz, D. M. et al. (2012). Physical ageing of the contact line on colloidal particles at liquid interfaces. *Nat Mater*, 11 (2), 138-142.
- Kentish, S., & Ashokkumar, M. (2011). The physical and chemical effects of ultrasound. In H. Feng, G. Barbosa-Canovas, & J. Weiss (Eds.). *Ultrasound technologies for food and bioprocessing* (pp. 1–12). New York, NY: Springer Food Engineering Series.
- Khawas, P., & Deka, S. C. (2016). Isolation and characterization of cellulose nanofibers from culinary banana peel using high-intensity ultrasonication combined with chemical treatment. *Carbohydrate Polymers*, 137, 608–616.
- Kim, J., Yun, S. & Ounaies, Z. (2006) Discovery of Cellulose as a Smart Material. *Macromolecules*, 39(12), 4202-4206.
- Kitamura, Y., Okawa, O., Kato, T., & Sugawara, K. (2016). Effect of ultrasound intensity on the size and morphology of synthesized scorodite particles. *Advanced Powder Technology*, 27, 891–897.
- Klinkesorn, U. & McClements, D. J. (2009) Influence of chitosan on stability and lipase digestibility of lecithin-stabilized tuna oil-in-water emulsions. *Food Chemistry*, 114(4), 1308-1315.
- Krebs, T., Schroën, K., Boomb, R. (2012). Coalescence dynamics of surfactant-stabilized emulsions studied with microfluidics. *Soft Matter*, 8, 10650–10657.
- Kurukji, D., Pichot, R., Spyropoulos, F., & Norton, I. T. (2013). Interfacial behaviour of sodium stearylactylate (SSL) as an oil-in-water pickering emulsion stabiliser. *Journal of Colloid and Interface Science*, 409, 88-97.
- Kutuzov, S., He, J., Tangirala, R., Emrick, T., Russell, T.P., Böker, A. (2007). On the kinetics of nanoparticle self-assembly at liquid/liquid interfaces. *Physical Chemistry Chemical Physics*, 9, 6351–6358.

- Kvien, I., Tanem, B. S., & Oksman, K. (2005). Characterization of cellulose whiskers and their nanocomposites by atomic force and electron microscopy. *Biomacromolecules*, 6(6), 3160- 3165.
- Leal-Calderon, F., & Schmitt, V. (2008). Solid-stabilized emulsions. *Current Opinion in Colloid & Interface Science*, 13(4), 217–227.
- Leclercq, L., & Nardello-Rataj, V. (2016). Pickering emulsions based on cyclodextrins: A smart solution for antifungal azole derivatives topical delivery. *European Journal of Pharmaceutical Sciences*, 82, 126–137.
- Lee, K.-Y., Aitomäki, Y., Berglund, L. A., Oksman, K., & Bismarck, A. (2014). On the use of nanocellulose as reinforcement in polymer matrix composites. *Composites Science and Technology*, 105, 15–27.
- Li, J., Hwang, I.-C., Chen, X. & Park, H. J. (2016) Effects of chitosan coating on curcumin loaded nano-emulsion: Study on stability and in vitro digestibility. *Food Hydrocolloids*, 60(Supplement C), 138-147.
- Li, J., Wei, X., Wang, Q., Chen, J., Chang, G., Kong, L., ... Liu, Y. (2012). Homogeneous isolation of nanocellulose from sugarcane bagasse by high pressure homogenization. *Carbohydrate Polymers*, 90(4), 1609–1613.
- Li, Y. & McClements, D. J. (2010) New Mathematical Model for Interpreting pH-Stat Digestion Profiles: Impact of Lipid Droplet Characteristics on in Vitro Digestibility. *Journal of Agricultural and Food Chemistry*, 58(13), 8085-8092.
- Liang, H. N., & Tang, C. H. (2014). Pea protein exhibits a novel Pickering stabilization for oil-in- water emulsions at pH 3.0. *LWT - Food Science and Technology*, 58(2), 463-469.
- Linke, C., Drusch, S. (2017). Pickering emulsions in foods - opportunities and limitations. *Journal Critical Reviews in Food Science and Nutrition*, 58, 1971-1985.
- Liu, F., & Tang, C. H. (2014). Emulsifying properties of soy protein nanoparticles: Influence of the protein concentration and/or emulsification process. *Journal of Agricultural and Food Chemistry*, 62(12), 2644–2654.
- Liu, F., & Tang, C.-H. (2013). Soy Protein Nanoparticle Aggregates as Pickering Stabilizers for Oil- in-Water Emulsions. *Journal of Agricultural and Food Chemistry*, 61(37), 8888-8898.

- Liu, F., & Tang, C.-H. (2016). Soy glycinin as food-grade Pickering stabilizers: Part. I. Structural characteristics, emulsifying properties and adsorption/arrangement at interface. *Food Hydrocolloids*, 60, 606–619.
- Liu, H., Wang, C., Zou, S., Wei, Z., & Tong, Z. (2012). Simple, reversible emulsion system switched by pH on the basis of chitosan without any hydrophobic modification. *Langmuir*, 28(30), 11017-11024.
- Lopetinsky, R. J. G., Masliyah, J. H., & Xu, Z. (2006). Solids-stabilized emulsions: A review. In: (Ed.). *Colloidal Particles at Liquid Interfaces*, 186-224.
- Luo, Z., Murray, B. S., Yusoff, A., Morgan, M. R. A., Povey, M. J. W., & Day, A. J. (2011). Particle- Stabilizing Effects of Flavonoids at the Oil-Water Interface. *Journal of Agricultural and Food Chemistry*, 59(6), 2636-2645.
- Majeed, H., Antoniou, J., Hategekimana, J., Sharif, H. R., Haider, J., Liu, F., . . . Zhong, F. (2016). Influence of carrier oil type, particle size on in vitro lipid digestion and eugenol release in emulsion and nanoemulsions. *Food Hydrocolloids*, 52, 415-422.
- Maljaars, P. W. J., Peters, H. P. F., Mela, D. J., & Masclee, A. A. M. (2008). Ileal brake: A sensible food target for appetite control. *A review. Physiology & Behavior*, 95(3), 271-281.
- McClements, D. J. (2005). *Food Emulsions: Principles, Practices, and Techniques*. Ed Crc Press. Washington, 632.
- McClements, D. J., Decker, E. A., & Weiss, J. (2007). Emulsion-based delivery systems for lipophilic bioactive components. *Journal of Food Science*, 72(8), R109-R124.
- McGorty, R., Fung, J., Kaz, D., Manoharan, V.N., 2010. Colloidal self-assembly at an interface. *Materials Today* 13, 34–42.
- Mengual, O., Meunier, G., Cayré, I., Puech, K., & Snabre, P. (1999). TURBISCAN MA 2000: Multiple light scattering measurement for concentrated emulsion and suspension instability analysis.
- Meyabadi, T. F., & Dadashian, F. (2012). Optimization of enzymatic hydrolysis of waste cotton fibers for nanoparticles production using response surface methodology. *Fibers and Polymers*, 13(3), 313–321.
- Mikulcová, V., Bordes, R., & Kašpárková, V. (2016). On the preparation and antibacterial activity of emulsions stabilized with nanocellulose particles. *Food Hydrocolloids*, 61, 780–792.

- Minekus, M., Alming, M., Alvito, P., Ballance, S., Bohn, T., Bourlieu, C., Carriere, F., Boutrou, R., Corredig, M., Dupont, D., Dufour, C., Egger, L., Golding, M., Karakaya, S., Kirkhus, B., Le Feunteun, S., Lesmes, U., Macierzanka, A., Mackie, A., Marze, S., McClements, D. J., Menard, O., Recio, I., Santos, C. N., Singh, R. P., Vegarud, G. E., Wickham, M. S. J., Weitschies, W. & Brodkorb, A. (2014) A standardised static in vitro digestion method suitable for food - an international consensus. *Food & Function*, 5(6), 1113-1124.
- Mohammed, M. H., Williams, P. A. & Tverezovskaya, O. (2013) Extraction of chitin from prawn shells and conversion to low molecular mass chitosan. *Food Hydrocolloids*, 31(2), 166-171.
- Mun, S., Decker, E. A. & McClements, D. J. (2007) Influence of emulsifier type on in vitro digestibility of lipid droplets by pancreatic lipase. *Food Research International*, 40(6), 770-781.
- Mun, S., Park, S., Kim, Y.-R. & McClements, D. J. (2016) Influence of methylcellulose on attributes of  $\beta$ -carotene fortified starch-based filled hydrogels: Optical, rheological, structural, digestibility, and bioaccessibility properties. *Food Research International*, 87, 18-24.
- Mwangi, W. W., Ho, K.-W., Tey, B.-T., & Chan, E.-S. (2016). Effects of environmental factors on the physical stability of pickering-emulsions stabilized by chitosan particles. *Food Hydrocolloids*, 60, 543–550.
- Pääkko, M., Ankerfors, M., Kosonen, H., Nykänen, A., Ahola, S., Österberg, M., ... Lindström, T. (2007). Enzymatic hydrolysis combined with mechanical shearing and high-pressure homogenization for nanoscale cellulose fibrils and strong gels. *Biomacromolecules*, 8(6), 1934–1941.
- Pandey, A., Derakhshandeh, M., Kedzior, S.A., Pilapil, B., Shomrat, N., Segal-Peretz, T., Bryant, S. L., Trifkovic, M. (2018). Role of interparticle interactions on microstructural and rheological properties of cellulose nanocrystal stabilized emulsions. *Journal of Colloid and Interface Science*, 532, 808-818.
- Paximada, P., Tsouko, E., Kopsahelis, N., Koutinas, A. A., & Mandala, I. (2016). Bacterial cellulose as stabilizer of o/w emulsions. *Food Hydrocolloids*, 53, 225–232.
- Payet, L., & Terentjev, E. M. (2008). Emulsification and stabilization mechanisms of O/W emulsions in the presence of chitosan. *Langmuir*, 24(21), 12247–12252.

- Pelissari, F. M., Andrade-Mahecha, M. M., Sobral, P. J.d. A., & Menegalli, F. C. (2012). Isolation and characterization of the flour and starch of plantain bananas (*Musa paradisiaca*). *Starch – Stärke*, 64(5), 382–391.
- Pelissari, F. M., Sobral, P. J.d. A., & Menegalli, F. C. (2014). Isolation and characterization of cellulose nanofibers from banana peels. *Cellulose*, 21(1), 417–432.
- Perrier-Cornet, J. M., Marie, P., & Gervais, P. (2005). Comparison of emulsification efficiency of protein-stabilized oil-in-water emulsions using jet, high pressure and colloid mill homogenization. *Journal of Food Engineering*, 66(2), 211-217.
- Philippova, O. E. & Korchagina, E. V. (2012) Chitosan and its hydrophobic derivatives: Preparation and aggregation in dilute aqueous solutions. *Polymer Science - Series A*, 54(7), 552-572.
- Pickering, S. U. (1907). CXCVI. –Emulsions. *Journal of the Chemical Society, Transactions*, 91(0), 2001–2021.
- Pirani, S., & Hashaikeh, R. (2013). Nanocrystalline cellulose extraction process and utilization of the byproduct for biofuels production. *Carbohydrate Polymers*, 93(1), 357–363.
- Priest, C., Reid, M. D., & Whitby, C. P. (2011). Formation and stability of nanoparticle-stabilised oil- in-water emulsions in a microfluidic chip. *Journal of Colloid and Interface Science*, 363(1), 301-306.
- Qaqish, R., & Amiji, M. (1999). Synthesis of a fluorescent chitosan derivative and its application for the study of chitosan–mucin interactions. *Carbohydrate Polymers*, 38(2), 99–107.
- Ranby, B. G. (1951). Fibrous macromolecular systems. Cellulose and muscle. The colloidal properties of cellulose micelles. *Discussions of the Faraday Society*, 11(0), 158-164.
- Rayner, M., Sjöö, M., Timgren, A., & Dejmek, P. (2012). Quinoa starch granules as stabilizing particles for production of Pickering emulsions. *Faraday Discussions*, 158, 139-155.
- Renzaho, A. M. N., & Mellor, D. (2010). Food security measurement in cultural pluralism: Missing the point or conceptual misunderstanding. *Nutrition*, 26(1), 1-9.
- Rosa, M. F., Medeiros, E. S., Malmonge, J. A., Gregorski, K. S., Wood, D. F., Mattoso, L. H. C., ... Imam, S. H. (2010). Cellulose nanowhiskers from coconut husk fibers: Effect of preparation conditions on their thermal and morphological behavior. *Carbohydrate Polymers*, 81(1), 83–92.

- Salari, J. W. O. et al. (2014) Deformation of the water/oil interface during the adsorption of sterically stabilized particles. *Langmuir*, 30(25), 7327-7333.
- Salas, C., Nypelö, T., Rodriguez-Abreu, C., Carrillo, C., & Rojas, O. J. (2014). Nanocellulose properties and applications in colloids and interfaces. *Current Opinion in Colloid & Interface Science*, 19(5), 383-396.
- Saravacos, G., Taoukis, P., Krokida, M., Karathanos, V., Lazarides, H., Stoforos, N., ... Dejmeek, P. (2011). 11th international congress on engineering and food (ICEF11) starch particles for food-based Pickering emulsions. *Procedia Food Science*, 1, 95–103.
- Sarkar, A., Horne, D. S. & Singh, H. (2010) Interactions of milk protein-stabilized oil-in-water emulsions with bile salts in a simulated upper intestinal model. *Food Hydrocolloids*, 24(2), 142-151.
- Sarkar, A., Zhang, S., Murray, B., Russell, J. A. & Boxal, S. (2017) Modulating in vitro gastric digestion of emulsions using composite whey protein-cellulose nanocrystal interfaces. *Colloids and Surfaces B: Biointerfaces*, 158(Supplement C), 137-146.
- Segal, L., Creely, J. J., Martin, A. E., & Conrad, C. M. (1959). An empirical method for estimating the degree of crystallinity of native cellulose using the X-ray diffractometer. *Textile Research Journal*, 29(10), 786–794.
- Shah, R. K., Shum, H. C., Rowat, A. C., Lee, D., Agresti, J. J, Utada, A. S., Chu, L. -Y., Kim, J. -W., Fernandez-Nieves, A., Martinez, C. J., Weitz, D. A., 2008. Designer emulsions using microfluidics. *Materials Today*, 11 (4), 18-27.
- Silva, E. K., Gomes, M. T. M. S., Hubinger, M. D., Cunha, R. L., & Meireles, M. A. A. (2015). Ultrasound-assisted formation of annatto seed oil emulsions stabilized by biopolymers. *Food Hydrocolloids*, 47, 1–13.
- Silva, E. K., Rosa, M. T. M. G., & Meireles, M. A. A. (2015). Ultrasound-assisted formation of emulsions stabilized by biopolymers. *Current Opinion in Food Science*, 5, 50–59.
- Silva, E. K., Zabot, G. L., & A Meireles, M. A. (2015). Ultrasound-assisted encapsulation of annatto seed oil: Retention and release of a bioactive compound with functional activities. *Food Research International*, 78, 159–168.
- Singh, H. (2011). Aspects of milk-protein-stabilised emulsions. *Food Hydrocolloids*, 25(8), 1938-1944.
- Siqueira, G., Bras, J., & Dufresne, A. (2010). Cellulosic bionanocomposites: A review of preparation, properties and applications. *Polymers*, 2(4).



- Song, X., Pei, Y., Qiao, M., Ma, F., Ren, H., & Zhao, Q. (2015). Preparation and characterizations of Pickering emulsions stabilized by hydrophobic starch particles. *Food Hydrocolloids*, 45, 256–263.
- Soria, A. C., & Villamiel, M. (2010). Effect of ultrasound on the technological properties and bioactivity of food: A review. *Trends in Food Science & Technology*, 21, 323–331.
- Stancik, E. J., & Fuller, G. G. (2004). Connect the drops: Using solids as adhesives for liquids. *Langmuir*, 20(12), 4805–4808.
- Stenstad, P., Andresen, M., Tanem, B. S., & Stenius, P. (2008). Chemical surface modifications of microfibrillated cellulose. *Cellulose*, 15(1), 35–45.
- Sun, X. F., Sun, R. C., Fowler, P., & Baird, M. S. (2004). Isolation and characterisation of cellulose obtained by a two-stage treatment with organosolv and cyanamide activated hydrogen peroxide from wheat straw. *Carbohydrate Polymers*, 55(4), 379–391.
- Suslick, K. S., & Price, G. J. (1999). Applications of ultrasound to materials chemistry. *Annual Review of Materials Science*, 29(1), 295–326.
- Svagan, A. J., Azizi Samir, M. A. S., & Berglund, L. A. (2007). Biomimetic Polysaccharide Nanocomposites of High Cellulose Content and High Toughness. *Biomacromolecules*, 8(8), 2556–2563.
- Talanta, 50(2), 445–456. Mohammed, M. H., Williams, P. A., & Tverezovskaya, O. (2013). Extraction of chitin from prawn shells and conversion to low molecular mass chitosan. *Food Hydrocolloids*, 31(2), 166–171.
- Tan, C., Xie, J., Zhang, X., Cai, J., & Xia, S. (2016). Polysaccharide-based nanoparticles by chitosan and gum arabic polyelectrolyte complexation as carriers for curcumin. *Food Hydrocolloids*, 57, 236–245.
- TAPPI (2011). Proposed new TAPPI standard: Standard terms and their definition for cellulose nanomaterial.
- Tarchichi, N., Chollet, F., Manceau, J.F. (2013). New regime of droplet generation in a T-shape microfluidic junction. *Microfluidic Nanofluidic*, 14, 45–51.
- Tcholakova, S., Denkov, N. D., & Lips, A. (2008). Comparison of solid particles, globular proteins and surfactants as emulsifiers. *Physical Chemistry Chemical Physics*, 10(12), 1608–1627.

- Teixeira, E.d. M., Bondancia, T. J., Teodoro, K. B. R., Corrêa, A. C., Marconcini, J. M., & Mattoso, L. H. C. (2011). Sugarcane bagasse whiskers: Extraction and characterizations. *Industrial Crops and Products*, 33(1), 63–66.
- Tibolla, H., Pelissari, F. M., & Menegalli, F. C. (2014). Cellulose nanofibers produced from banana peel by chemical and enzymatic treatment. *LWT – Food Science and Technology*, 59(2P2), 1311–1318.
- Tibolla, H., Pelissari, F. M., Rodrigues, M. I., & Menegalli, F. C. (2017). Cellulose nanofibers produced from banana peel by enzymatic treatment: Study of process conditions. *Industrial Crops and Products*, 95, 664–674.
- Tikekar, R. V., Pan, Y., & Nitin, N. (2013). Fate of curcumin encapsulated in silica nanoparticle stabilized Pickering emulsion during storage and simulated digestion. *Food Research International*, 51(1), 370–377.
- Torres, L. G., Iturbe, R., Snowden, M. J., Chowdhry, B. Z., & Leharne, S. A. (2007). Preparation of o/w emulsions stabilized by solid particles and their characterization by oscillatory rheology. *Colloids and Surfaces A: Physicochemical and Engineering Aspects*, 302(1–3), 439–448.
- Turbak, A. F., Snyder, F. W., & Sandberg, K. R. (1982). US 4.341.807. Washington, DC, US: Patent and Trademark Office.
- Turbak, A. F., Snyder, F. W., & Sandberg, K. R. (1983a). Microfibrillated cellulose, a new cellulose product: Properties, uses, and commercial potential. *Journal of Applied Polymer Science: Applied Polymer Symposiom*, 37, 815–827.
- Turbak, A. F., Snyder, F. W., & Sandberg, K. R. (1983b). US 4.378.381. Washington DC, US: Patent and Trademark Office.
- Tzoumaki, M. V., Moschakis, T., Kiosseoglou, V., & Biliaderis, C. G. (2011). Oil-in-water emulsions stabilized by chitin nanocrystal particles. *Food Hydrocolloids*, 25(6), 1521–1529.
- Tzoumaki, M. V., Moschakis, T., Scholten, E., & Biliaderis, C. G. (2013). In vitro lipid digestion of chitin nanocrystal stabilized o/w emulsions. *Food and Function*, 4(1), 121–129.
- Umbanhowar, P., Prasad, V., Weitz, D.A. (2000). Monodisperse emulsion generation via drop break off in a coflowing stream. *Langmuir*, 16, 347–351.

- Urban, K. et al. (2006). Rotor-stator and disc systems for emulsification processes. *Chemical Engineering and Technology*, 29(1), 24-31.
- Utada, A. S., Lorenceau, E., Link, D. R., Kaplan, P. D., Stone, H. A., Weitz, D. A. (2005). Monodisperse double emulsions generated from a microcapillary device. *Science*, 308 (5721), 537-541.
- Van Soest, J. J. G., Hullemans, S. H. D., de Wit, D., & Vliegenthart, J. F. G. (1996). Changes in the mechanical properties of thermoplastic potato starch in relation with changes in B-type crystallinity. *Carbohydrate Polymers*, 29(3), 225-232.
- Vicentini, N. M., Dupuy, N., Leitzelman, M., Cereda, M. P., & Sobral, P. J. A. (2005). Prediction of cassava starch edible film properties by chemometric analysis of infrared spectra. *Spectroscopy Letters*, 38(6), 749-767.
- Walstra, P. (2005). Emulsions. *Fundamentals of Interface and Colloid Science*, 5, 8.1-8.94.
- Wang, W., Du, G., Li, C., Zhang, H., Long, Y., & Ni, Y. (2016). Preparation of cellulose nanocrystals from asparagus (*Asparagus officinalis* L.) and their applications to palm oil/water Pickering emulsion. *Carbohydrate Polymers*, 151, 1-8.
- Wen, C., Yuan, Q., Liang, H., & Vriesekoop, F. (2014). Preparation and stabilization of d-limonene Pickering emulsions by cellulose nanocrystals. *Carbohydrate Polymers*, 112, 695-700.
- Wilde, P. J., & Chu, B. S. (2001). Interfacial & colloidal aspects of lipid digestion. *Advances in Colloid and Interface Science*, 165(1), 14-22.
- Wilhelm, M., Zhao, C.-L., Wang, Y., Xu, R., Winnik, M. A., Mura, J.-L., ... Croucher, M. D. (1991). Poly(styrene-ethylene oxide) block copolymer micelle formation in water. A fluorescence probe study. *Macromolecules*, 24(5), 1033-1040.
- Winuprasith, T., & Supphantharika, M. (2013). Microfibrillated cellulose from mangosteen (*Garcinia mangostana* L.) rind: Preparation, characterization, and evaluation as an emulsion stabilizer. *Food Hydrocolloids*, 32(2), 383-394.
- Winuprasith, T., & Supphantharika, M. (2015). Properties and stability of oil-in-water emulsions stabilized by microfibrillated cellulose from mangosteen rind. *Food Hydrocolloids*, 43, 690-699.
- Xhanari, K., Syverud, K., Chinga-Carrasco, G., Paso, K., & Stenius, P. (2011). Structure of nanofibrillated cellulose layers at the o/w interface. *Journal of Colloid and Interface Science*, 356(1), 58-62.

- Xu, F., Sun, J.-X., Sun, R., Fowler, P., & Baird, M. S. (2006). Comparative study of organosolv lignins from wheat straw. *Industrial Crops and Products*, 23(2), 180–193.
- Xu, Q. Y., Nakajima, M., & Binks, B. P. (2005). Preparation of particle-stabilized oil-in-water emulsions with the microchannel emulsification method. *Colloids and Surfaces A: Physicochemical and Engineering Aspects*, 262(1–3), 94–100.
- Yan, H., Chen, X., Song, H., Li, J., Feng, Y., Shi, Z., Wang, X. & Lin, Q. (2017) Synthesis of bacterial cellulose and bacterial cellulose nanocrystals for their applications in the stabilization of olive oil pickering emulsion. *Food Hydrocolloids*, 72(Supplement C), 127–135.
- Yao, X., Wang, N., Fang, Y., Phillips, G. O., Jiang, F., Hu, J., Lu, J., Xu, Q. & Tian, D. (2013) Impact of surfactants on the lipase digestibility of gum arabic-stabilized O/W emulsions. *Food Hydrocolloids*, 33(2), 393–401.
- Ye, A., Zhu, X., & Singh, H. (2013). Oil-in-water emulsion system stabilized by protein coated nanoemulsion droplets. *Langmuir*, 29(47), 14403–14410.
- Yuan, Q., Cayre, O. J., Manga, M., Williams, R. A., & Biggs, S. (2010). Preparation of particle-stabilized emulsions using membrane emulsification. *Soft Matter*, 6(7), 1580–1588.
- Yusoff, A., & Murray, B. S. (2011). Modified starch granules as particle-stabilizers of oil-in-water emulsions. *Food Hydrocolloids*, 25(1), 42–55.
- Zhang, R., Zhang, Z., Zhang, H., Decker, E. A. & McClements, D. J. (2015) Influence of emulsifier type on gastrointestinal fate of oil-in-water emulsions containing anionic dietary fiber (pectin). *Food Hydrocolloids*, 45, 175–185.
- Zhao, C. X. (2013). Multiphase flow microfluidics for the production of single or multiple emulsions for drug delivery. *Advanced Drug Delivery Reviews*, 65(11–12), 1420–1446.
- Zhao, C.-X., & Middelberg, A. P. J. (2011). Two-phase microfluidic flows. *Chemical Engineering Science*, 66(7), 1394–1411.
- Zhao, H., Kwak, J. H., Conrad Zhang, Z., Brown, H. M., Arey, B. W., & Holladay, J. E. (2007). Studying cellulose fiber structure by SEM, XRD, NMR and acid hydrolysis. *Carbohydrate Polymers*, 68(2), 235–241.
- Zhou, G., Zhao, Y., Hu, J., Shen, L., Liu, W., & Yang, X. (2013). A new drug-loading technique with high efficiency and sustained-releasing ability via the Pickering emulsion interfacial assembly of temperature/pH-sensitive nanogels. *Reactive and Functional Polymers*, 73(11), 1537–1543.

- 
- Zhu, Y., Jiang, J., Liu, K., Cui, Z., & Binks, B. P. (2015). Switchable pickering emulsions stabilized by silica nanoparticles hydrophobized in situ with a conventional cationic surfactant. *Langmuir*, 31(11), 3301-3307.
- Zuluaga, R., Putaux, J. L., Cruz, J., Vélez, J., Mondragon, I., & Gañán, P. (2009). Cellulose microfibrils from banana rachis: Effect of alkaline treatments on structural and morphological features. *Carbohydrate Polymers*, 76(1), 51–59.

## **ANEXOS**

---

- PERMISSÃO PARA USO DE ARTIGO

10/1/2018

Rightslink® by Copyright Clearance Center



RightsLink®

Home

Create Account

Help



**Title:** One-step ultrasound producing O/W emulsions stabilized by chitosan particles

**Author:** Ana Letícia Rodrigues Costa, Andresa Gomes, Rosiane Lopes Cunha

**Publication:** Food Research International

**Publisher:** Elsevier

**Date:** May 2018

© 2018 Elsevier Ltd. All rights reserved.

## LOGIN

If you're a **copyright.com user**, you can login to RightsLink using your copyright.com credentials. Already a **RightsLink user** or want to [learn more?](#)

Please note that, as the author of this Elsevier article, you retain the right to include it in a thesis or dissertation, provided it is not published commercially. Permission is not required, but please ensure that you reference the journal as the original source. For more information on this and on your other retained rights, please visit: <https://www.elsevier.com/about/our-business/policies/copyright#Author-rights>

BACK

CLOSE WINDOW

Copyright © 2018 [Copyright Clearance Center, Inc.](#) All Rights Reserved. [Privacy statement](#). [Terms and Conditions](#). Comments? We would like to hear from you. E-mail us at [customercare@copyright.com](mailto:customercare@copyright.com)

10/1/2018

Rightslink® by Copyright Clearance Center

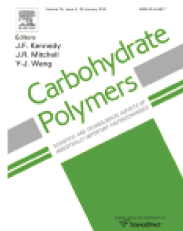


RightsLink®

Home

Create  
Account

Help



**Title:** Cellulose nanofibers from banana peels as a Pickering emulsifier: High-energy emulsification processes

**Author:** Ana Letícia Rodrigues Costa, Andresa Gomes, Heloisa Tibolla, Florencia Cecilia Menegalli, Rosiane Lopes Cunha

**Publication:** Carbohydrate Polymers

**Publisher:** Elsevier

**Date:** 15 August 2018

© 2018 Elsevier Ltd. All rights reserved.

## LOGIN

If you're a **copyright.com user**, you can login to RightsLink using your copyright.com credentials. Already a **RightsLink user** or want to [learn more?](#)

Please note that, as the author of this Elsevier article, you retain the right to include it in a thesis or dissertation, provided it is not published commercially. Permission is not required, but please ensure that you reference the journal as the original source. For more information on this and on your other retained rights, please visit: <https://www.elsevier.com/about/our-business/policies/copyright#Author-rights>

BACK

CLOSE WINDOW

Copyright © 2018 [Copyright Clearance Center, Inc.](#) All Rights Reserved. [Privacy statement](#). [Terms and Conditions](#). Comments? We would like to hear from you. E-mail us at [customercare@copyright.com](mailto:customercare@copyright.com)